

First Bulk and Surface Results for the ATLAS ITk Stereo Annulus Sensors

, S.H. Abidi^l, A.A. Affolder^k, J. Boehm^j, J. Botte^a, B. Ciungu^l, K. Dette^l, Z. Dolezal^l
C. Escobar^g, V. Fadeyev^k, J. Fernandez-Tejero^b, C. García Argos^{c,g}, D. Gillberg^a, K. Hara^m, M. Hauser^c,
R.F.H. Hunter^a, K. Jakobs^c, J.S. Keller^a, P. Kodysⁱ, T. Koffas^a, Z. Kotek^j, J. Krol^l, C. Lacasta^g, V. Latonova^j,
J. Loenker^d, D. Madaffari^g, M. Mikestikova^j, M. Miñano^g, S. Y. Ng^f, R.S. Orr^l, U. Parzefall^c, D. Rodriguez^g,
U. Soldevila^g, J. Stastny^j, M. Stegler^c, J. Suzuki^m, R. Teuscher^l, Y. Unno^h, S. Wada^m, M. Wiehe^c, L. Wiik-Fucks^c,
F. Wizemann^d, V. Zahradnik^j

^aPhysics Department, Carleton University, 1125 Colonel By Drive, Ottawa, Ontario, K1S 5B6, Canada

^bCentro Nacional de Microelectronica (IMB-CNM, CSIC), Campus UAB-Bellaterra, 08193 Barcelona, Spain

^cDeutsches Elektronen-Synchrotron, Notkestraße 85, 22607 Hamburg, Germany

^dExperimentelle Physik IV, TU Dortmund, Dortmund, Germany

^ePhysikalisches Institut, Albert-Ludwigs-Universität Freiburg, Hermann-Herder-Str. 3, 79104 Freiburg-im-Breisgau, Germany

^fInstitut für Physik, Humboldt-Universität zu Berlin, Newtonstraße, Berlin, Germany

^gInstituto de Física Corpuscular (IFIC) - CSIC-University of Valencia, Parque Científico, C/Catedrático José Beltrán 2, E-46980 Paterna, Spain

^hIPNS, KEK, 1-1 Oho, Tsukuba, Ibaraki 305-0801, Japan

ⁱFaculty of Mathematics and Physics, Charles University, V Holesovickach 2, Prague, CZ18000 The Czech Republic

^jAcademy of Sciences of the Czech Republic, Institute of Physics, Na Slovance 2, 18221 Prague 8, Czech Republic

^kSanta Cruz Institute for Particle Physics (SCIPP), University of California, Santa Cruz, CA 95064, USA

^lDepartment of Physics, University of Toronto, 60 Saint George St., Toronto M5S 1A7, Ontario, Canada

^mInstitut of Pure and Applied Sciences, University of Tsukuba, 1-1-1 Tennodai, Tsukuba Ibaraki 305-8571, Japan

ⁿComment out this line once the proper institute is assigned to the corresponding author

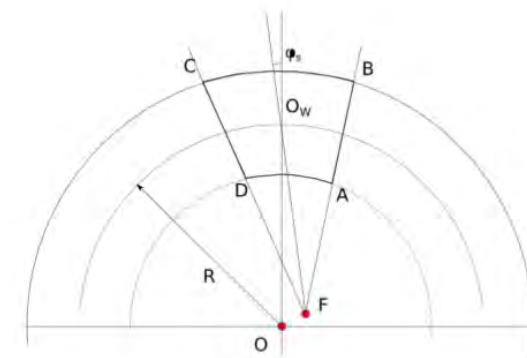
December 12th, 2017

Okinawa, Japan

11th International "Hiroshima" Symposium

On the Development and Application of Semiconductor Tracking Detectors

- Background
- Stereo Annulus Geometry and Its Advantages



- The R0 Prototype Sensor

See poster by Carlos Lacasta Llacer: "Design of the first full size ATLAS ITk Strip sensor for the endcap region"

- Bulk Sensor Characteristics

- With comparison to conventionally shaped comparable sensor

See talk by Vladimir Cindro for irradiated bulk performance. Coming up next!

- Surface Property Investigation

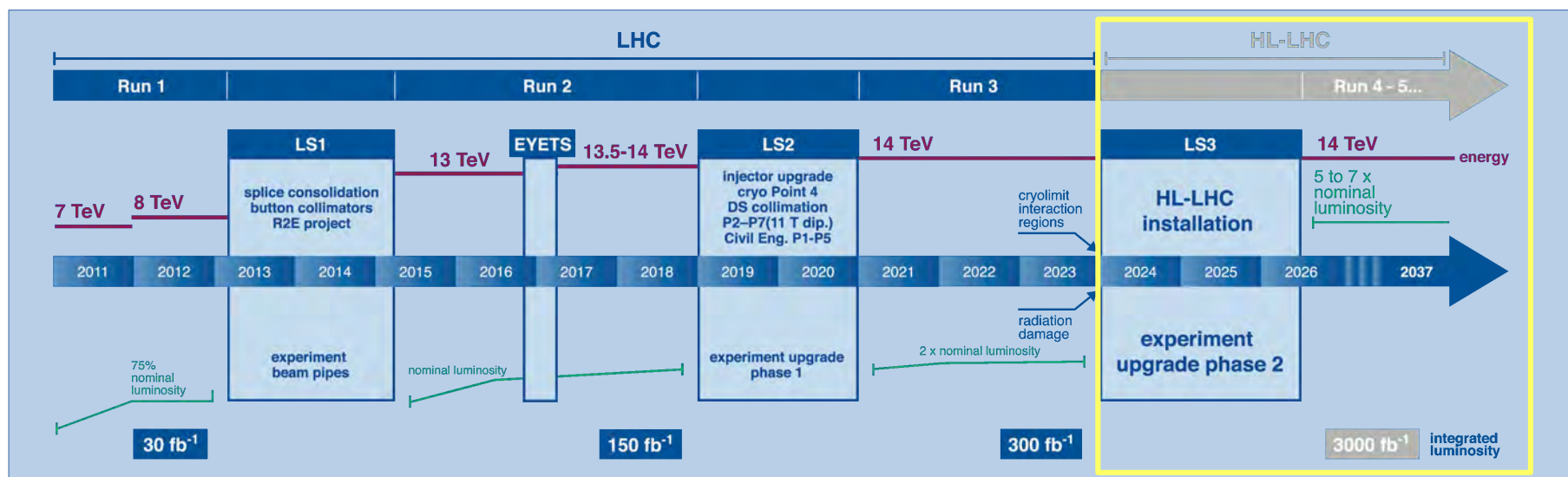
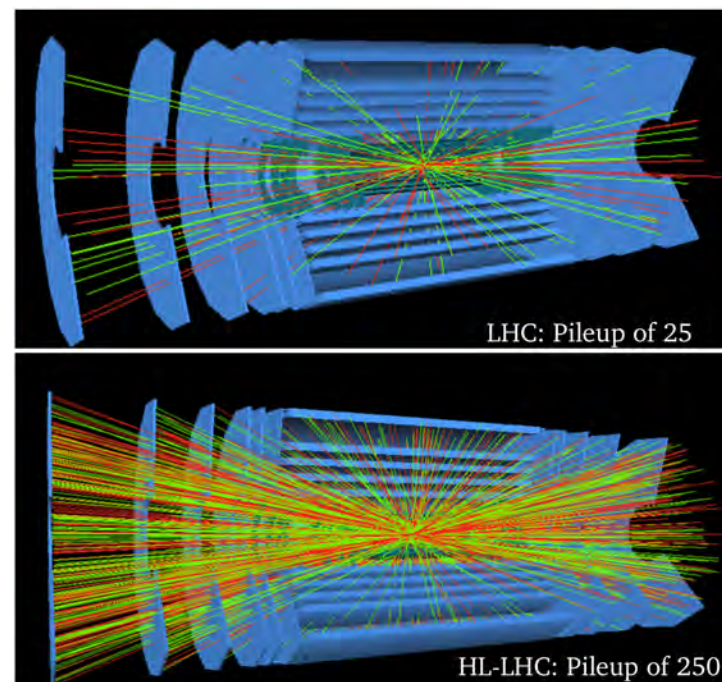
- With evaluation of irradiated performance

See also, R0 Prototype poster by Carlos Garcia Argos : "Assembly and Electrical Tests of the First Full-size Forward Module for the ATLAS ITk Strip Detector"

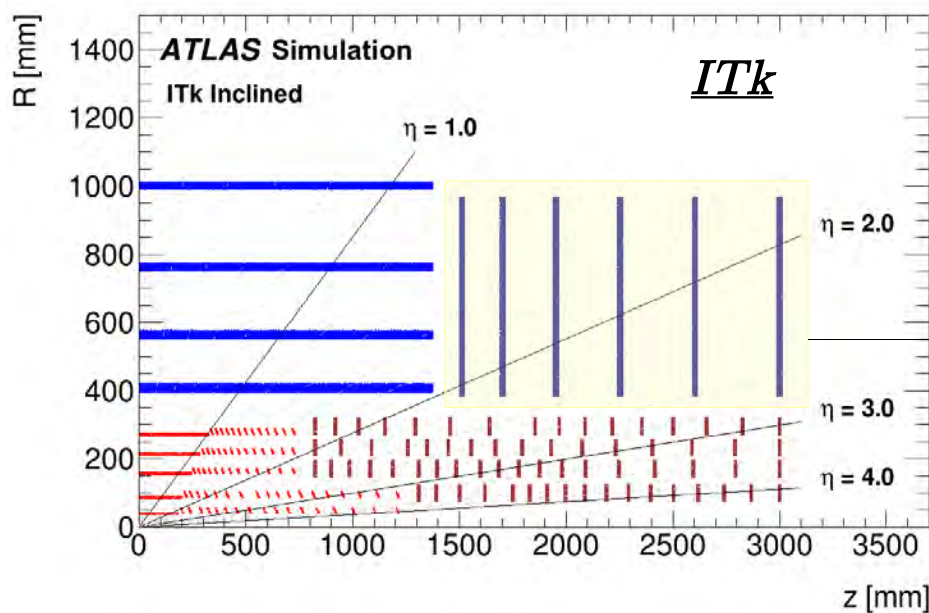
The HL-LHC and Challenges Faced

- 10x more premier p⁺-p⁺ data (3000fb⁻¹)
 ⇒ Higher sensitivity for LHC measurements
 ⇒ A leading possibility to uncover new physics
- 500-750% increase in instantaneous luminosity
 (levelled 5-7.5x10³⁴ cm⁻² s⁻¹)
- 600%-850% increase in number of interactions per 25ns bunch crossing (levelled 140-200 vs. 23/40 avg/peak)
- 170% increase in projected lifetime (27yr vs 10yr)
- 10x more radiation damage (10¹⁶ n_{eqv}/cm² NIEL, 10⁷ Gy TID)

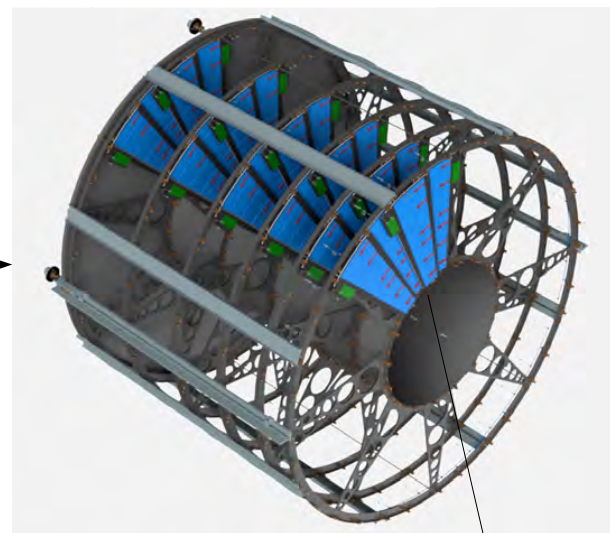
⇒ High granularity, reliability, radiation hardness required from detector upgrades



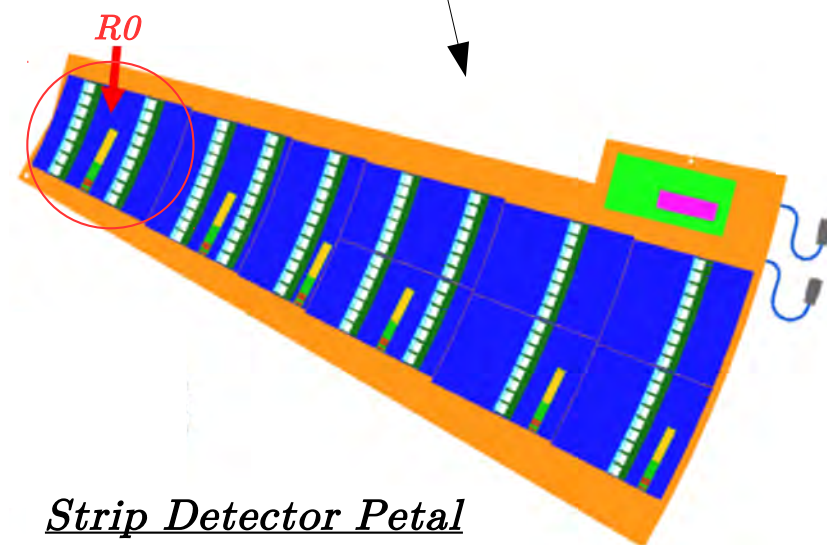
The ITk; Home of the First Stereo Annulus Sensor



Strip Detector Endcap

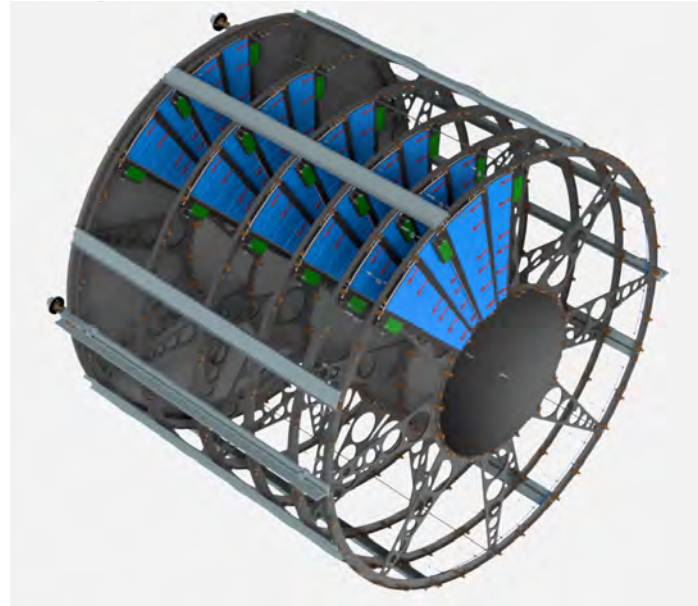


- *ITk*; all-silicon HL-LHC replacement of ATLAS ID utilizing pixels and strips
- *The Strip Detector*; $\sim 165\text{m}^2$ silicon surface area
- *Endcaps*; two each with six disks each with 32 petals
- *Petals*;
 - Double-sided (mirror image)
 - Nine sensors per side in six designs
 - All stereo annulus



Strip Detector Petal

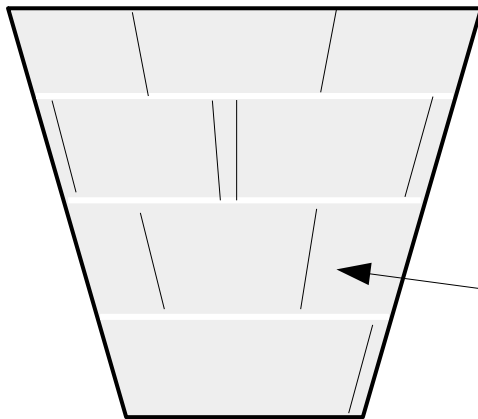
The Stereo Annulus Geometry



- What is the best way to do strip tracking in the restricted endcap geometry?
 - *Primary* dimension to measure is the azimuthal angle (bending dimension)
 - Use the most sensitive feature \Rightarrow strips oriented radially
 - *Secondary* dimension is the radius from the beam-pipe
 - Add a small (20-40mrad) stereo angle to vastly improve resolution
 - (*Tertiary* dimension is the axial distance and is obtained from the disk location)

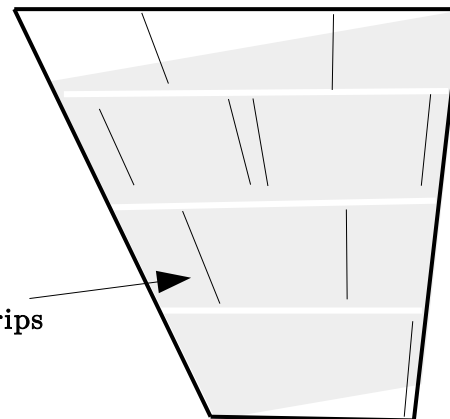
The Stereo Annulus Design; 'Reinventing' the Wheel

Conventional Geometry:
Symmetric Trapezoidal Wedge
(Sensor itself is rotated by stereo angle)



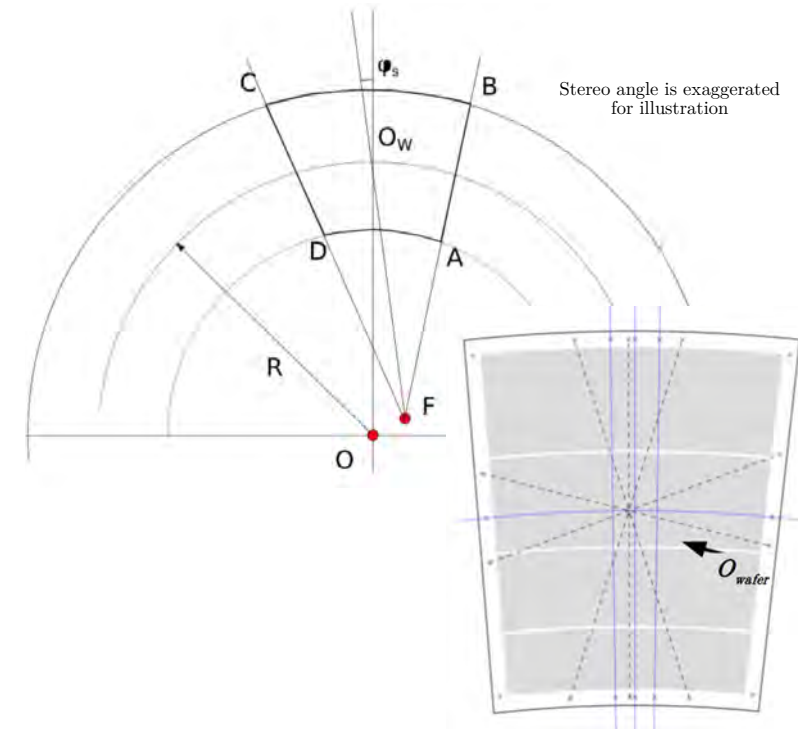
eg. ATLAS SCT

Upgraded Geometry:
Stereo Trapezoidal Wedge



Stereo angle is Greatly exaggerated for illustration

Optimized Geometry:
Stereo Annulus



eg. ATLAS ITk

Stereo strips in symmetric sensor?

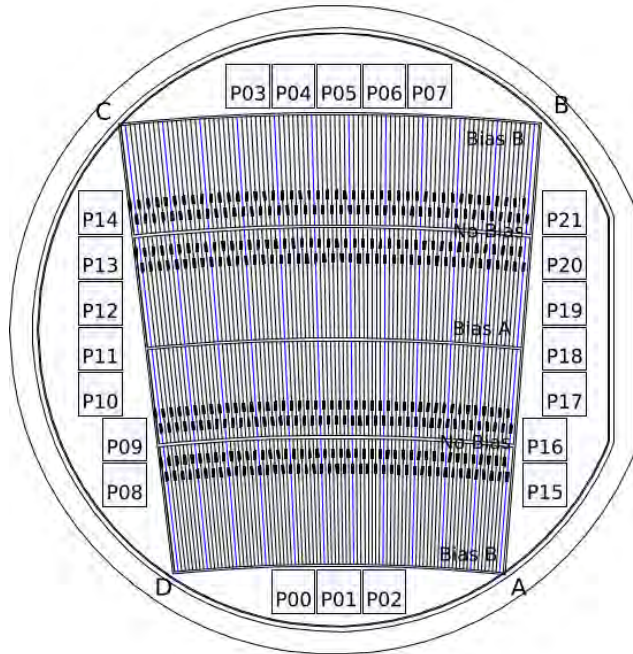
- Truncated and orphaned strips

Disadvantages:

- Most difficult interlocking
- Space is limited on petals
- Incomplete coverage at large and small radii
- Uneven strip lengths
- Interlocking is more manageable
- Incomplete coverage at large and small radii
- Uneven strip lengths
- Inexperience

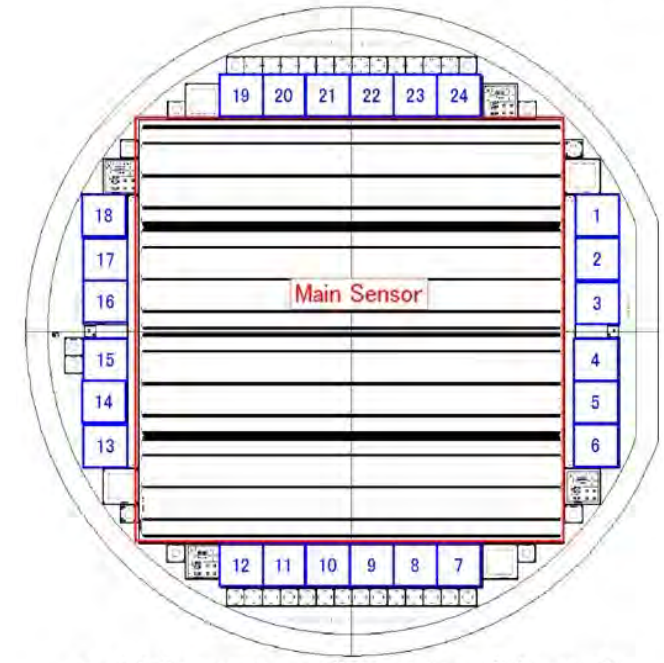
Bulk Character Comparison Samples

R0 Prototype (Stereo Annulus)



- Large surface area: (90.0cm²,91.8cm²)
- n⁺-in-p, ac-coupled, single-sided
- 6", FZ-grown, ~325 μm thick, <100> wafer
- Optimized common p-stops, gated PTP
- SiO₂ and AlN:H passivation
- Similar strip and contact pad numbers (4360,5128 strips in 4 segments)
- Hamamatsu Photonics

ATLAS12 (Conventional Barrel)



- Square with parallel strips of constant pitch (74.5 μm) and length (23.9 mm)
- Slim edge width for 25% of sensors (450 μm with a standard 980 μm)
- ~120 sensors from 4 batches

L.B.A. Hommels *et al.*, *Nucl. Instr. Meth. Phys. Res. A*, vol. 831, pp. 167–173, 2016. (10th International “Hiroshima” Symposium)

- Stereo annulus with constant angular pitch in each segment (73.5-83.9 μm) and variant length (19-32 mm)

- Slim edge width for 100% of sensors (450 μm annular edge, 500 μm stereo edge)

- ~60 sensors from 2 batches

See talks by Liv Wiik-Fuchs and Andy Blue for annealing and irradiated testbeam performance of ATLAS12. Coming up soon!

Surface Properties; Irradiated Samples

- **730 (1cm)² minis**
 - ie. square with parallel strips
- **252 minis** have already been **irradiated** up to $2.2 \times 10^{15} n_{eqv}/cm^2$ with protons and neutrons
- Minis have ~8 mm long strips and come with variant pitch, coupling, and punch through protection configurations

Narrow / Default / Wide pitch (μm): 70 / 75 / 85

(R0 Prototype pitches range from approximately 73-84 μm)

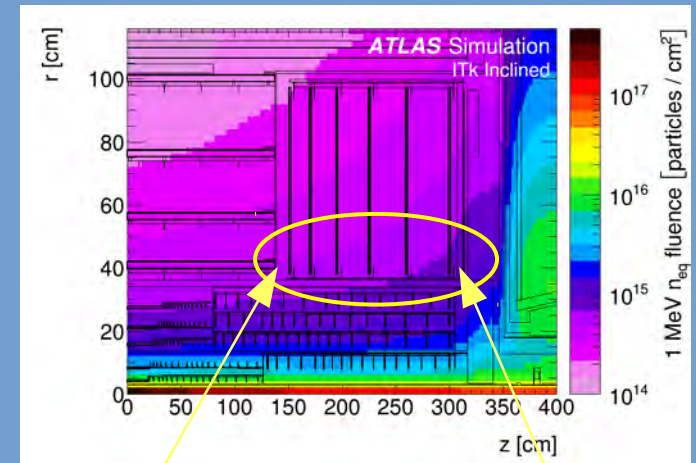
- *Today's results: AC-coupled, PTP minis from one mini test set irradiated with p^+ and annealed 80 minutes at 60°C*

A Mini Test Set:

Fluence unit: $\times 10^{14} n_{eqv}/cm^2$

Pitch	Coupling	PTP	0x	5x	10x	20x	TOTAL
Default	AC	Yes	2	2	2	2	8
	DC	Yes	2	2	2	2	8
	DC	No	2	2	2	2	8
Narrow	AC	Yes	2	1	2	1	6
	DC	Yes		1	1	1	3
	DC	No		1	1	1	3
Wide	AC	Yes	2	1	2	1	6
	DC	Yes					0
	DC	No					0
Total			10	10	12	10	42

Radiation Projections for the R0 Sensor



NIEL Fluence:
 $3.8 \times 10^{14} n_{eqv}/cm^2$
TID: 9.8 Mrad

NIEL Fluence:
 $1.2 \times 10^{15} n_{eqv}/cm^2$
TID: 50.4 Mrad

4500fb⁻¹ (1.5 safety factor)

The ATLAS Collaboration, "ATLAS Inner Tracker Strip Detector: Technical Design Report," CERN Tech. Rep. ATL-TDR-025 / LHCC-2017-005, 2017.

Three mini test sets are *each* irradiated with:

n

reactor neutrons
 Ljubljana Reactor
 Jožef Stefan Institute,
 Slovenia

p^+

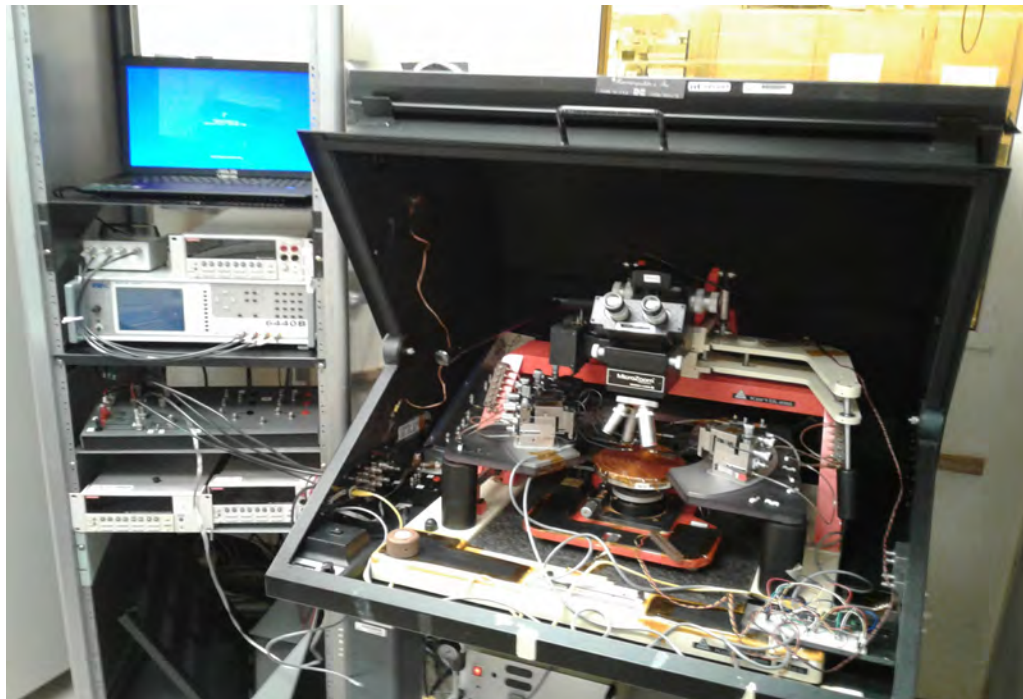
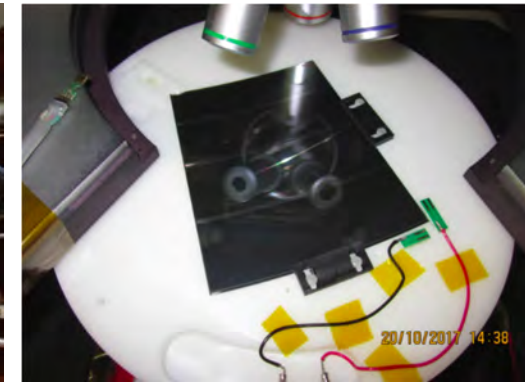
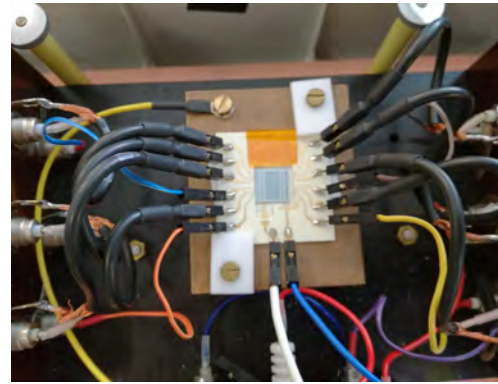
70MeV protons
 CYRIC
 Tohoku University,
 Japan

Test Setups

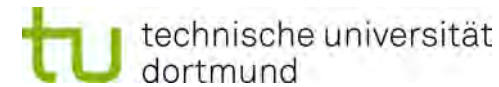
- Tests conducted in probestation or with sensor wirebonded into custom jigs
- Clean environment, dry storage
- Irradiated devices tested cold (in freezer or with a cooled chuck)

Unirradiated Devices +20°C to +30°C

Irradiated Devices -20°C to -30°C



R0 Prototype Test Institutes



Jožef Stefan Institute



筑波大学
University of Tsukuba



UNIVERSITY OF
CAMBRIDGE



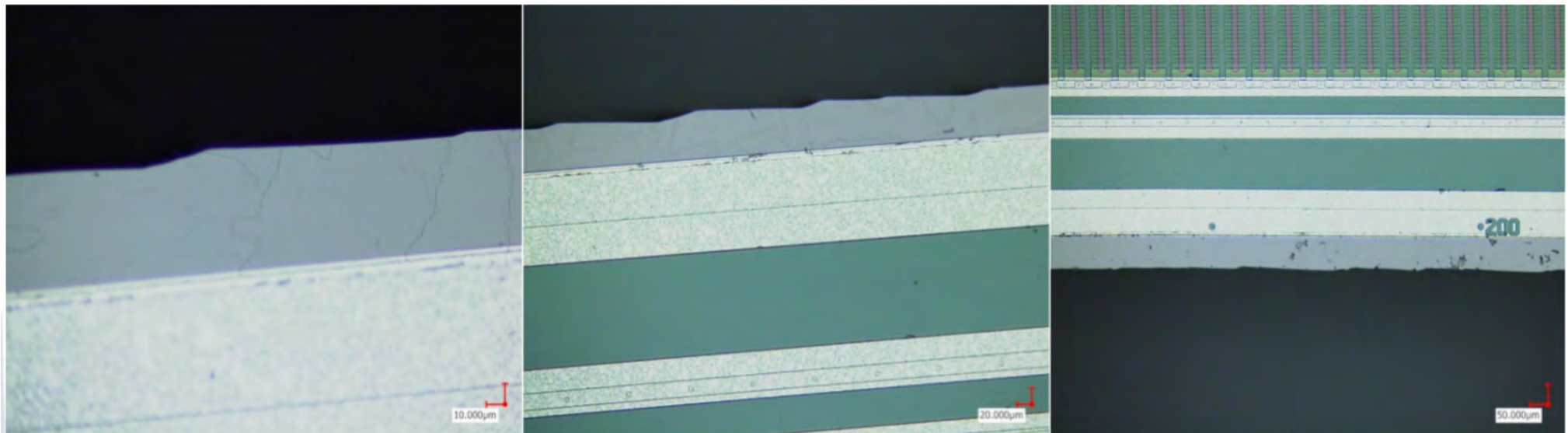
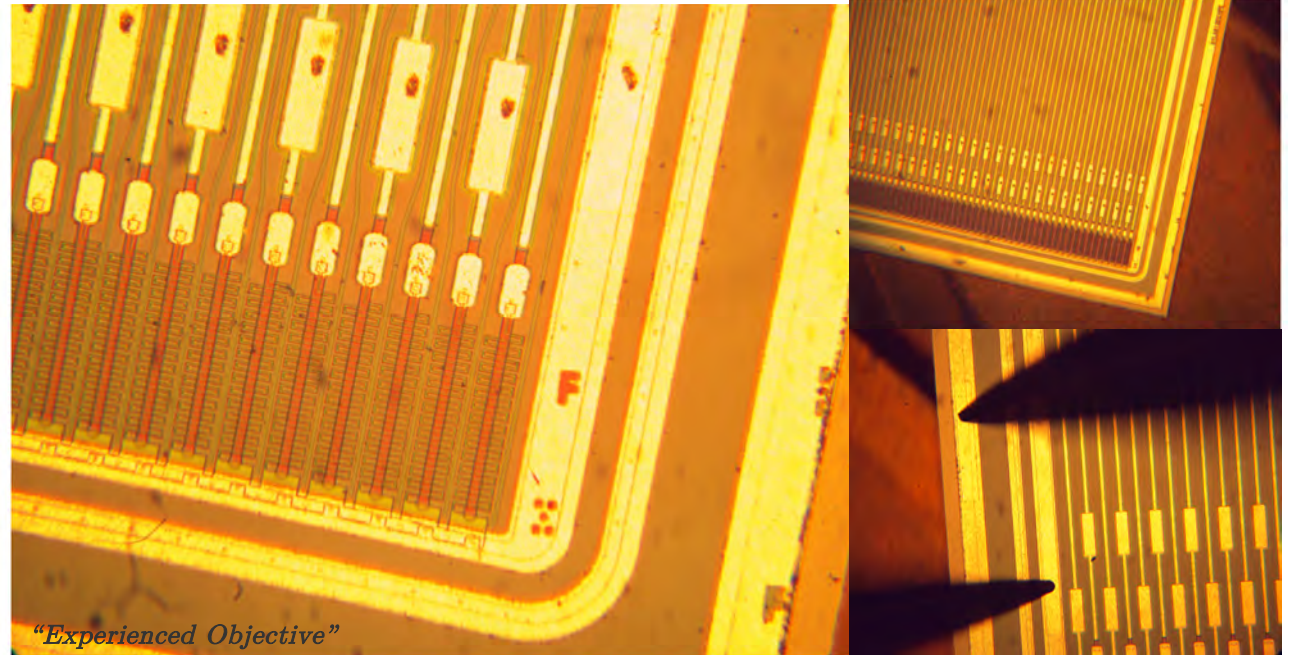
UNIVERSITY OF
TORONTO

Visual Inspection

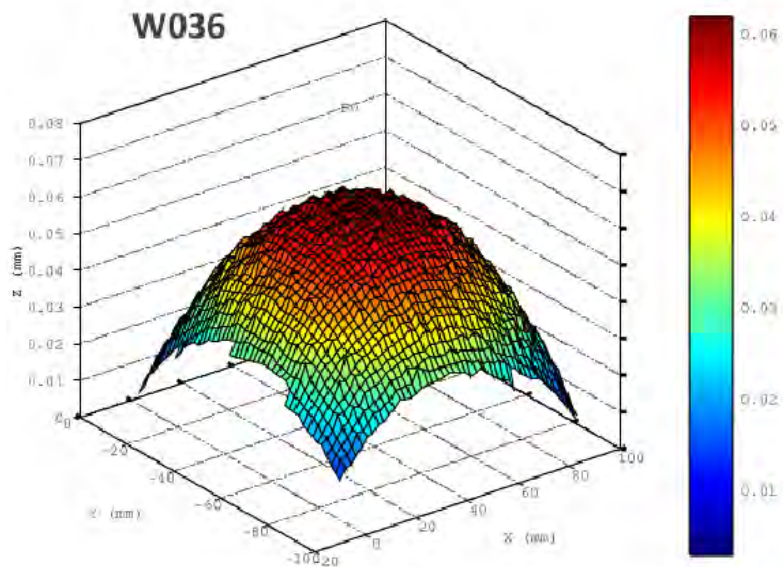
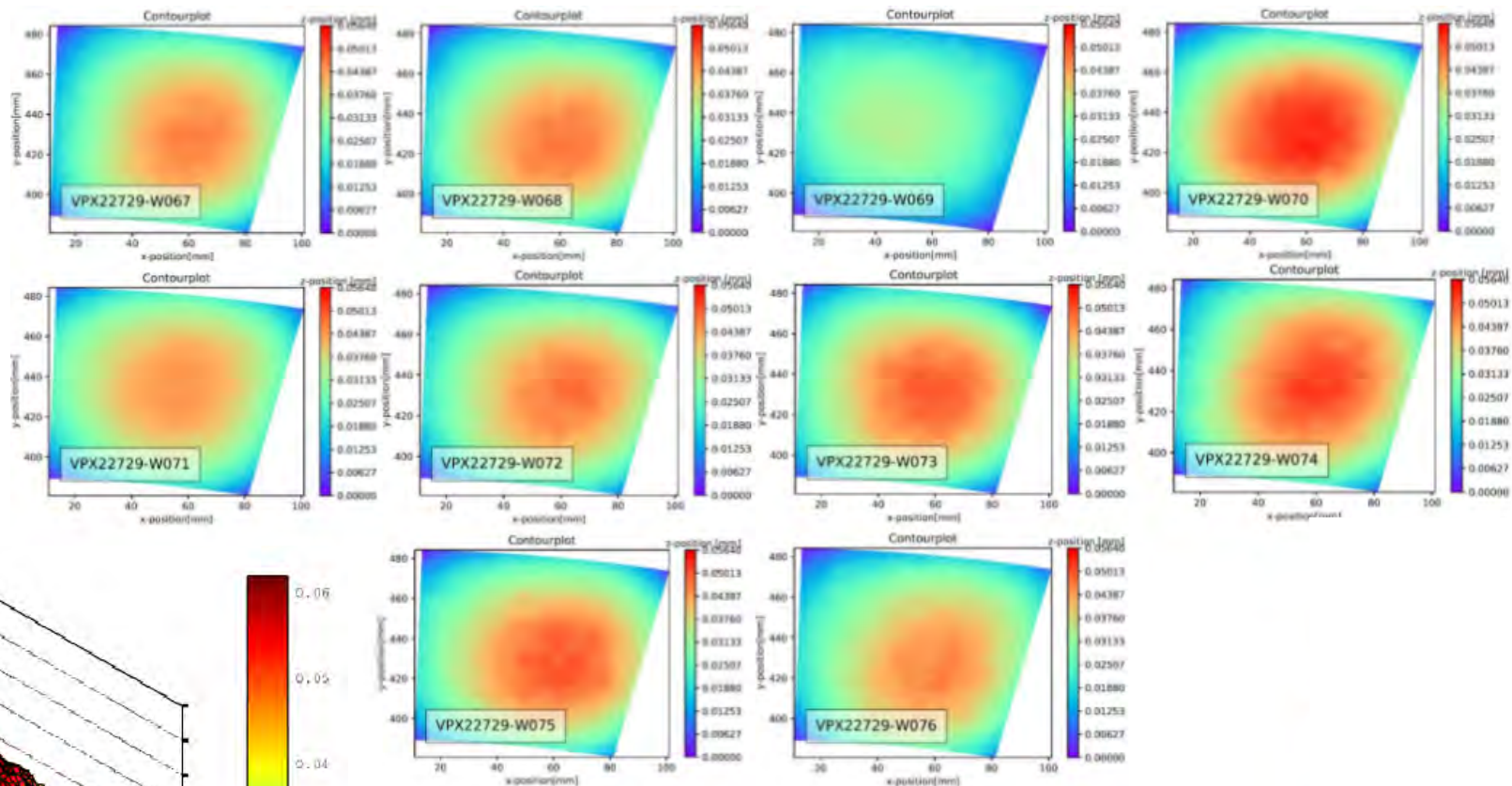
- Sensors in good condition
- Observed $\sim 10 \mu\text{m}$ meander on annular edge flats correlated with crystal orientation



Specification: Devoid of chips or cracks extending $50 \mu\text{m}$ inward



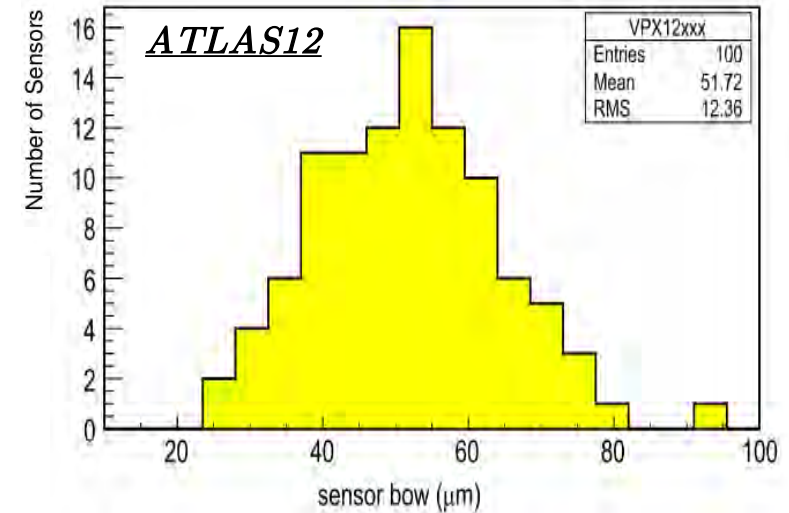
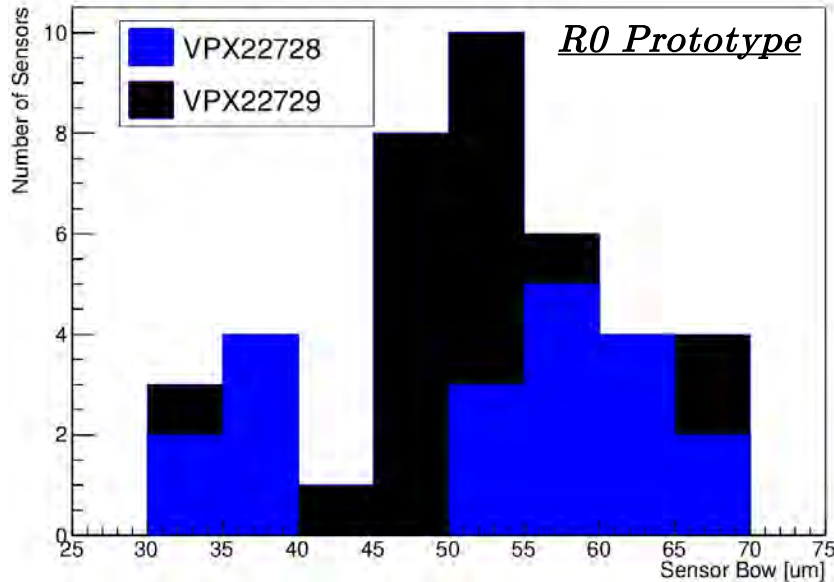
Metrology; Sensor Bow



- Considerations for stresses in assembled components restricts the sensor bow
- Sensors had typical dome-like bow profiles well within specification

Specification: < 200μm

Metrology; Sensor Bow



	<u>Sensor Bow (μm) *</u>	<u>Number of Sensors (Batches) in Sample</u>
<i>ATLAS12</i>	51.72 ± 12.36	100 (4)
<i>R0 Prototype</i>	51.18 ± 9.30	40 (2)

- High consistency across all 40 samples measured
- Well within specification
- Thickness also within specification

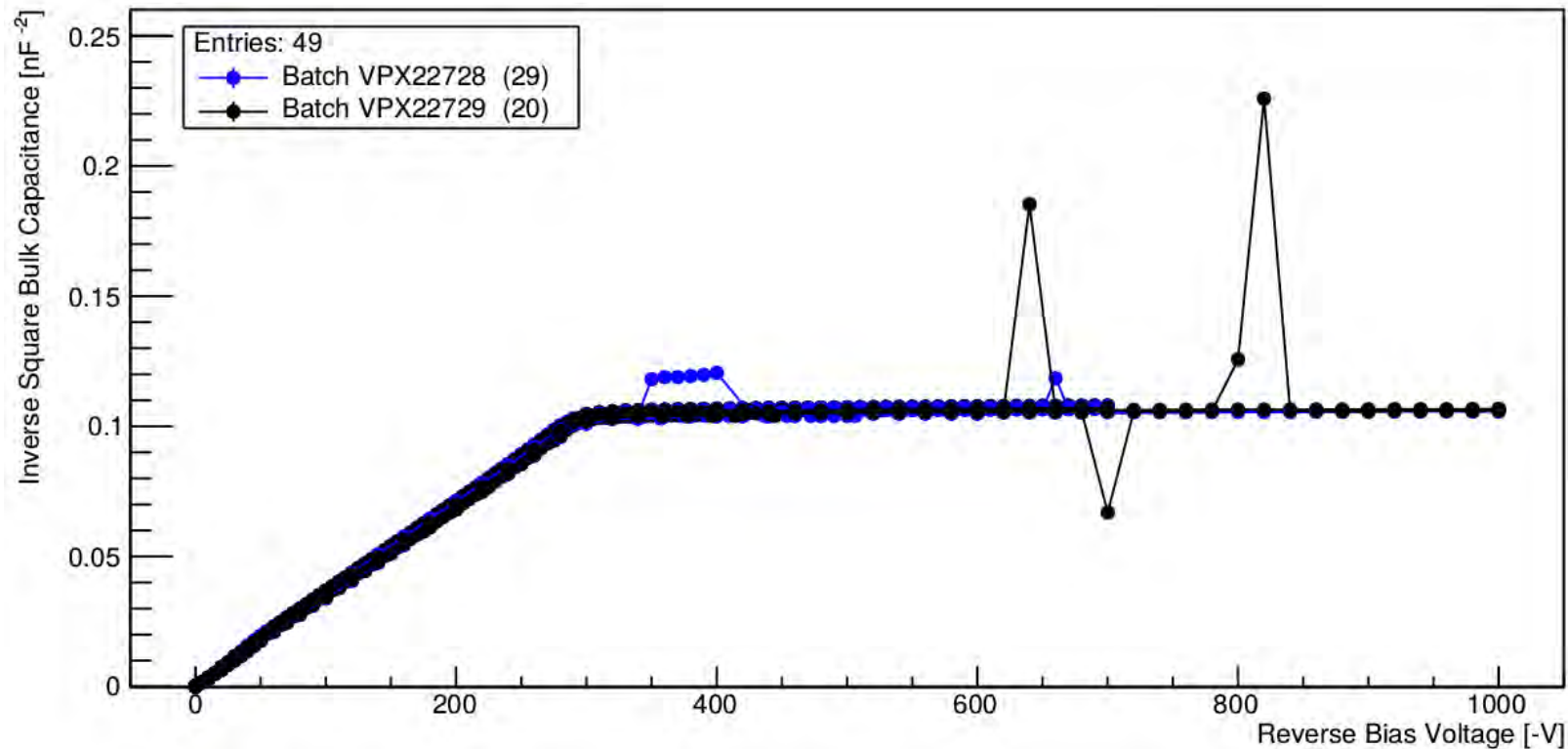
Specification: $< 200\mu\text{m}$

*RMSE against a Gaussian
(Default in following tables)

Thickness: $\sim 320\text{-}325 \mu\text{m}$
Specification: $310 \pm 25 \mu\text{m}$

Depletion Capacitance

- Low full depletion voltage (high resistivity) is especially desired due to the high fluence expectations
- High active depth to full thickness ratio is desired to maximize charge collection

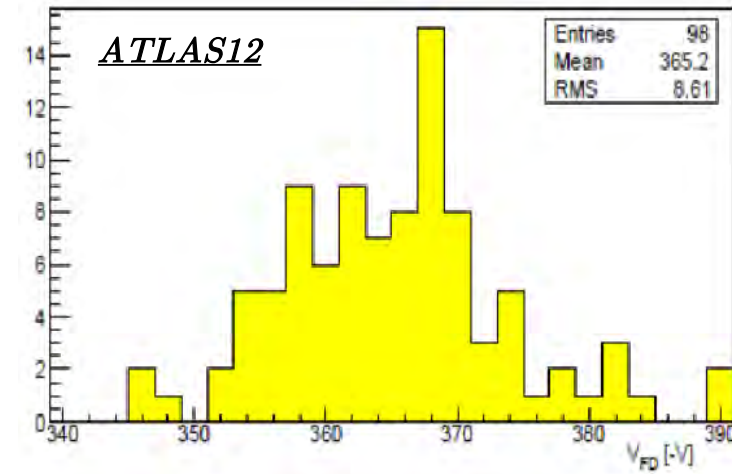
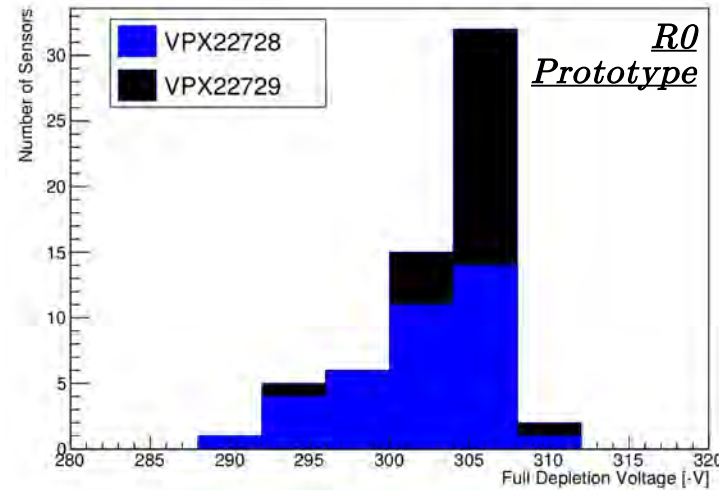


- Excellent consistency in full depletion voltage
- High active depth proportion inferred from active area and depleted capacitance

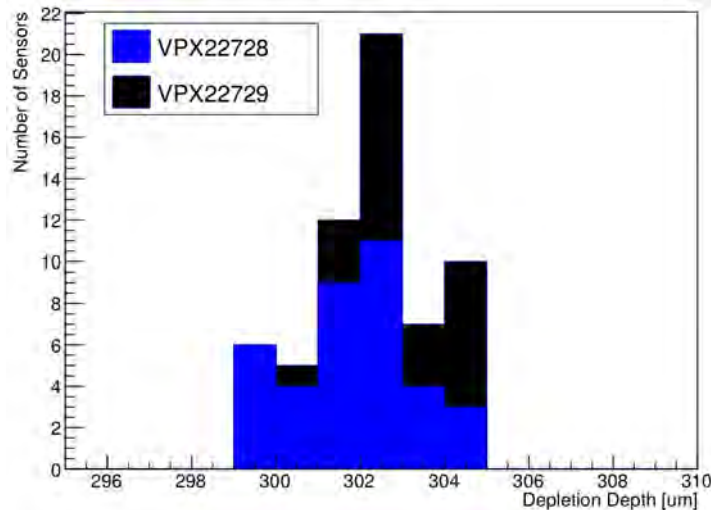
Depletion Capacitance

- High consistency in full depletion voltage
- **93%** of full thickness active depths ($302.3 \pm 1.4 \mu\text{m}$)
- Resistivity meets specification

Full Depletion Voltage



Active Depletion Depth



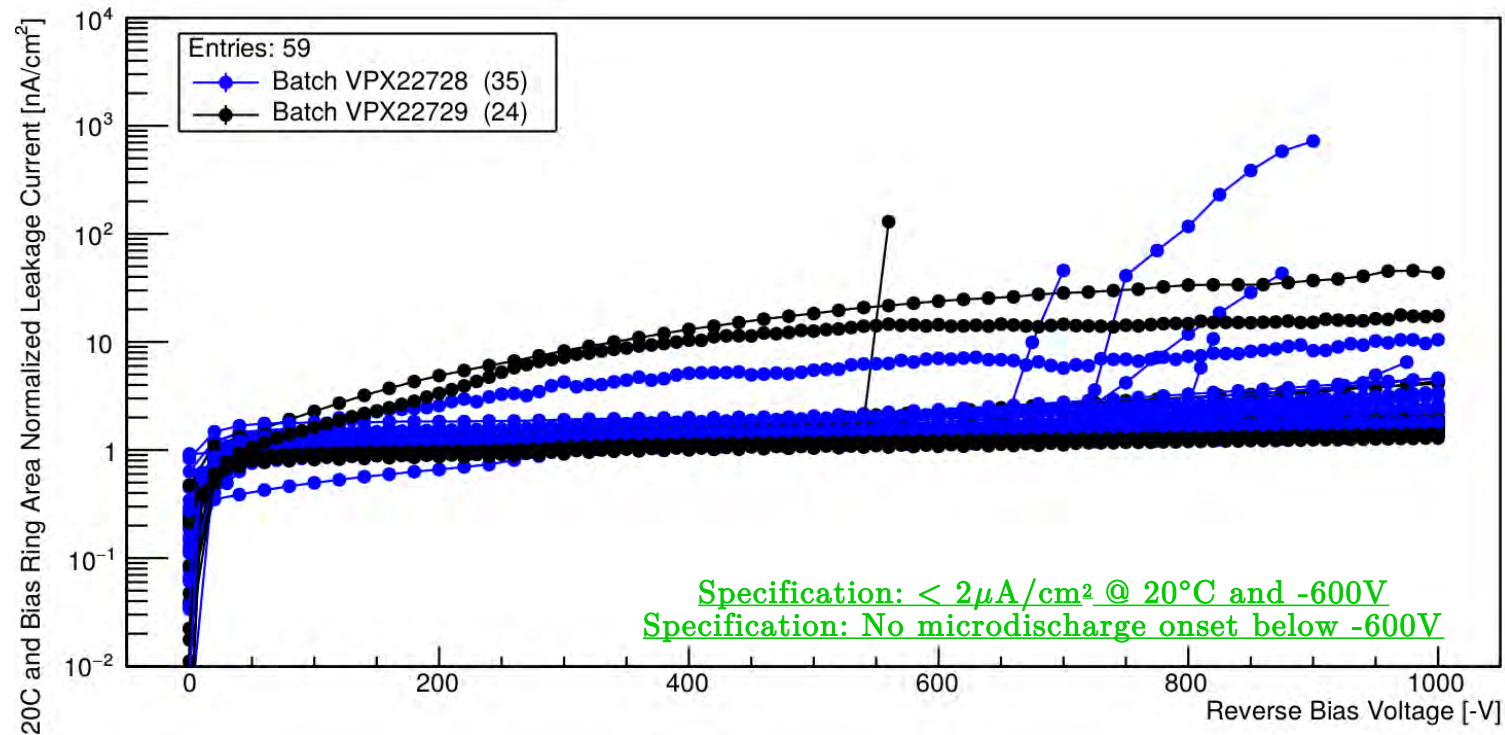
	Full Depletion Voltage [-V]	Resistivity ($k\Omega \text{ cm}$)	Number of Sensors (Batches) in Sample
<i>ATLAS12</i>	365.2 ± 8.61	~ 2.5	98 (4)
<i>R0 Prototype</i>	303.04 ± 4.17	3.24	58 (2)

Calculated resistivity: $3.24 \pm 0.03 k\Omega \text{ cm}$

Specification: $\geq 3 k\Omega \text{ cm}$

Leakage Current – IV Curve

- Sensors must have low leakage current to maintain a feasible power budget at end-of-lifetime
- For reliability sensors must be stable up to the voltage of -600V

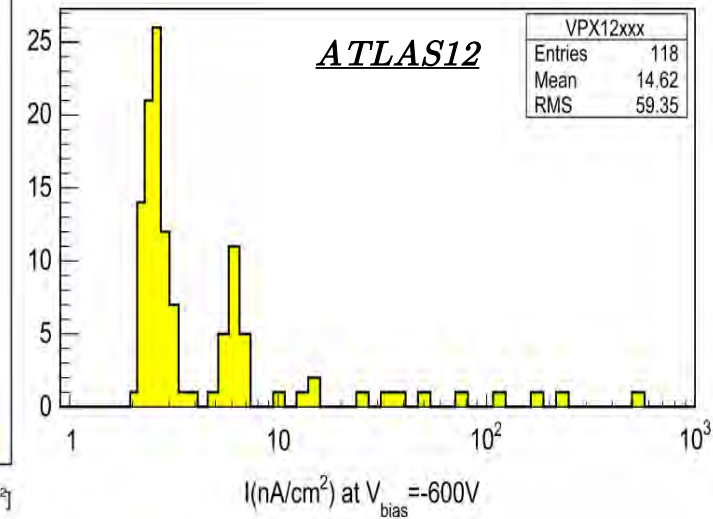
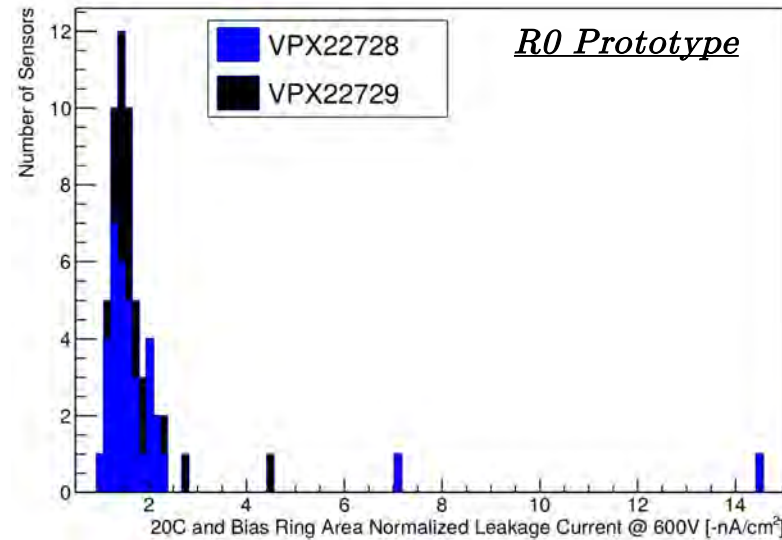


- Orders of magnitude sufficient leakage current obtained
- Levels of instability are very reasonable

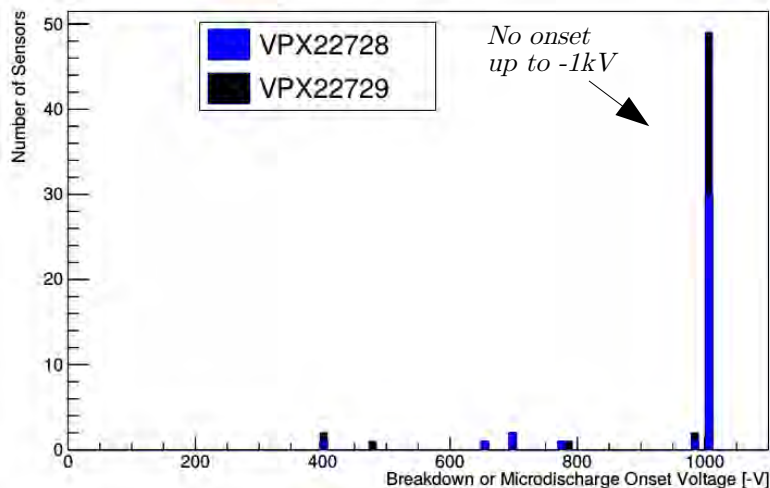
Leakage Current – IV Curve

- Vast majority of sensors show very low leakage current [$O(1\text{nA}/\text{cm}^2)$]
- Orders of magnitude within specification
- Lower level of leakage instability than the conventional sensor shape (ATLAS12)
- Instability attributed to passivation

20°C and Bias Ring Area Normalized Leakage Current at -600V



Breakdown or Microdischarge Onset Voltage



	<i>20°C Leakage Current at -600V [-nA/cm²]</i>	<i>Percentage of Sensors with Increased Leakage below -600V (-1kV)</i>	<i>Number of Sensors (Batches) in Sample</i>
<i>ATLAS12</i>	14.62 ± 59.35	14 (28)	118 (4)
<i>R0 Prototype</i>	1.95 ± 1.87	7 (15)	59 (2)

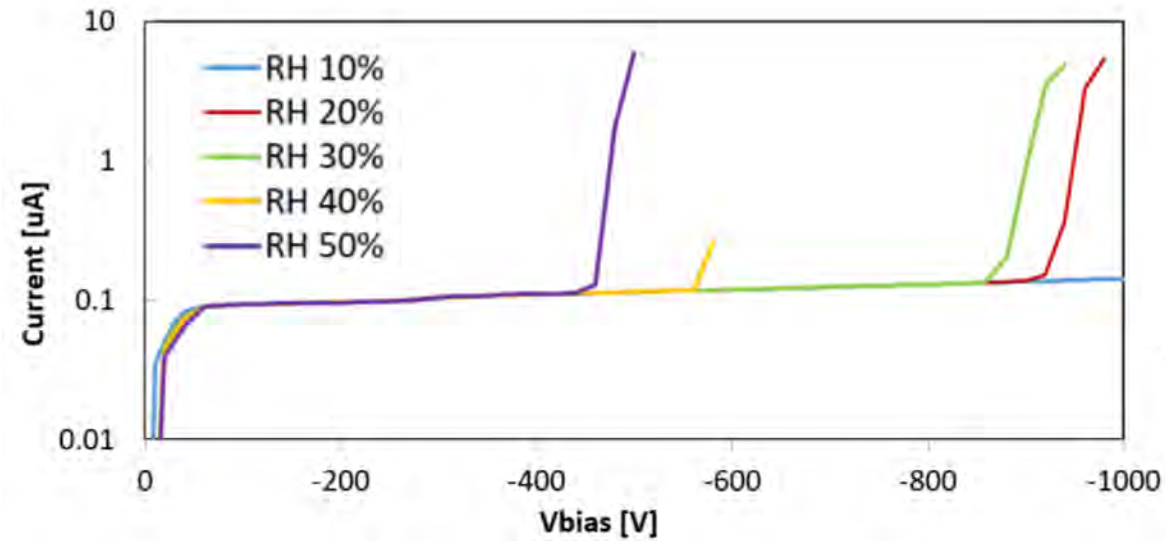
Specification: $< 2\mu\text{A}/\text{cm}^2$ @ 20°C and -600V
Specification: No microdischarge onset below -600V

Microdischarge Humidity Dependence

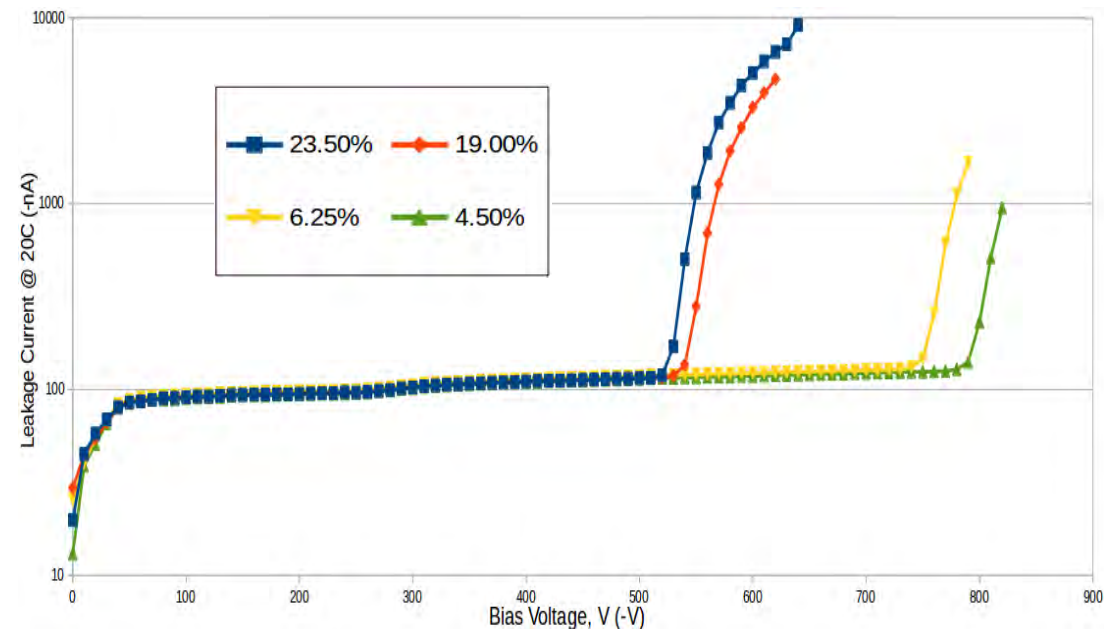
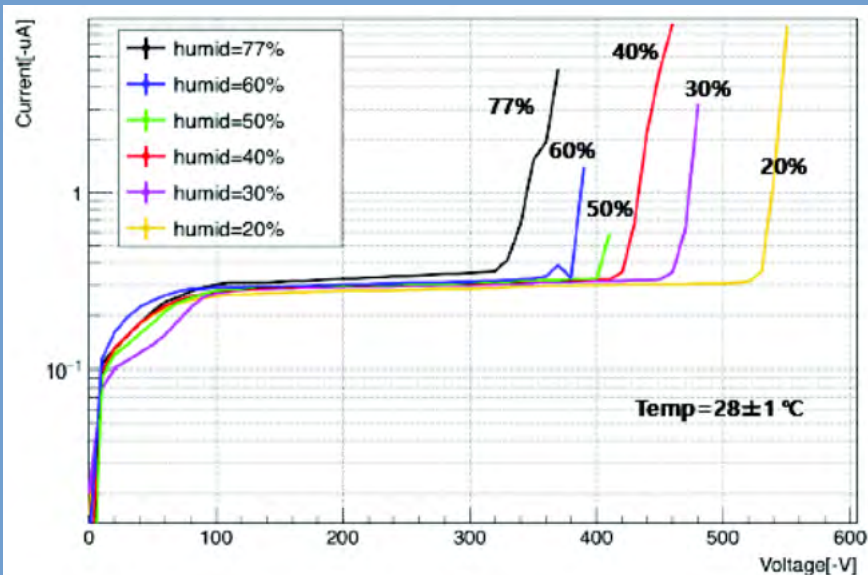
- Sensors with early microdischarge onset show a humidity dependency in the onset voltage
→ Lower humidity, higher microdischarge onset voltages
- Similar observations for previous generations

Percentage of R0 sensors with leakage instability below -600V (-1kV): 7 (15)

Specification: No microdischarge onset below -600V

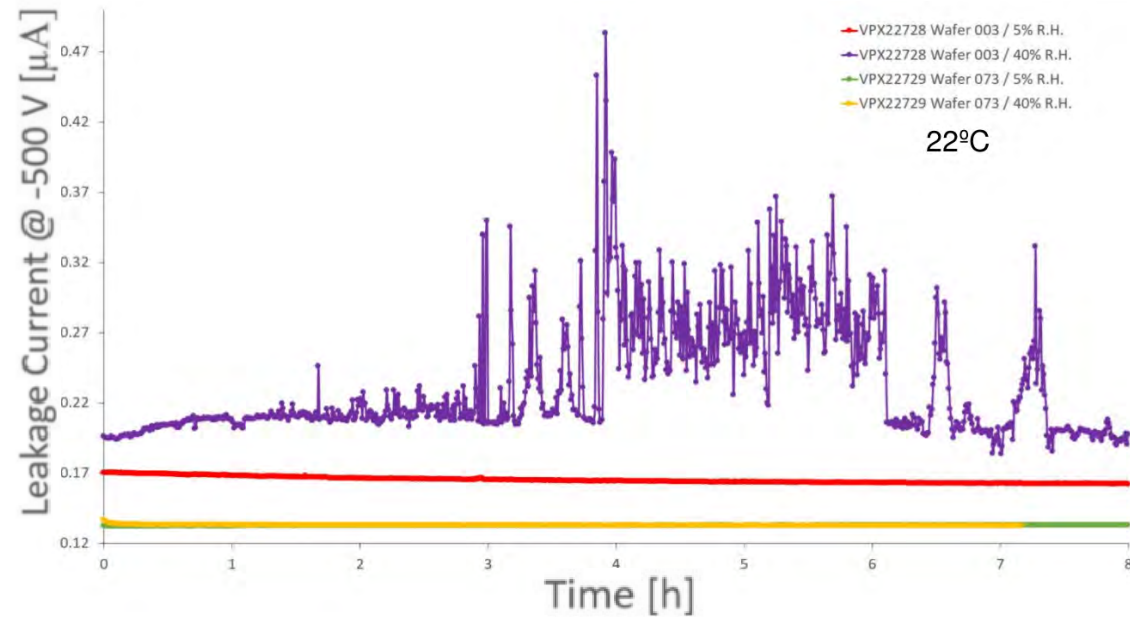


ATLAS12

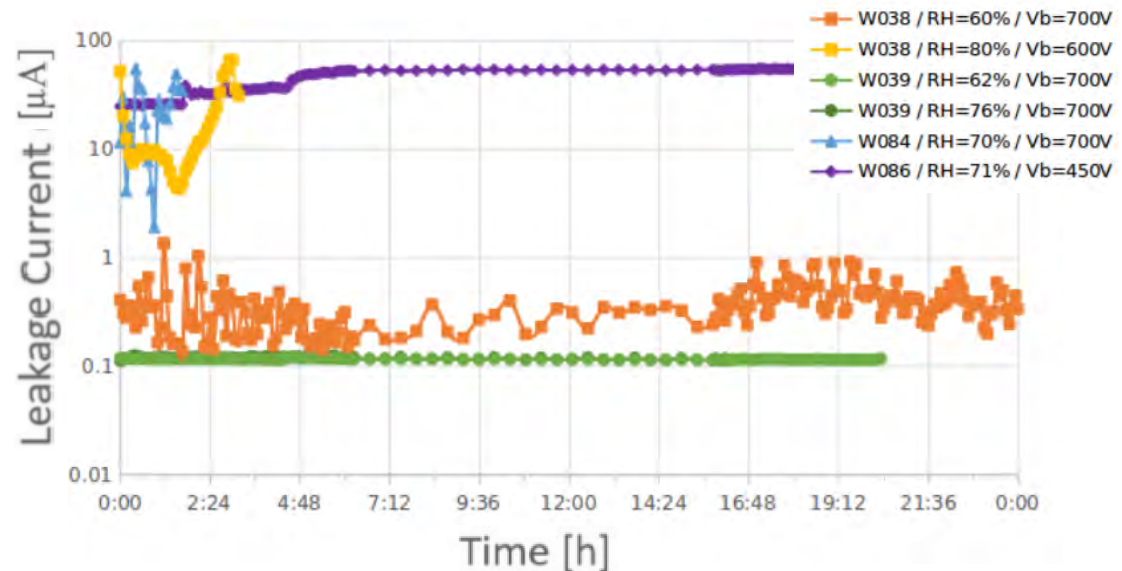
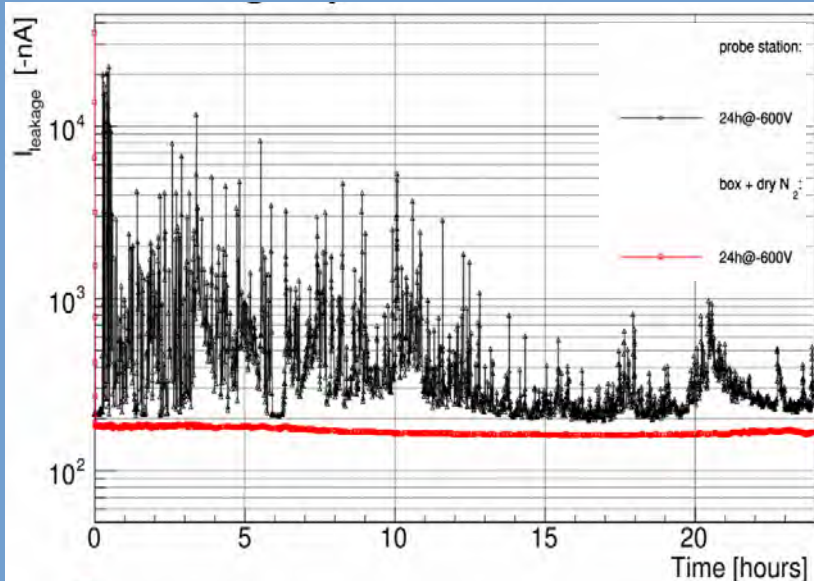


Long Term IV Stability

- Many sensors perform very well; fluctuations $O(10\text{nA})$ over several days even at elevated humidity
- Some sensors show sensitivity to higher humidities
 - Especially prevalent in the sensors with early breakdown/microdischarge
 - Some are recoverable after dry storage and sensor 'training' exercise
- Observations of instability correlated with changes in the rate of humidity change

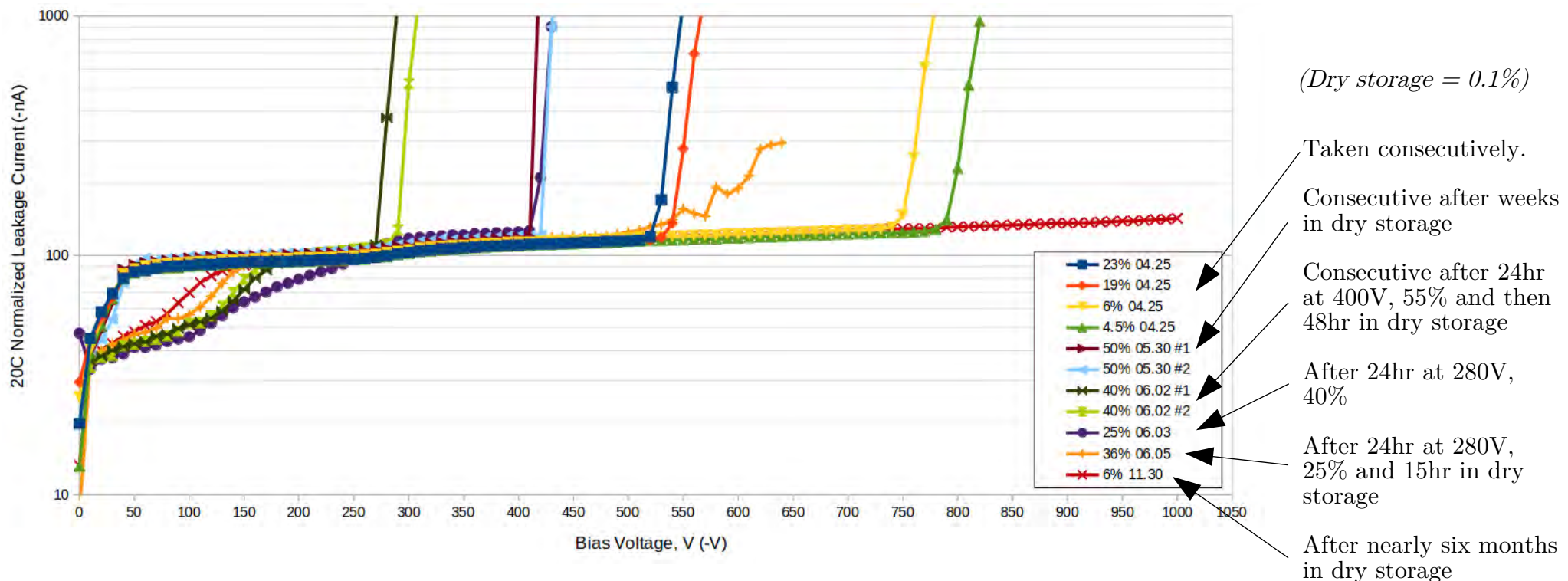


ATLAS12



Instability Conclusions

- Sensors showing early onset leakage instability exhibit much higher humidity sensitivity than their well-behaved counterparts
- Lowered microdischarge breakdown effect is recoverable after long-term dry storage
- Similar observations for conventional sensor shape of comparable size and complexity; not an issue with the stereo annulus geometry
- Evidence for mobile ions and interface trap activation (passivation issues)

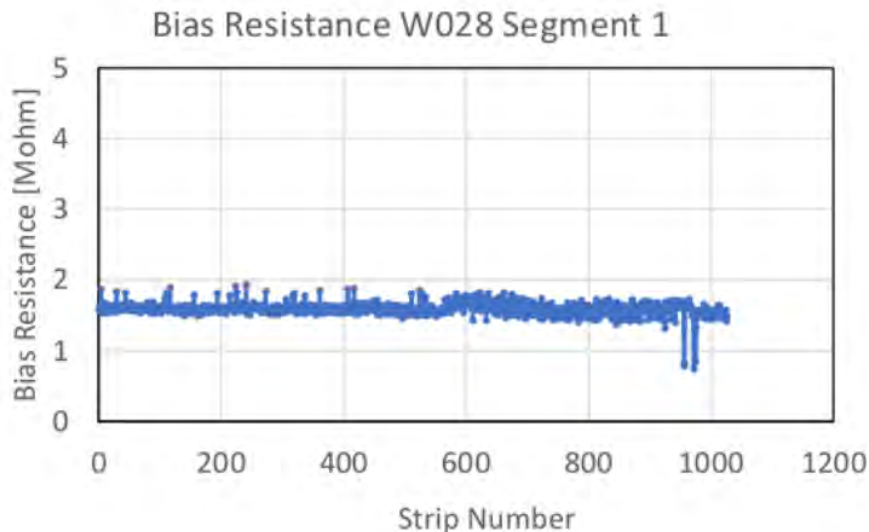
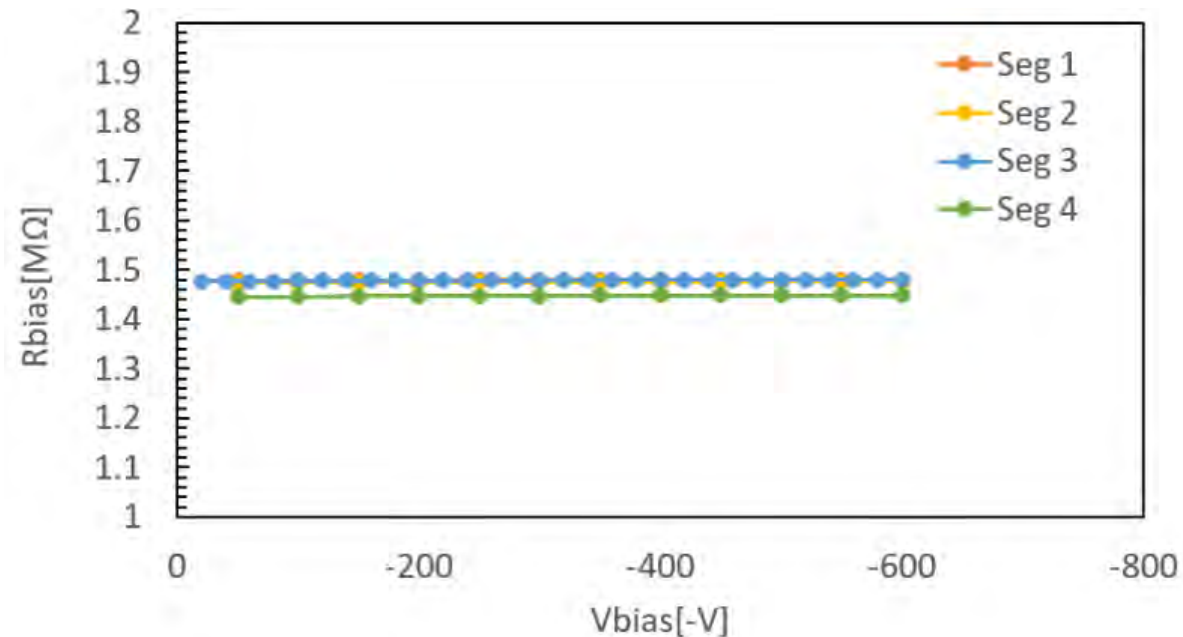


Strip Isolation: Bias and Interstrip Resistances

Full Size Sensors

Bias Resistance

- Must be large to isolate strips
- Must be large and consistent across the sensor to distribute bias effectively
- High consistency, safely within specification observed in all samples measured



Full Segment Average: $1.59 \pm 0.01 \text{ M}\Omega^*$

*No. of Strips Measured: 1026

Other Measurements Range: $1.47\text{-}1.52 \text{ M}\Omega^{**}$

**No. of Strips (Sensors) Measured: 10 (3)

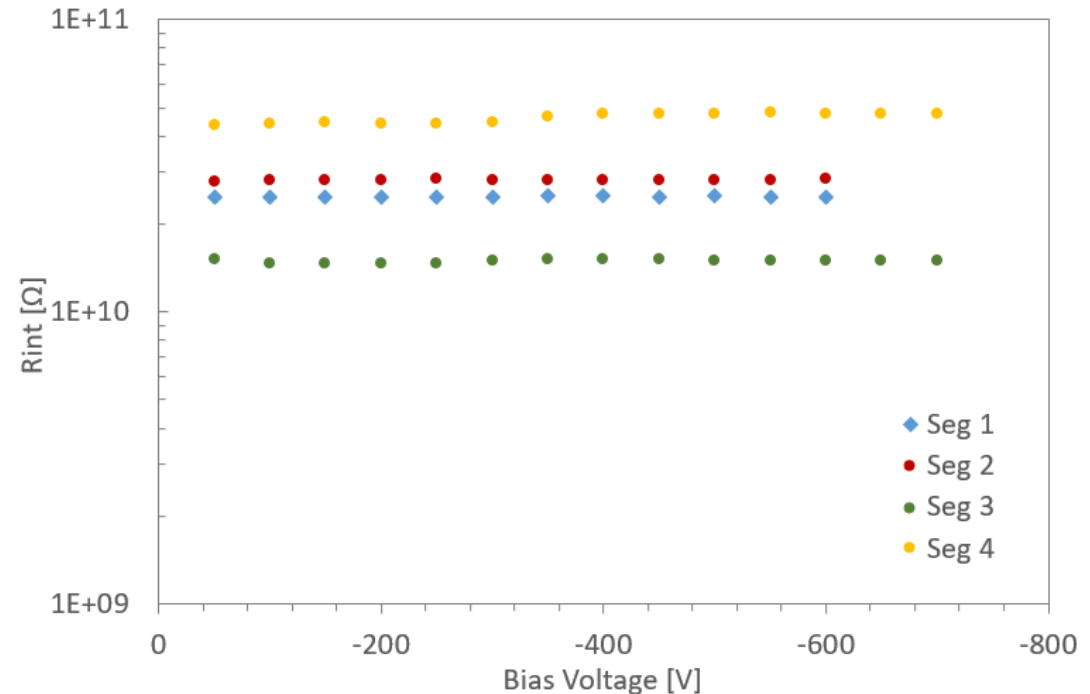
Specification: $1.5 \pm 0.5 \text{ M}\Omega$

Strip Isolation: Bias and Interstrip Resistances

Full Size Sensors

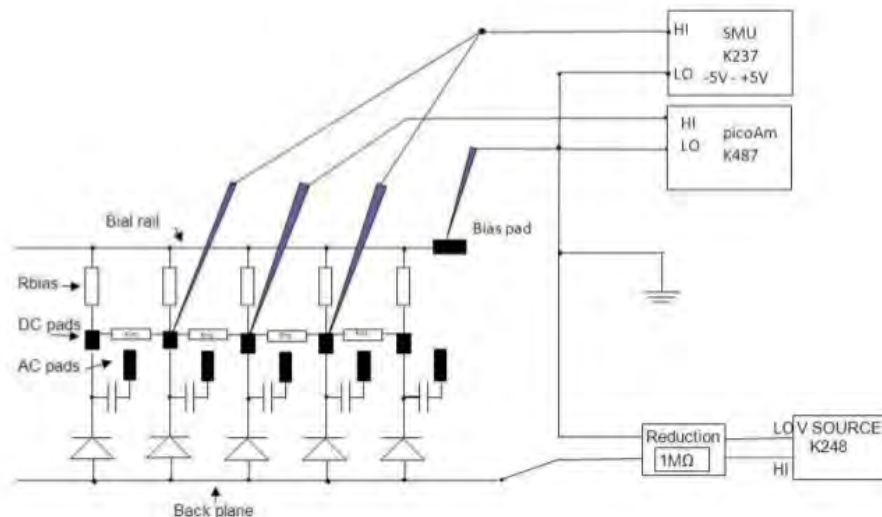
Interstrip Resistance

- Must be much greater than the bias resistance to maintain channel isolation
- In the ATLAS ITk design the inversion channel inherent in the n⁺-in-p sensor is overcome with a narrow common p-stop
 - Orders of magnitude within specification



Measurements: **All above $10G\Omega$ ***
 *No. of Strips Measured: 26

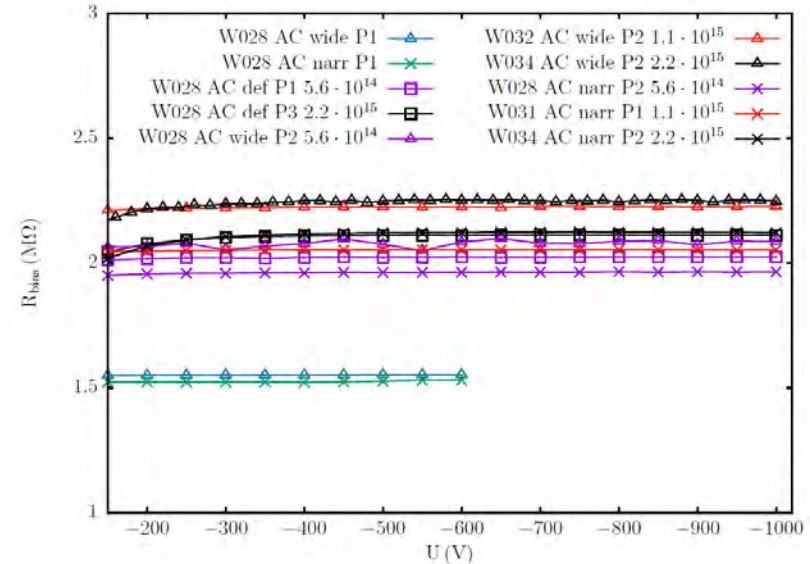
Specification: $> 10 \times R_{bias}$ at 300V ($150M\Omega$)



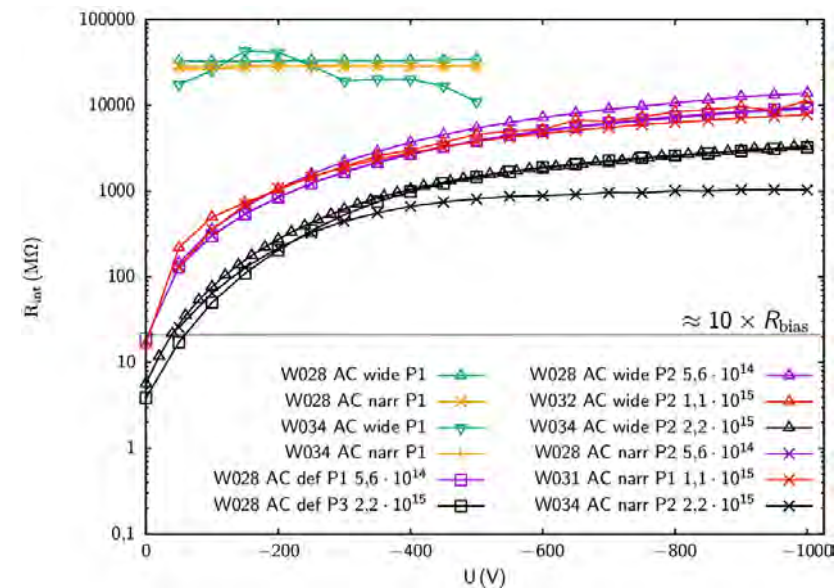
Strip Isolation after Proton Irradiation

Mini Sensors

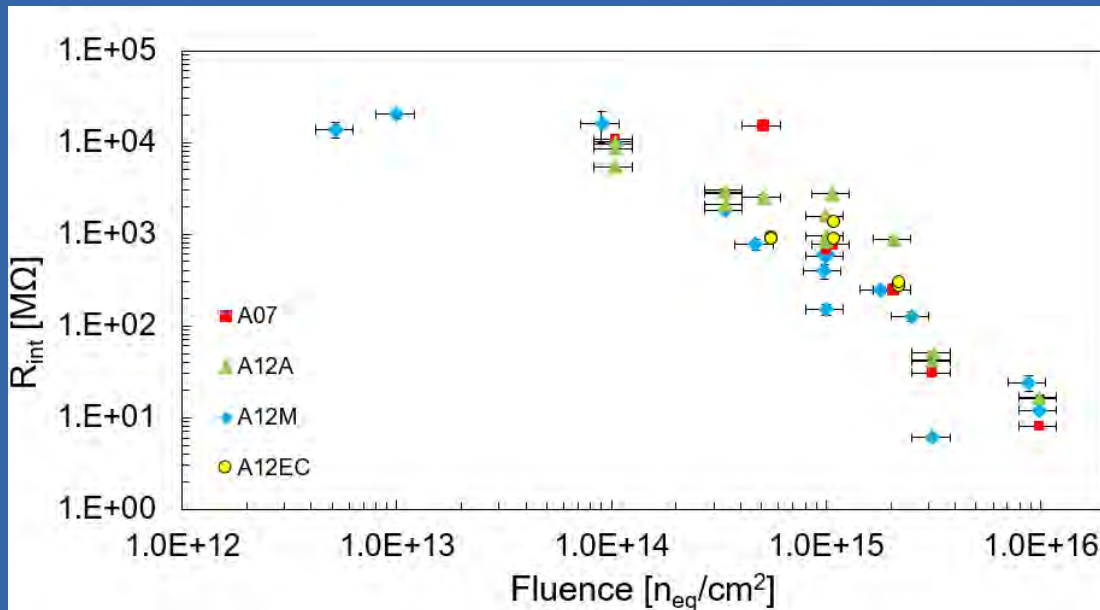
Bias Resistance



Interstrip Resistance



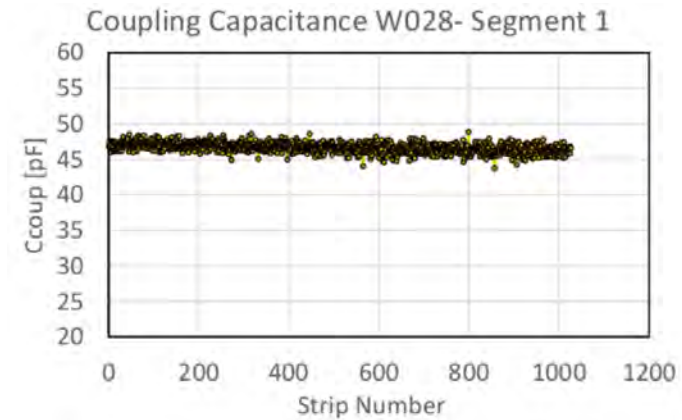
Comparison of Interstrip Resistance vs. Fluence Across the Generations



- Strip isolation requirements met at 50V for a fluence of $2.2 \times 10^{15} \text{ n}_{\text{eqv}}/\text{cm}^2$
- Bias Resistance shows very small, positive fluence and negative temperature dependencies
- Interstrip Resistance decreases with fluence and increases smoothly with bias after irradiation
- Measurements very comparable to previous generations

Coupling Capacitance

- Must be large to maximize signal and its integrity
- Very consistent and within specification
- Follows expected trends in strip length
- No radiation induced change
- Dielectric breakdown voltage is twice the specified value of 100V (~170V for negative voltage on the implants, ~210V for positive)

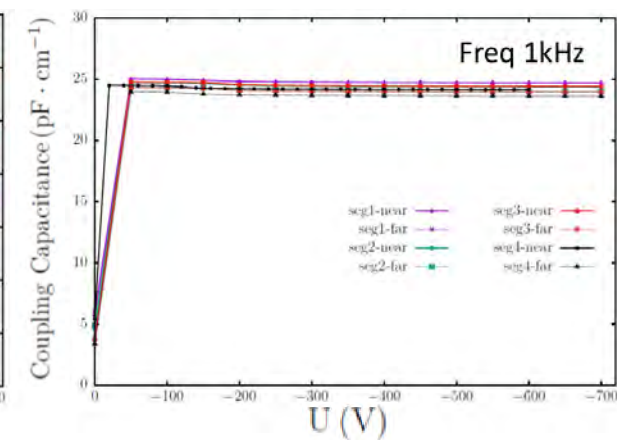
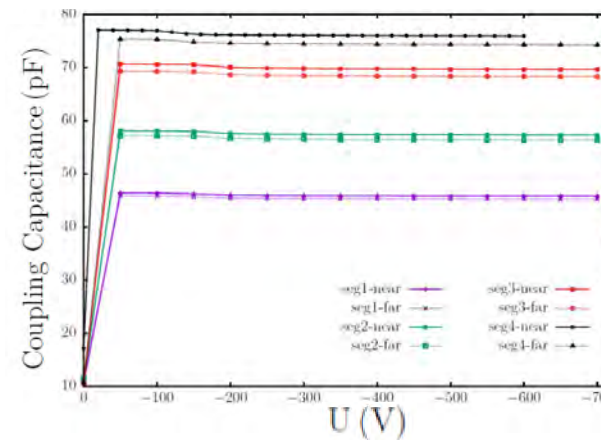
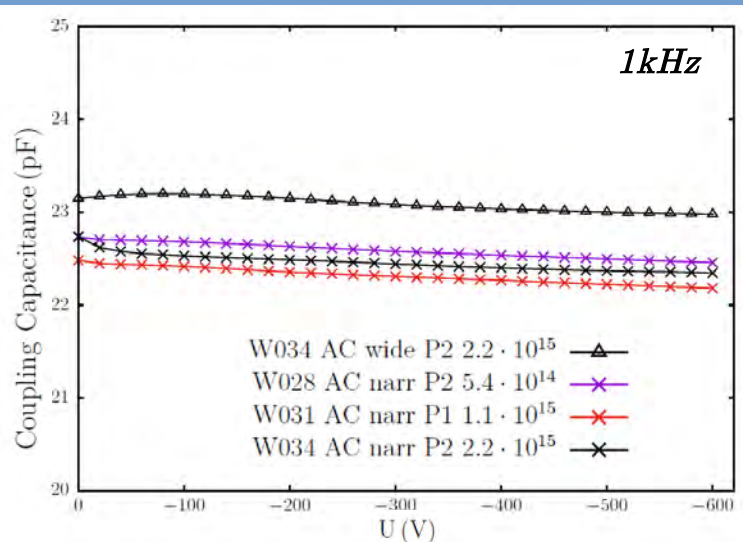


Full Segment Average: 25.21 ± 0.02 pF/cm*
*No. of Strips Measured: 1026

Other Measurements Range: $24.89-28.37$ pF/cm**
**No. of Strips Measured: 35

Specification: > 20 pF/cm

p^+ IRRADIATED MINIS

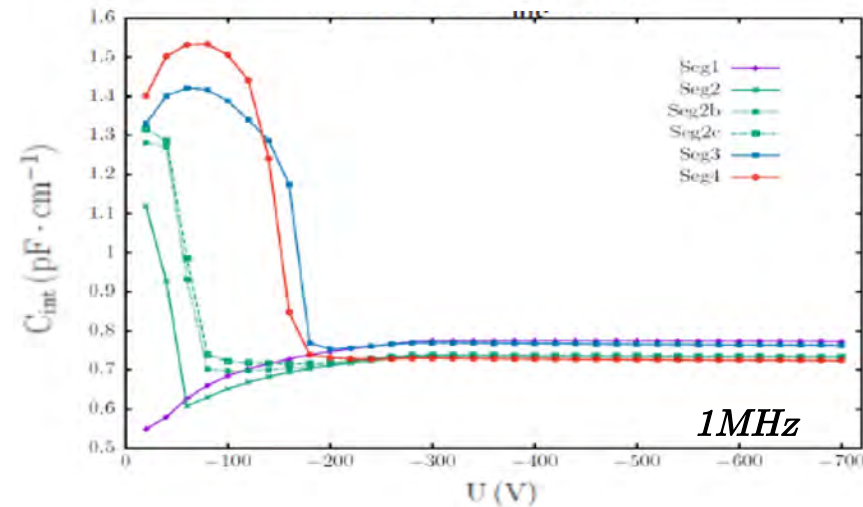
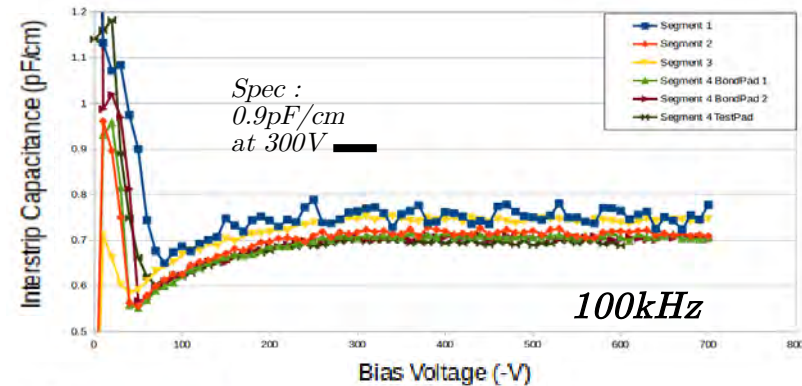
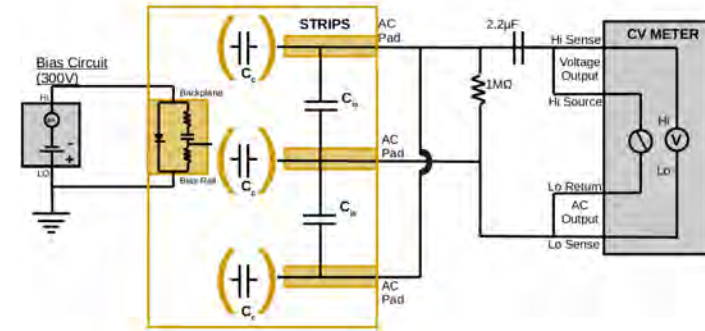


Interstrip Capacitance

- Needs to be small to minimize noise at the front end and needs to be much smaller than coupling capacitance for isolation of channels
- Capacitance follows expected trends in pitch
- Good consistency
- No change with proton irradiation
- All measurements within specification

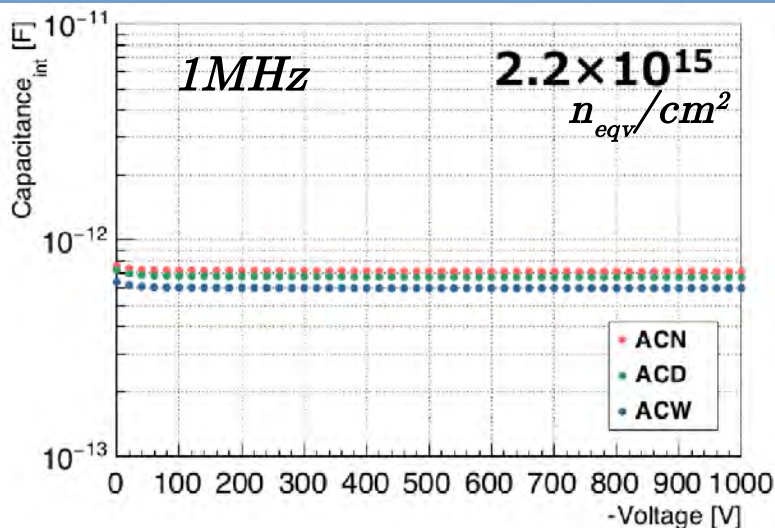
Range: **0.61 – 0.89 pF/cm** (at 700V)*
 *No. of Strips Measured: 15

Specification: < 0.9 pF/cm @ 300V, 100kHz



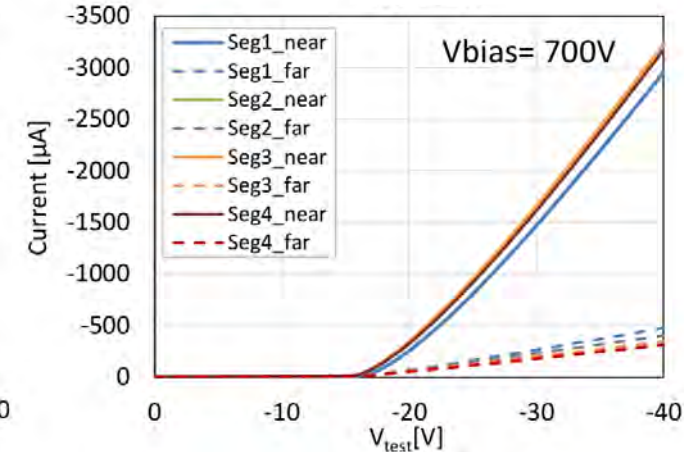
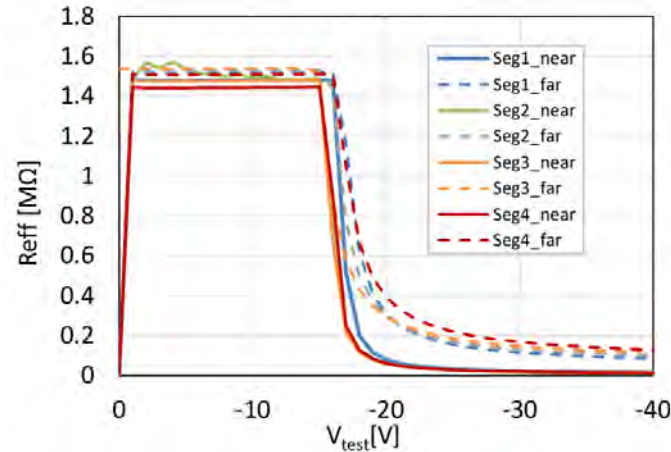
Coupling capacitance range: **24.89–28.37 pF/cm**

p⁺ IRRADIATED MINIS

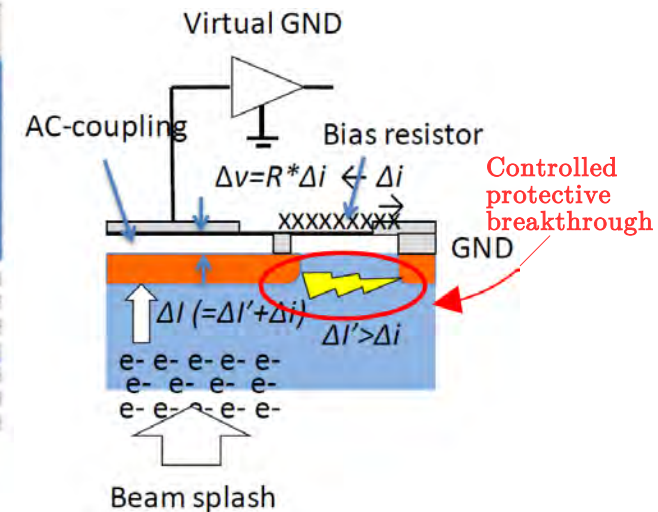
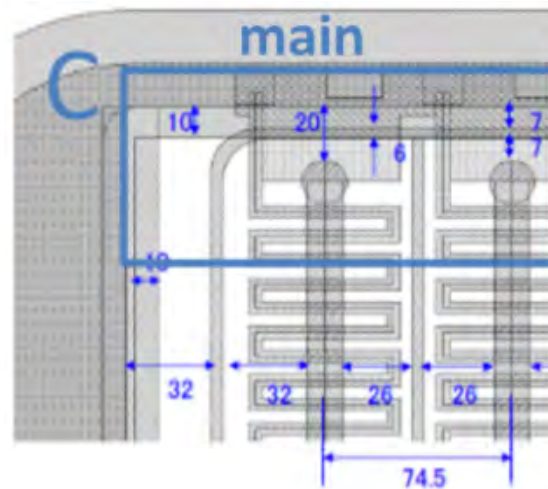
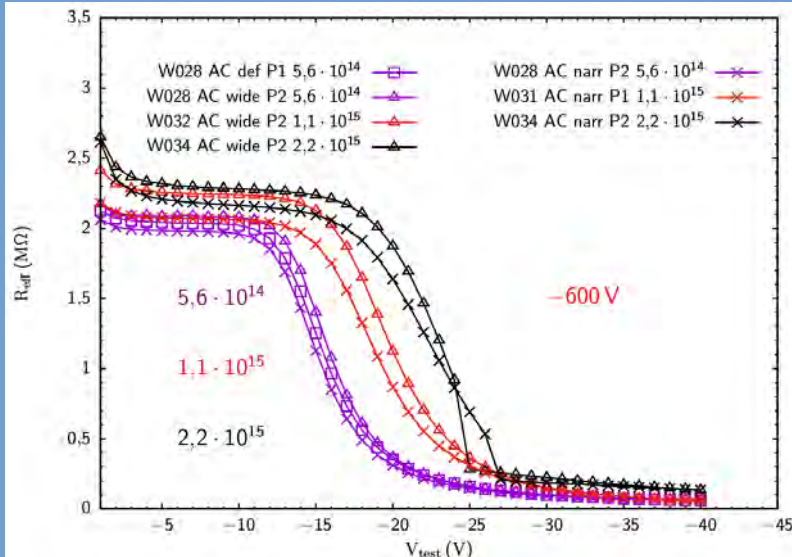


Punch Through Protection (PTP)

- Protects the coupling capacitor in the event of large charge liberation in the bulk
- Desire early onset voltage and high current flow at -100V
- Onset voltage increases with fluence but is only -30V at $2.2 \times 10^{15} \text{ n}_{\text{eqv}}/\text{cm}^2$ (at $V_{\text{bias}} = -600\text{V}$)
- **Suitable PTP performance**



p^+ IRRADIATED MINIS



Y. Unno *et al.*, *Nucl. Instr. Meth. Phys. Res. A*, vol. 765, pp. 80–90, 2014. (ATLAS12 Design)

- Stereo annulus is an optimized geometry for the restricted space of an endcap strip tracker
 - Stereo angle gains in secondary resolution without negative effects
 - Equal length strips and better annular disk coverage
- The first R0 prototype sensors show excellent results
 - Meets specification in all categories
 - High consistency in bulk character
 - Low leakage and good levels of leakage instability
 - Also high consistency in the surface processing
 - All structures performing as expected
- The stereo annulus geometry is considered to have negligible effect on sensor performance from the comparisons of the R0 prototype to the ATLAS12
 - Instability is not isolated to the R0 prototype and is attributed to passivation
 - The passivation issue will be addressed in the next iteration of R0 prototype sensor

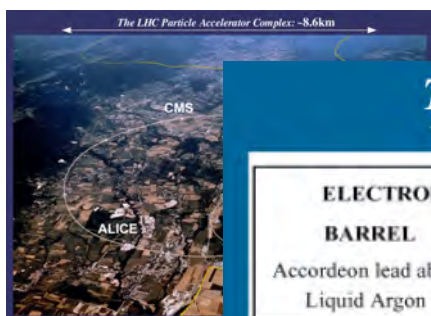
Thank you!



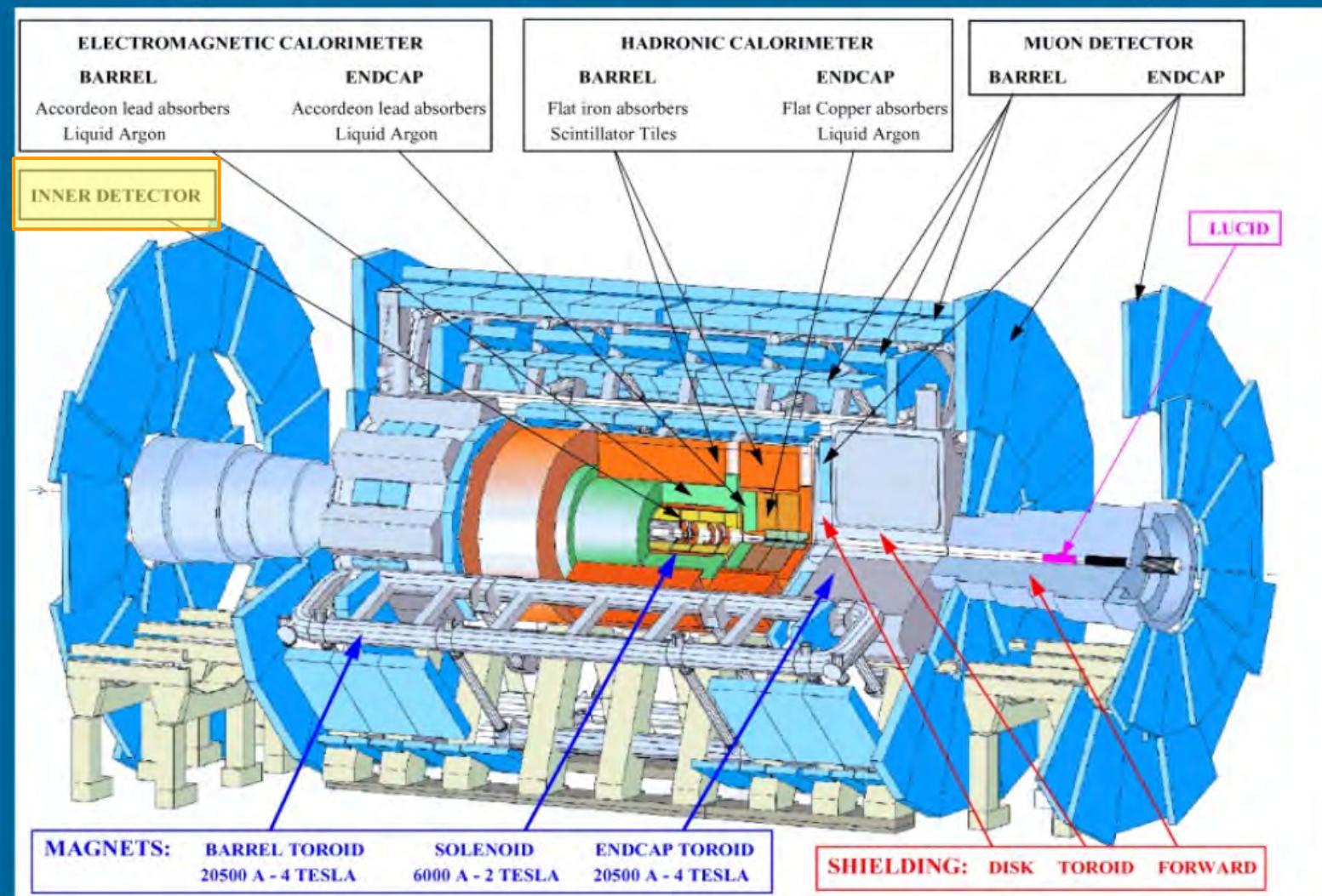
The research was supported and financed in part by Canada Foundation for Innovation, the National Science and Engineering Research Council (NSERC) of Canada under the Research and Technology Instrumentation (RTI) grant 23 SAPEQ-2016-00015; the Ministry of Education, Youth and Sports of the Czech Republic coming from the project 24 LM2015058 - Research infrastructure for experiments at CERN; USA Department of Energy, Grant DE-SC0010107, the Federal Ministry of Education and Research, BMBF, Germany

BACKUP

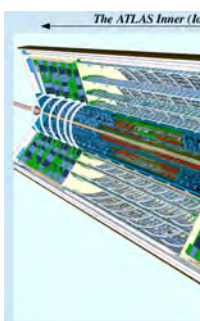
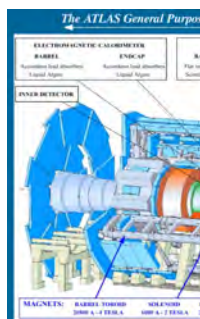
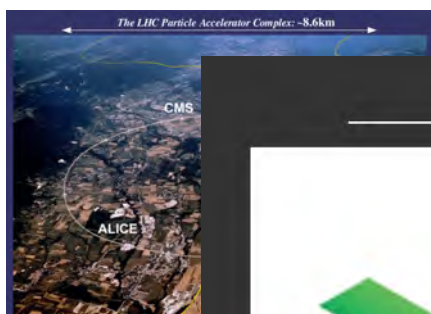
The Itk Strip Detector: Home of the First Stereo Annulus Sensors



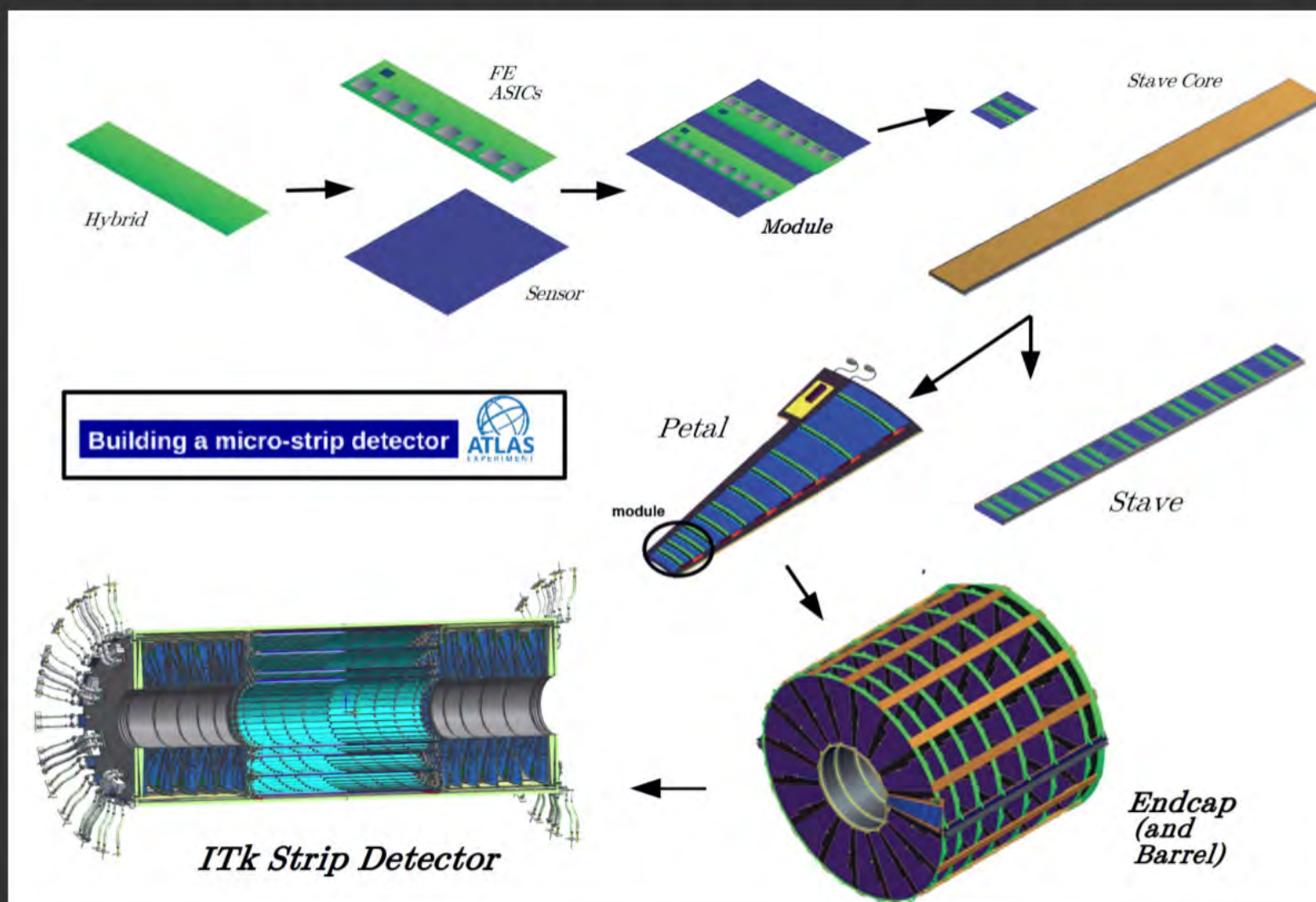
The ATLAS General Purpose Particle Detector: ~45m (x 25m)



The Itk Strip Detector: Home of the First Stereo Annulus Sensors



The ITk (Silicon Micro-)Strip Detector: ~6m (x 70cm)



Approximately 165m² silicon surface detection area.

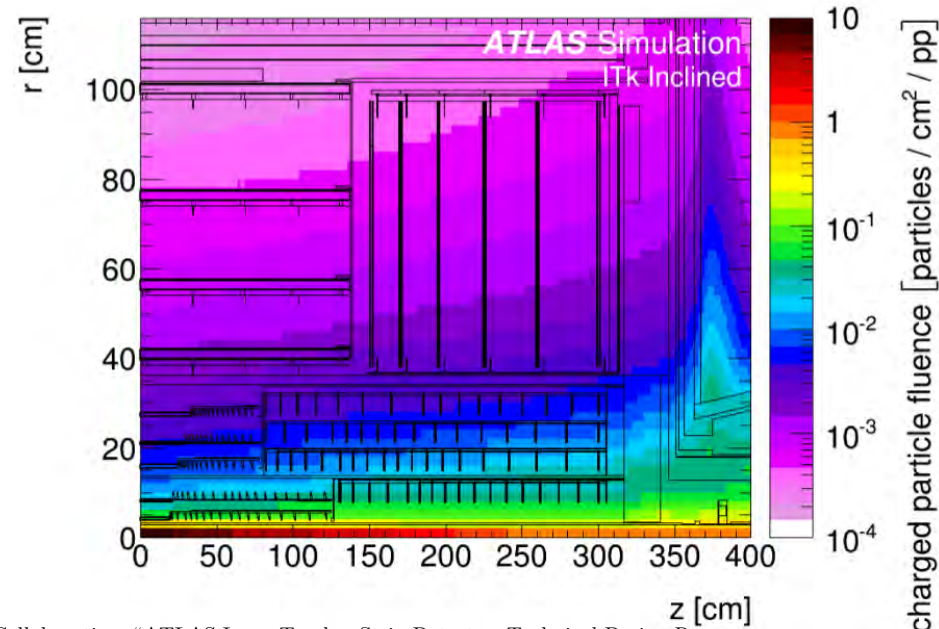
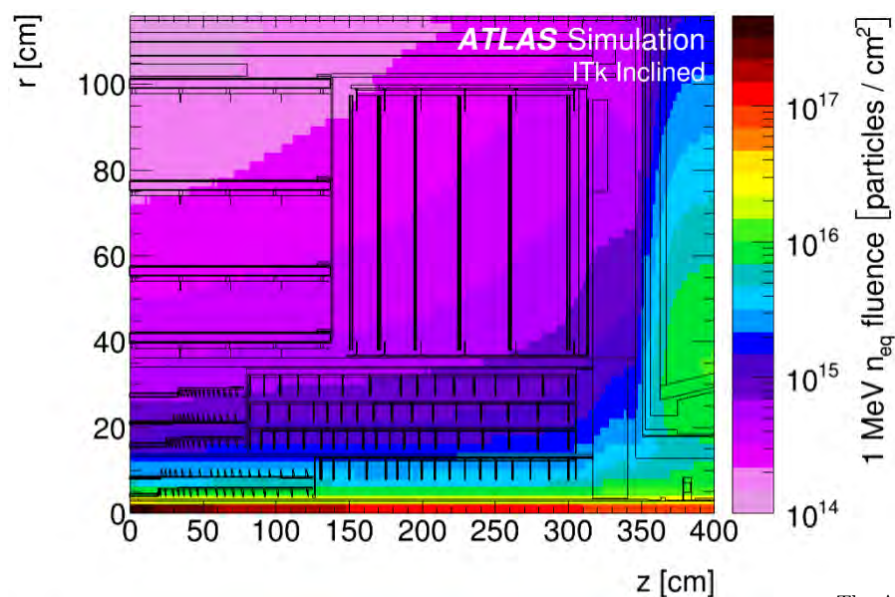
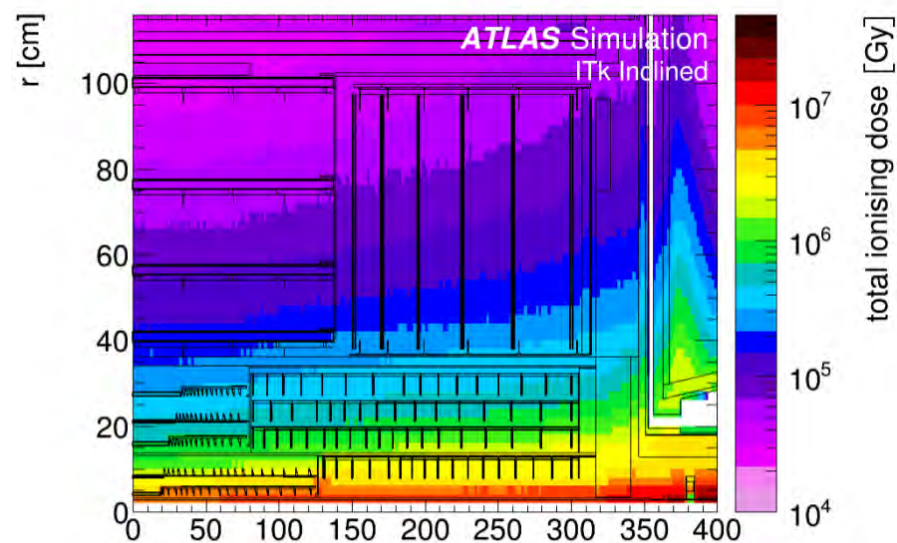
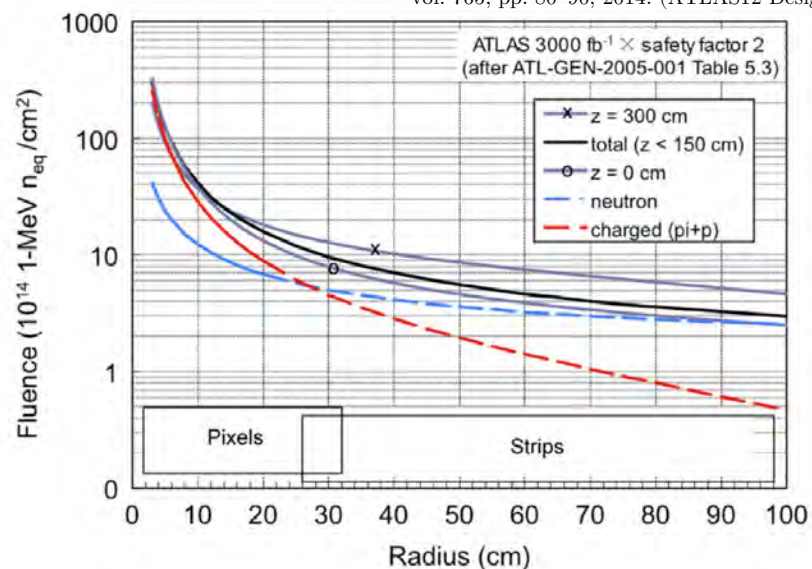
ITk Justifications

Operational Parameter	ID, LHC, and ATLAS Design Limits	HL-LHC Capabilities and Upgraded ATLAS Requirements
Experiment Lifetime	10 years	Current age: ~ 7 years Age at upgrade: 14 years Full duration: 27 years
Peak Instantaneous Luminosity ($\times 10^{34} \text{ cm}^{-2} \text{ s}^{-1}$)	1.0	Nominal: 5.0 Ultimate: 7.5 *with leveling
Pileup (proton collisions per 25 ns bunch crossing)	Design: 23 Operational Max: ~40 (peak), ~24 (avg.)	Nominal: 140 Ultimate: 200 *with leveling
ATLAS Trigger Rate (kHz)	Level-1: 100	Single Mode; Level-0: 1000 Dual Mode; Level-0: 4000 Level-1 (new): 400-600
Integrated Luminosity (fb^{-1})	Pixels: 400 SCT: 700 Inserted Beam Layer: 850	Nominal: 3000 Ultimate: 4000
Maximum High Energy Particle Fluence ($\times 10^{15} \text{ 1 MeV } n_{eq} \text{ cm}^{-2}$)	Pixels: 5.0 SCT: 0.2	ITk Pixel: 18.7 ITk Strip: 1.2
Maximum Total Ionizing Dose (MGy)	Pixels: 3.0	ITk Pixel: 12.7 ITk Strip: 0.5

The ID was not designed for the HL-LHC and **will not survive it.**

ITk Radiation Environment

Y. Unno *et al.*, *Nucl. Instr. Meth. Phys. Res. A*,
vol. 765, pp. 80–90, 2014. (ATLAS12 Design)

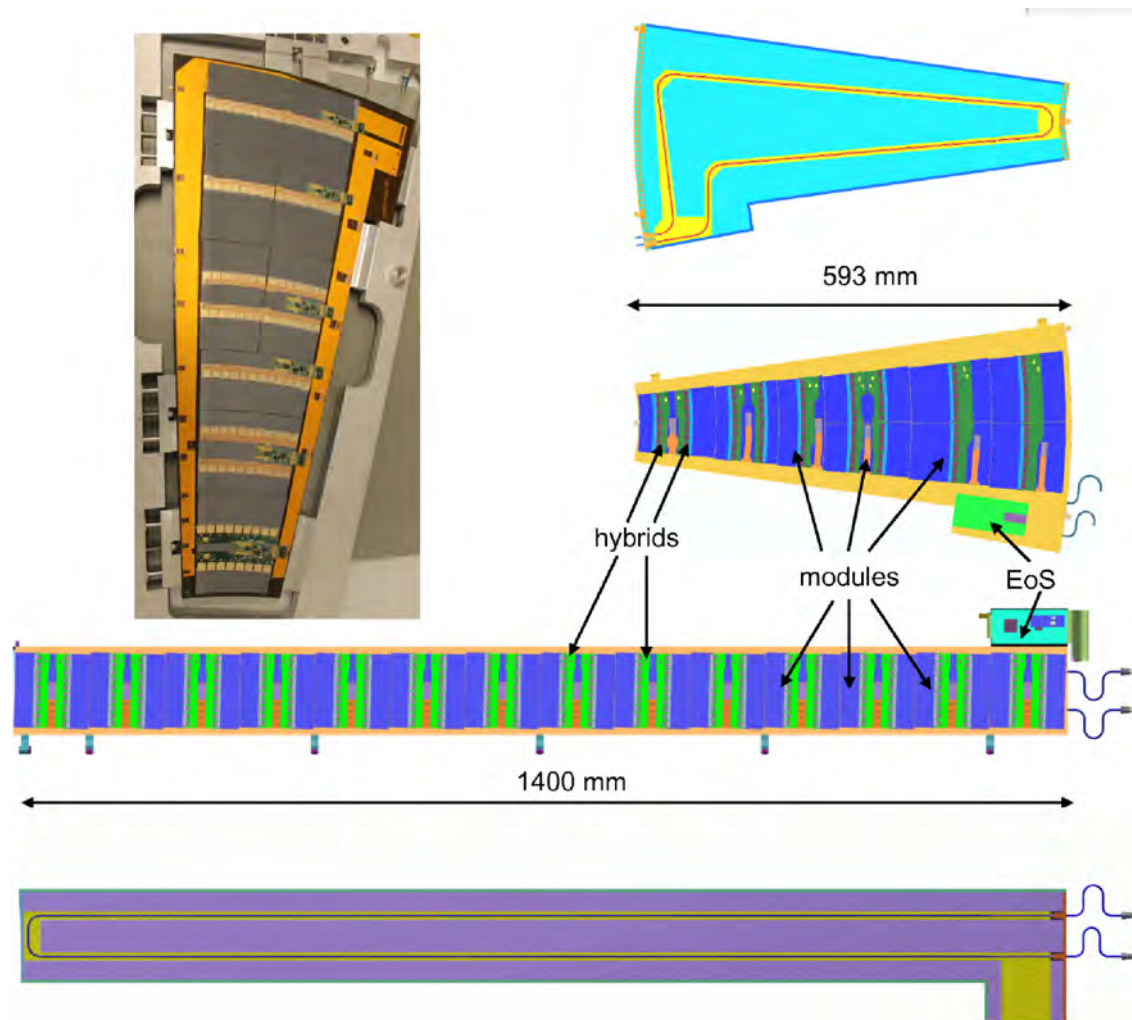
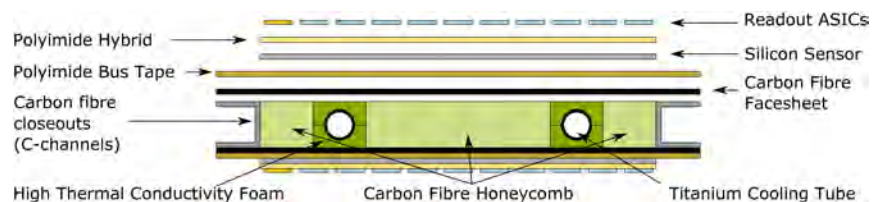


The ATLAS Collaboration, “ATLAS Inner Tracker Strip Detector: Technical Design Report,” Tech. Rep. ATL-TDR-025 / LHCC-2017-005, 2017.

Petals and ITk Strip Component Numerology

Barrel Layer:	Radius [mm]	# of staves	# of modules	# of hybrids	# of ABCStar	# of channels	Area [m ²]
L0	405	28	784	1568	15680	4.01M	7.49
L1	562	40	1120	2240	22400	5.73M	10.7
L2	762	56	1568	1568	15680	4.01M	14.98
L3	1000	72	2016	2016	20160	5.16M	19.26
Total half barrel		196	5488	7392	73920	18.92M	52.43
Total barrel		392	10976	14784	147840	37.85M	104.86







End-cap Disk:	z-pos. [mm]	# of petals	# of modules	# of hybrids	# of ABCStar	# of channels	Area [m ²]
D0	1512	32	576	832	6336	1.62M	5.03
D1	1702	32	576	832	6336	1.62M	5.03
D2	1952	32	576	832	6336	1.62M	5.03
D3	2252	32	576	832	6336	1.62M	5.03
D4	2602	32	576	832	6336	1.62M	5.03
D5	3000	32	576	832	6336	1.62M	5.03
Total one EC		192	3456	4992	43008	11.01M	30.2
Total ECs		384	6912	9984	86016	22.02M	60.4
Total		776	17888	24768	233856	59.87M	165.25

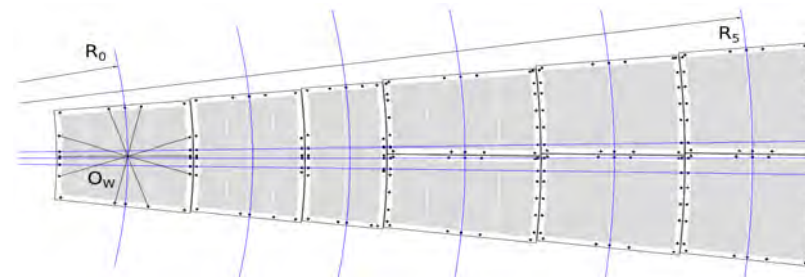


The ATLAS Collaboration, "ATLAS Inner Tracker Strip Detector: Technical Design Report," Tech. Rep. ATL-TDR-025 / LHCC-2017-005, 2017.

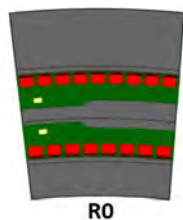
Stereo Annulus Sensors of the ITk Endcaps

Sensor type	Number of sensors	Shape	Number of rows	Channels per sensor	Min/max pitch (μm)
Short-strips	3808	Square	4	5128	75.5
Long-strips	7168	Square	2	2564	75.5

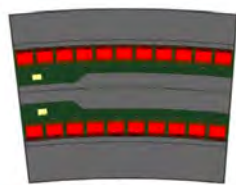
EC Ring 0	768		4	4360	73.5/84
EC Ring 1	768		4	5640	69/81
EC Ring 2	768		2	3076	73.5/84
EC Ring 3	1536		4	3592	70.6/83.5
EC Ring 4	1536		2	2052	73.4/83.9
EC Ring 5	1536		2	2308	74.8/83.6



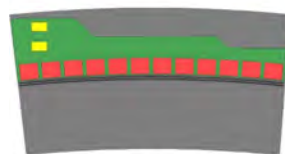
Ring/Row	Inner Radius [mm]	Strip Length [mm]	Strip Pitch [μm]
Ring 0 Row 0	384.5	19	75.0
Ring 0 Row 1	403.5	24	79.2
Ring 0 Row 2	427.5	29	74.9
Ring 0 Row 3	456.4	32	80.2
Ring 1 Row 0	489.8	18.1	69.9
Ring 1 Row 1	507.9	27.1	72.9
Ring 1 Row 2	535	24.1	75.6
Ring 1 Row 3	559.1	15.1	78.6
Ring 2 Row 0	575.6	30.8	75.7
Ring 2 Row 1	606.4	30.8	79.8
Ring 3 Row 0	638.6	32.2	71.1
Ring 3 Row 1	670.8	26.2	74.3
Ring 3 Row 2	697.1	26.2	77.5
Ring 3 Row 3	723.3	32.2	80.7
Ring 4 Row 0	756.9	54.6	75.0
Ring 4 Row 1	811.5	54.6	80.3
Ring 5 Row 0	867.5	40.2	76.2
Ring 5 Row 1	907.6	60.2	80.5



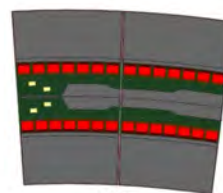
R0



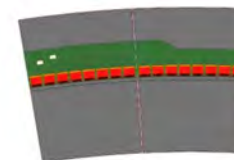
R1



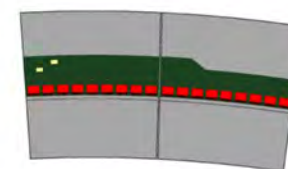
R2



R3

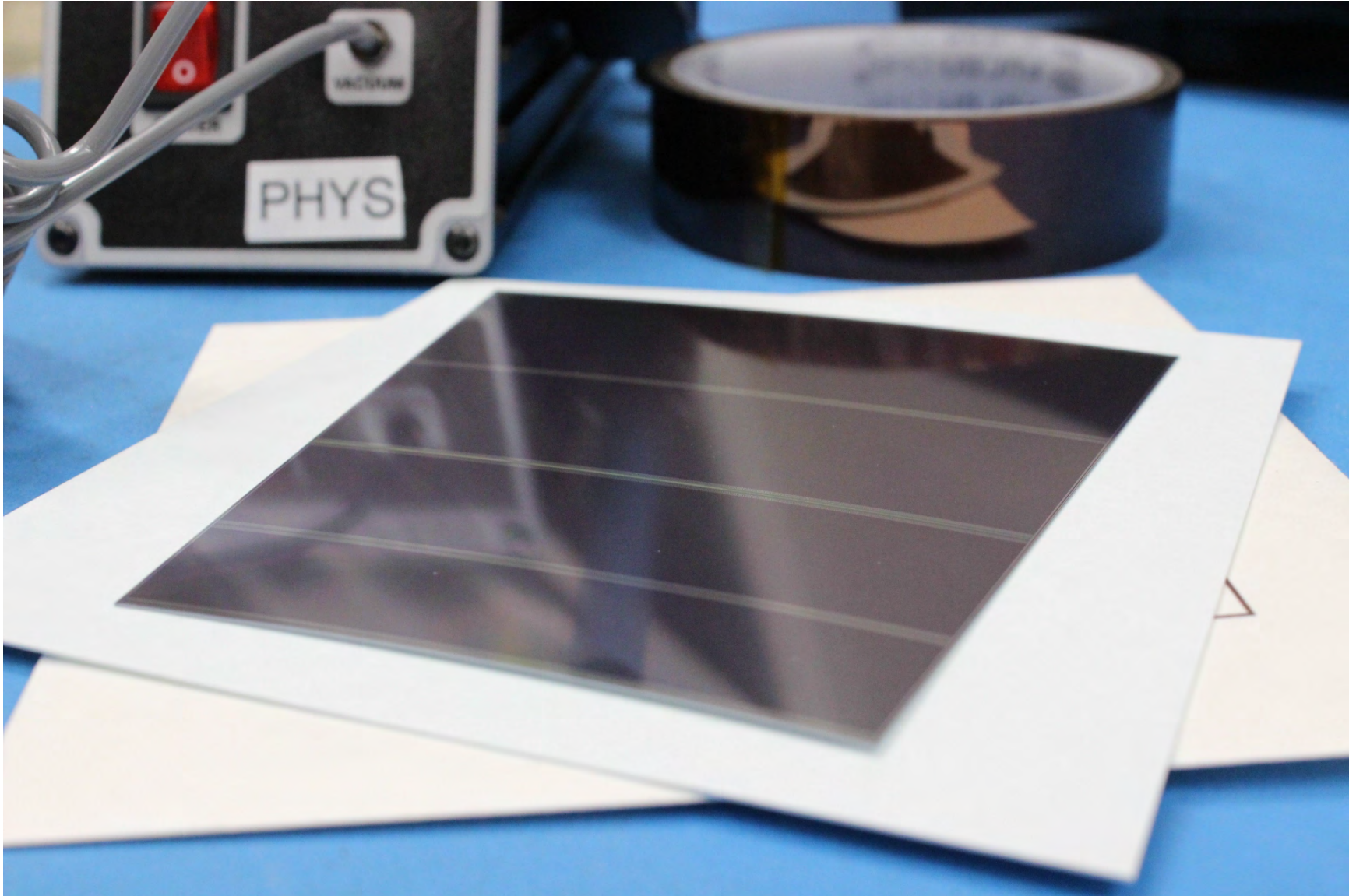


R4



R5

An ATLAS12EC Sensor



Sensor Specifications

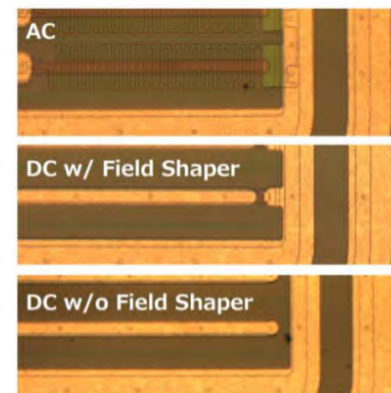
	ATLAS12EC
Wafer size	150 mm
Thickness	310 +/- 25 μm
Orientation	<100>
Type	P
Ingot	FZ
Resistivity	>3 k Ωcm
Strip segments	4
Strip implant	N
Strip implant Width	16 μm
Strip bias resistor	Polysilicon
Strip bias resistance (R_b)	1.5+/-0.5 M Ω
Strip readout coupling	AC
Strip readout metal	Pure Aluminium
Strip readout metal width	20 μm
Strip AC coupling capacitance	>20 pF/cm
Strip isolation	>10 $\times R_b$ at 300 V
Strip isolation method	Narrow-common p-stop
Gap between strip segments	56 μm (rail region) 70 μm (no rail region)
Microdischarge onset voltage	>600 V
Maximum operation voltage ^(*)	600 V
Leakage current	<2 $\mu\text{A}/\text{cm}^2$ at 600 V
Radiation tolerance	1.5×10^{15} 1-MeV $n_{\text{eq}}/\text{cm}^2$

^(*) The voltage rating of the external high voltage cable is 500V and tested 1 KV.

ATLAS12EC Mini Sensors

Mini distribution:

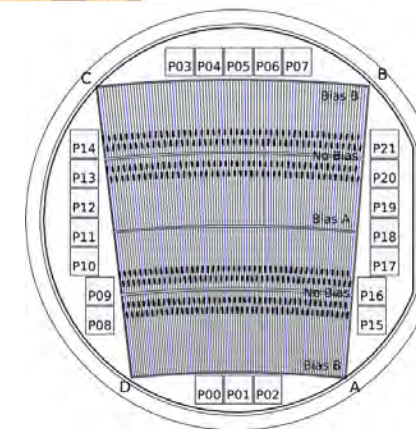
Pitch	Coupling	PTP	Total	Irradiated	Left
Default	AC	Yes	166	48	118
	DC	Yes	166	48	118
	DC	No	166	48	118
Narrow	AC	Yes	58	36	22
	DC	Yes	29	18	11
	DC	No	29	18	11
Wide	AC	Yes	58	36	22
	DC	Yes	29	0	29
	DC	No	29	0	29
			730	252	478



sample	Strips	Width [μm]
Default	103	75
Narrow	111	70
Wide	92	85

Irradiation test set: $(\times 10^{14} n_{\text{eqv}}/\text{cm}^2)$

Pitch	Coupling	PTP	0x	5x	10x	20x	TOTAL
Default	AC	Yes	2	2	2	2	8
	DC	Yes	2	2	2	2	8
	DC	No	2	2	2	2	8
Narrow	AC	Yes	2	1	2	1	6
	DC	Yes		1	1	1	3
	DC	No		1	1	1	3
Wide	AC	Yes	2	1	2	1	6
	DC	Yes					0
	DC	No					0
Total			10	10	12	10	42



Three mini test sets are *each* irradiated with:

n
reactor neutrons
 Ljubljana Reactor
 Jožef Stefan Institute,
 Slovenia

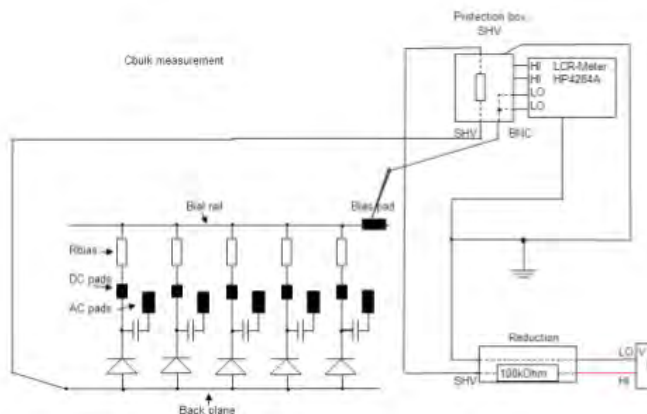
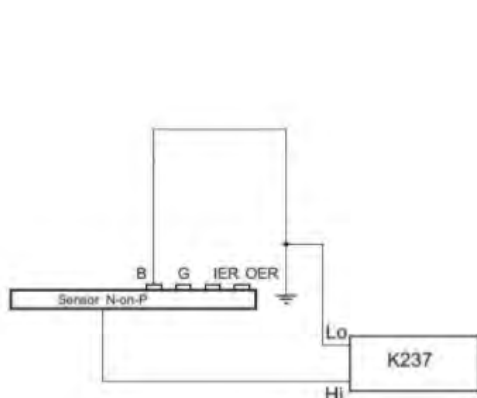
p^+
70MeV protons
 CYRIC
 Tohoku University,
 Japan

First ATLAS12EC Module

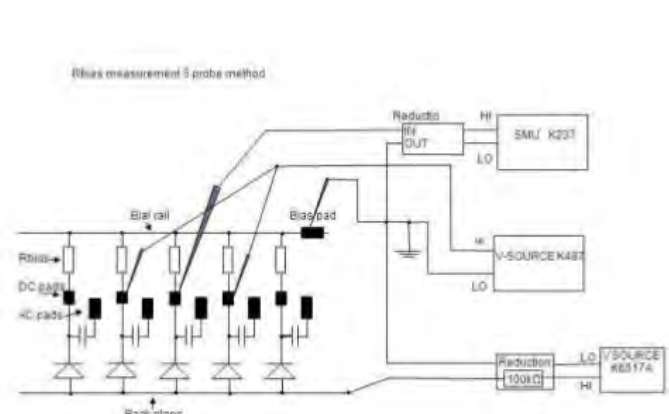
See poster by Carlos Garcia Argos : “Assembly and Electrical Tests of the First Full-size Forward Module for the ATLAS ITk Strip Detector”



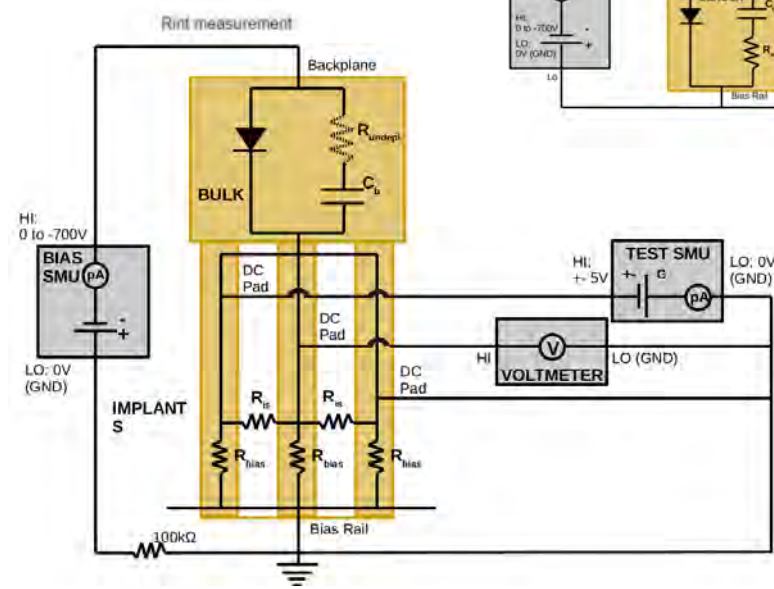
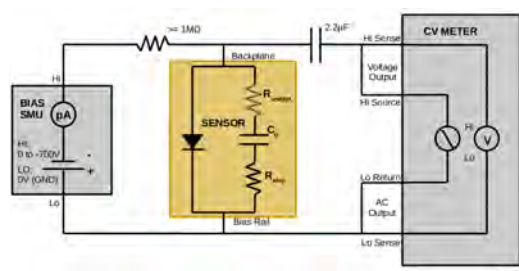
Measurement Techniques



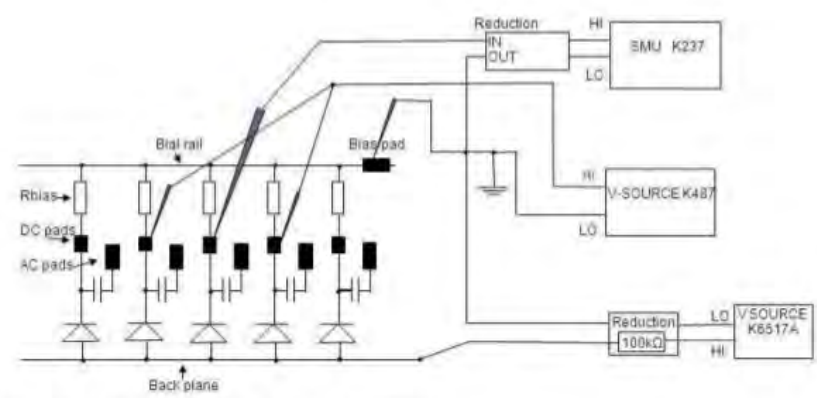
HP4284 - precise capacity meter, CR in Serie, 1kHz, level 2V
K8517 Vsource 0 to -1000V



K237 Source Measure Unit, V_{appt} = -5V to +5V, R_{bias} = dU/applid, I measured
K8517 Vsource 0 to -600V, R_{bias} = dU/applid

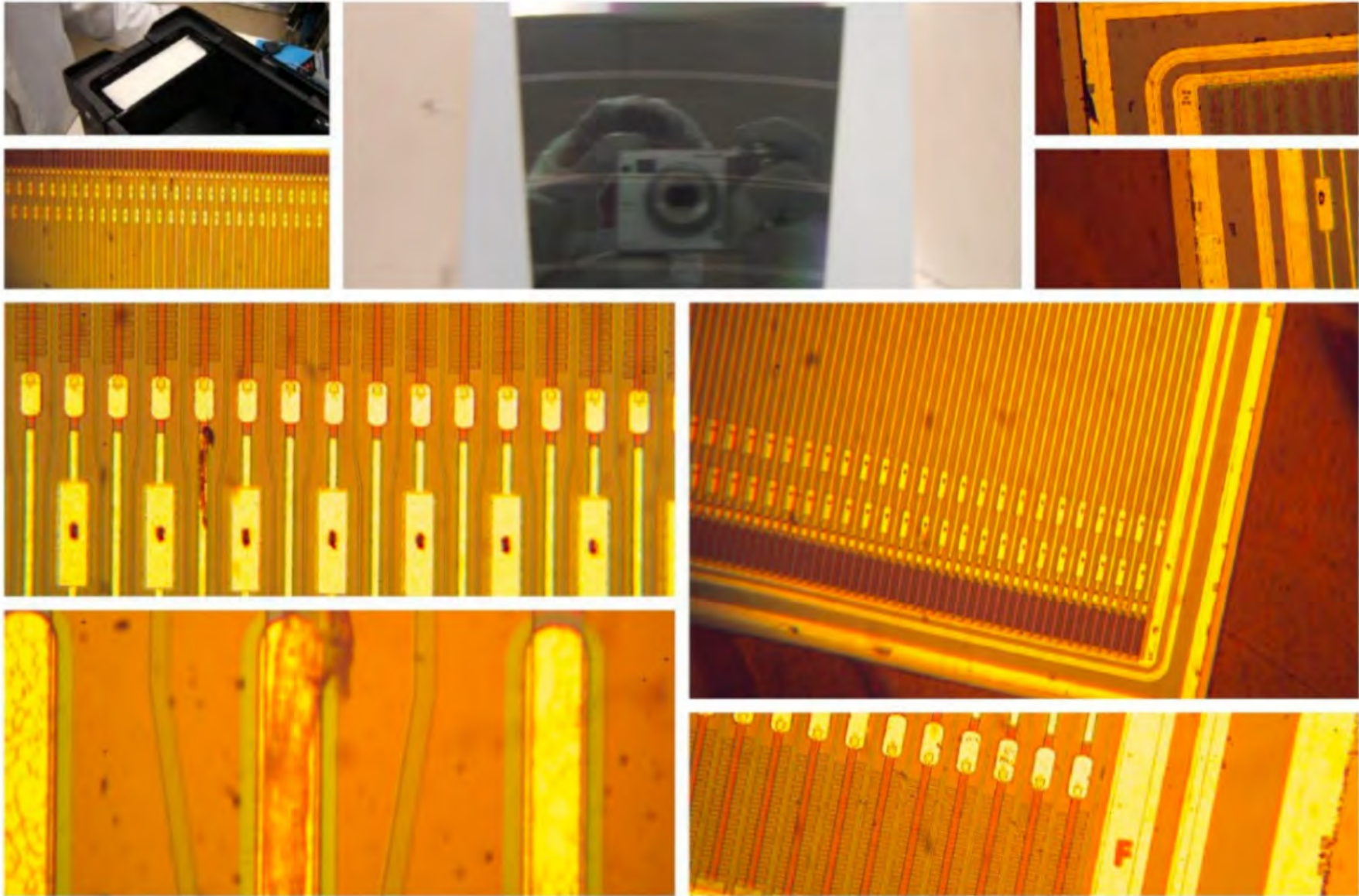


PTP measurement 3 probe method.



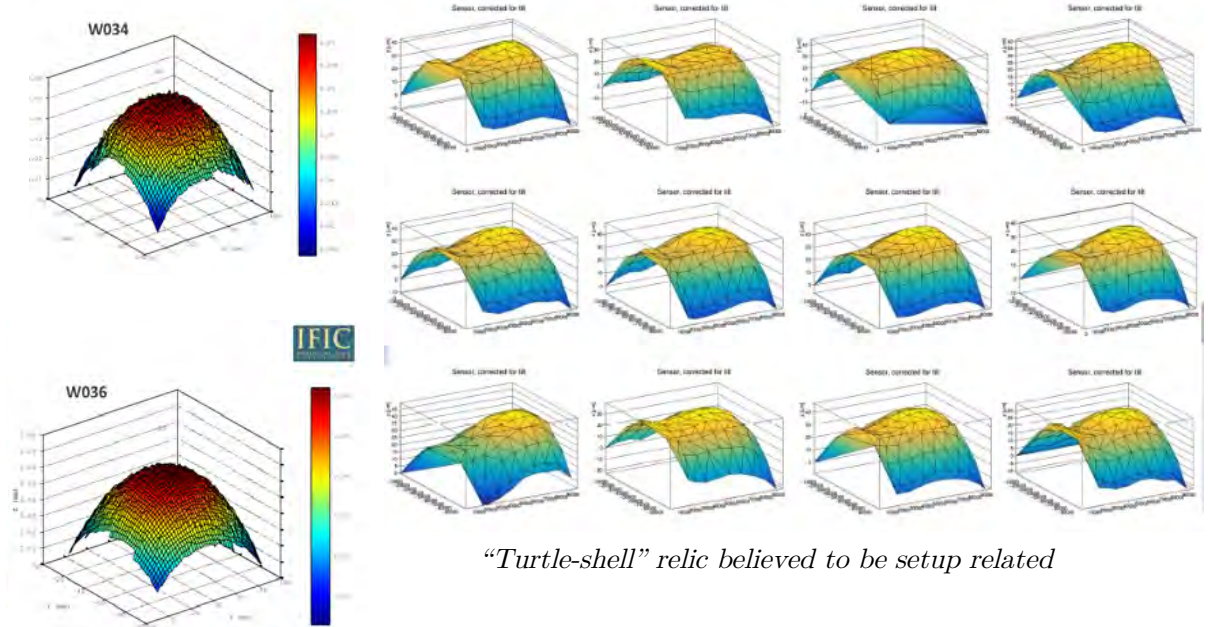
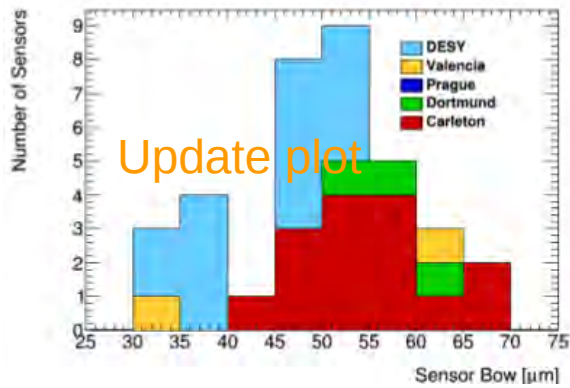
K237 Source Measure Unit, V_{test} = 0 to -50V, Ref_i = dVtest/ditest, I_{test} measured
K8517 Vsource 0 to -600V

More Visual Inspection Results

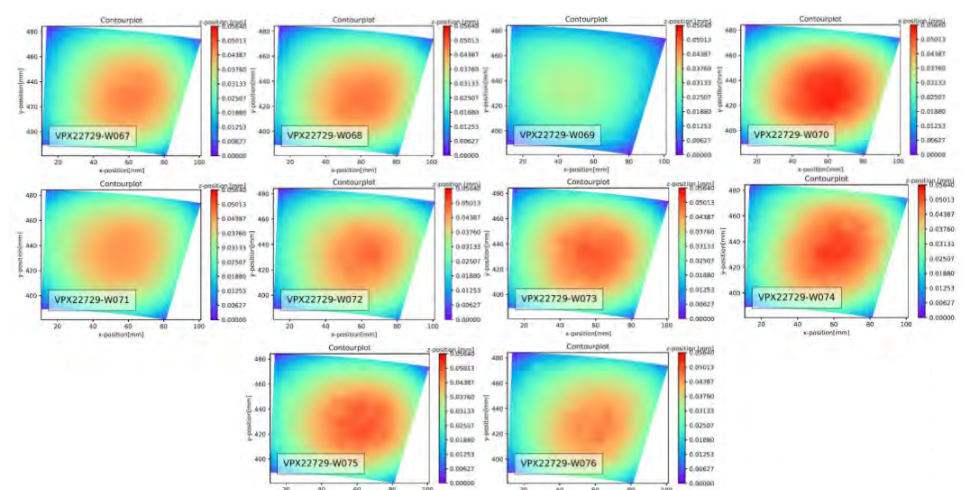
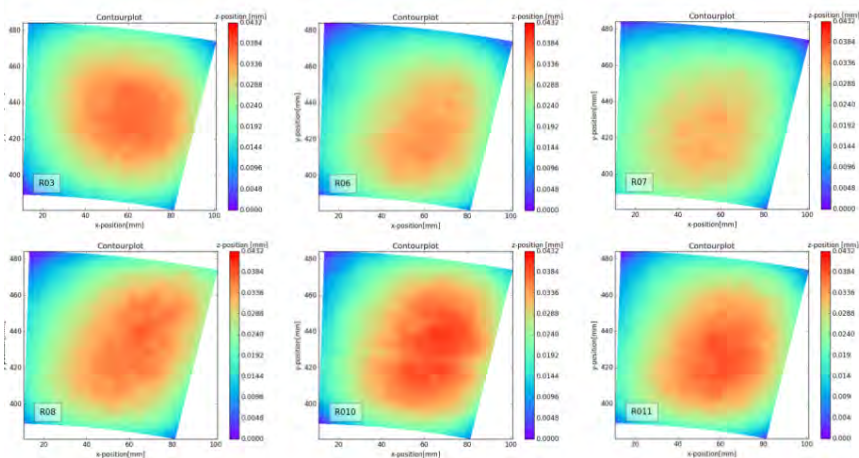


More Metrology Results

- High consistency *well* within specification

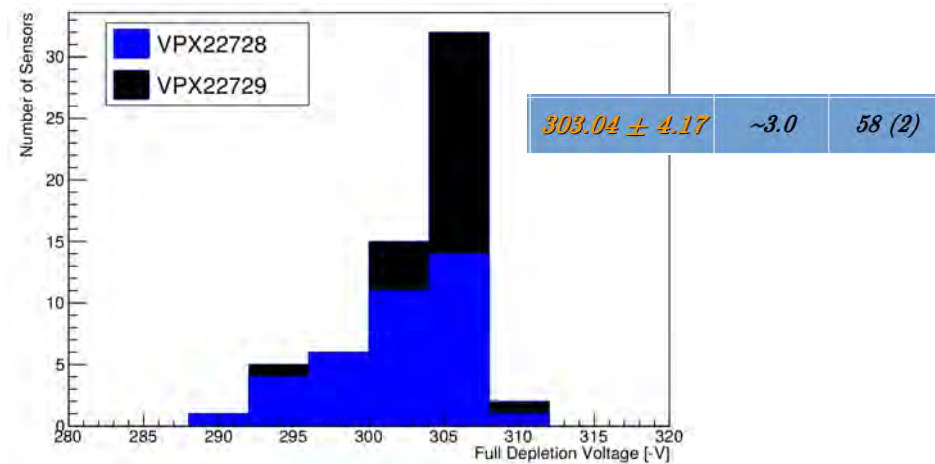
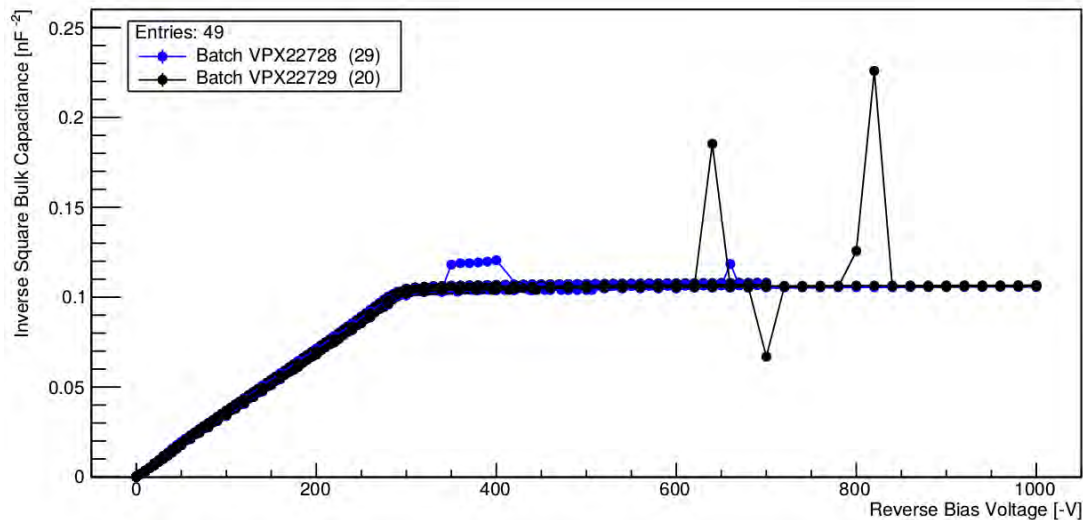
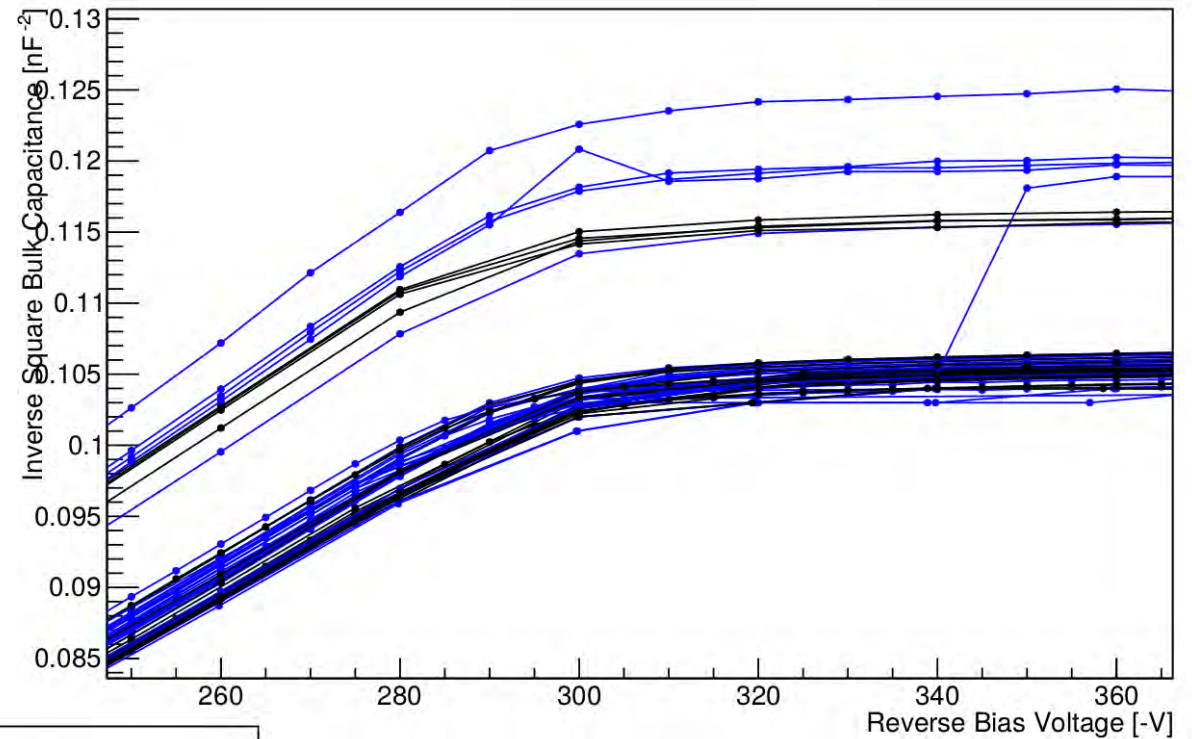


“Turtle-shell” relic believed to be setup related

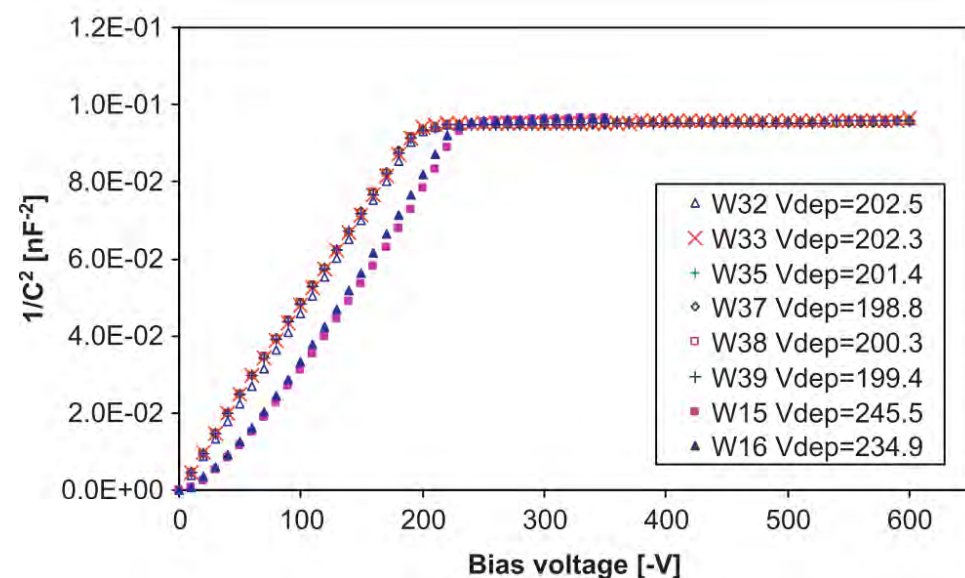
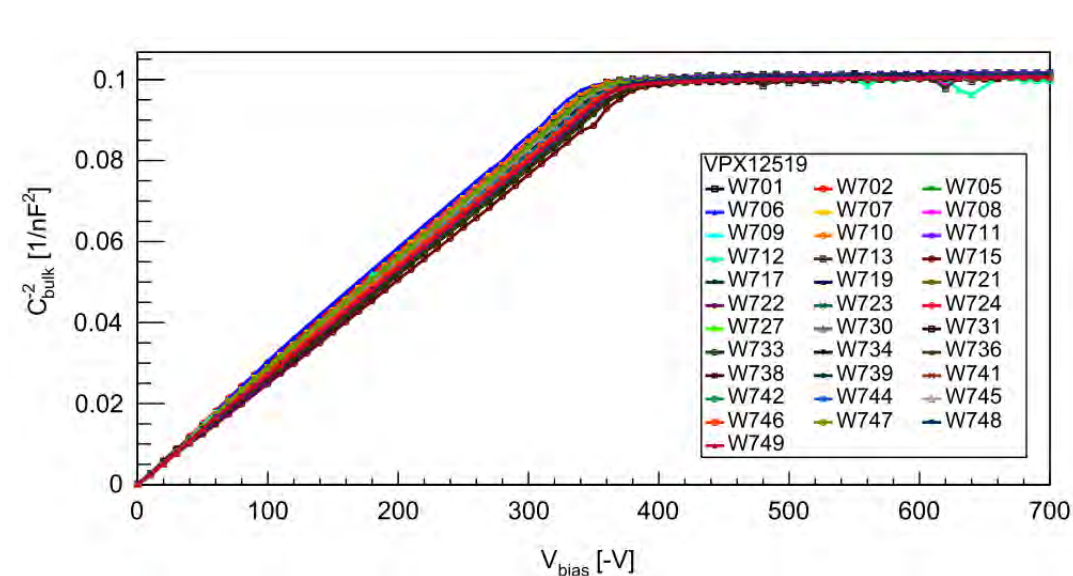


Full Depletion Kink

- Sensors from one institute removed from CV plot due to systematic parasitic capacitance that is not yet fully understood
 - 9 sensors sit above the 49 sensors in the lower curve seen
- This systematic does not affect the full depletion voltage extraction, as seen

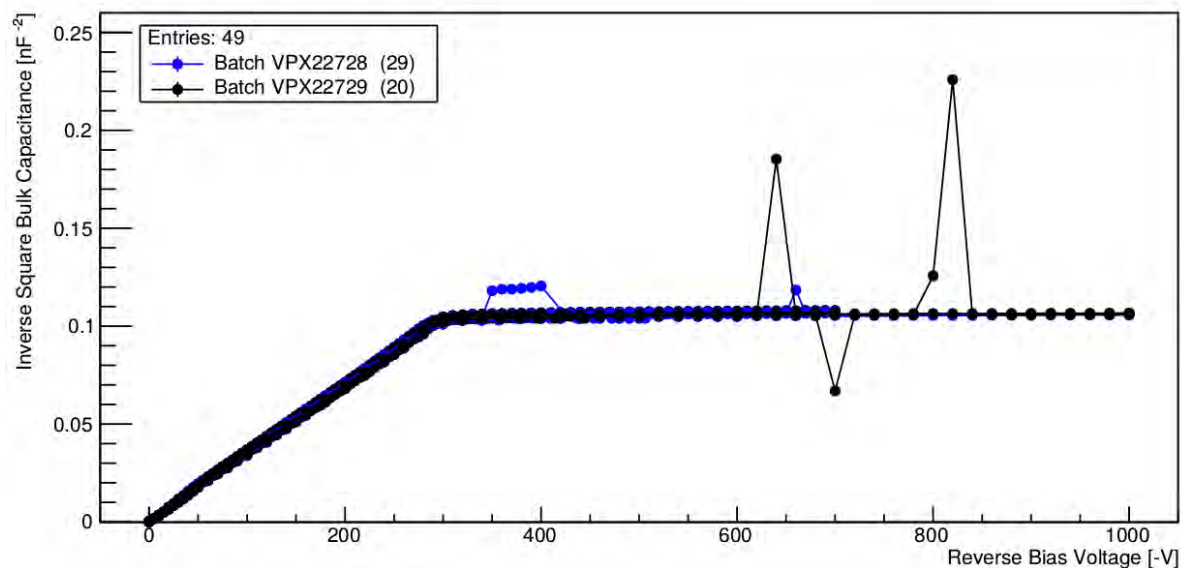


CV Curves (Over the Generations)

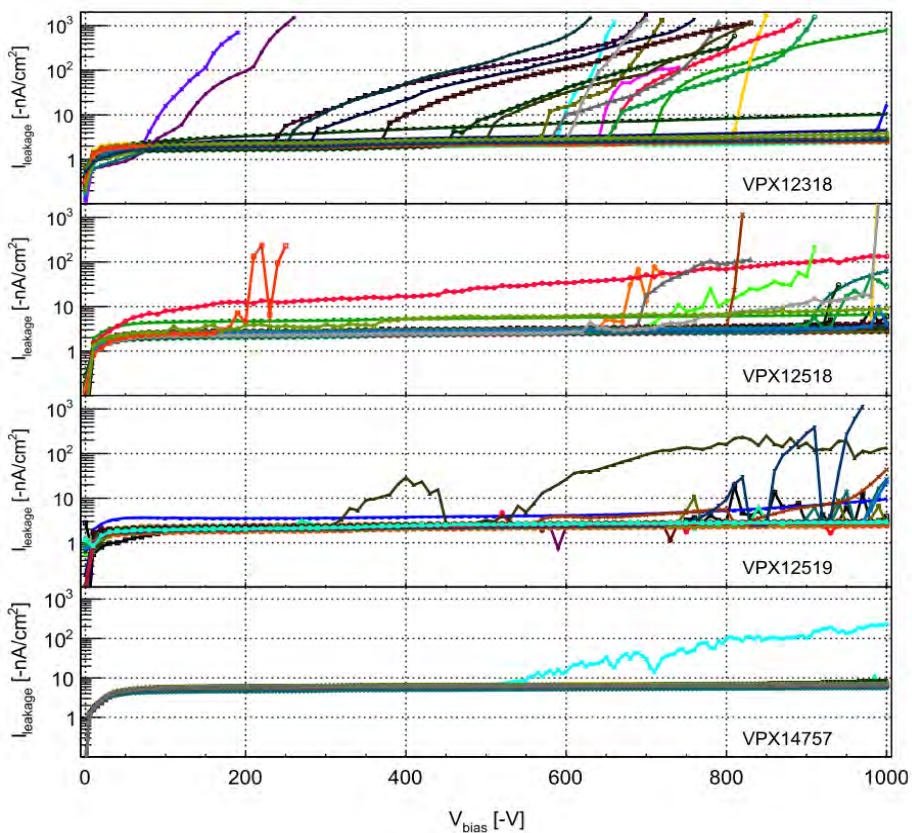


L.B.A. Hommels *et al.*, "Detailed Studies of Full-Size ATLAS12 Sensors". *Nucl. Instr. Meth. Phys. Res. A*, vol. 831, pp. 167–173, 2016.

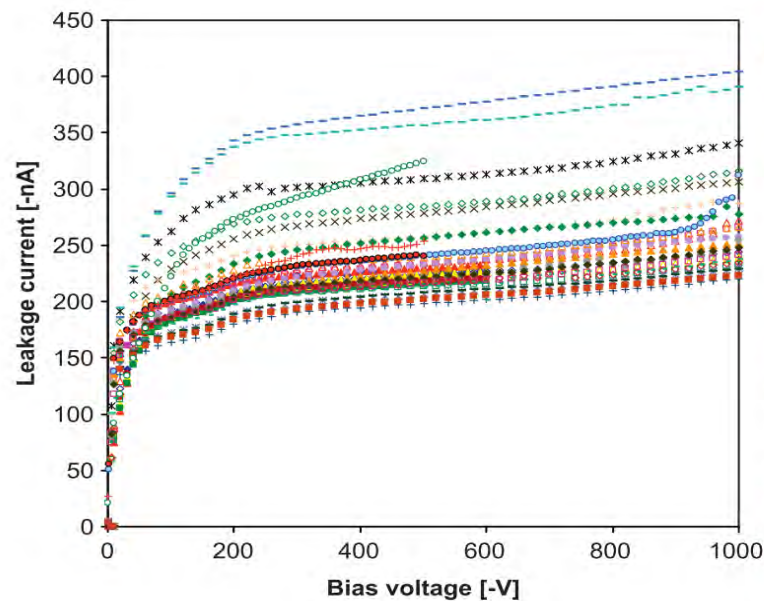
J. Bohm. *et al.*, "Evaluation of the bulk and strip characteristics of large area n-in-p silicon sensors intended for a very high radiation environment," *Nucl. Instr. Meth. Phys. Res. A*, vol. 636, pp. S104–S110, 2011.



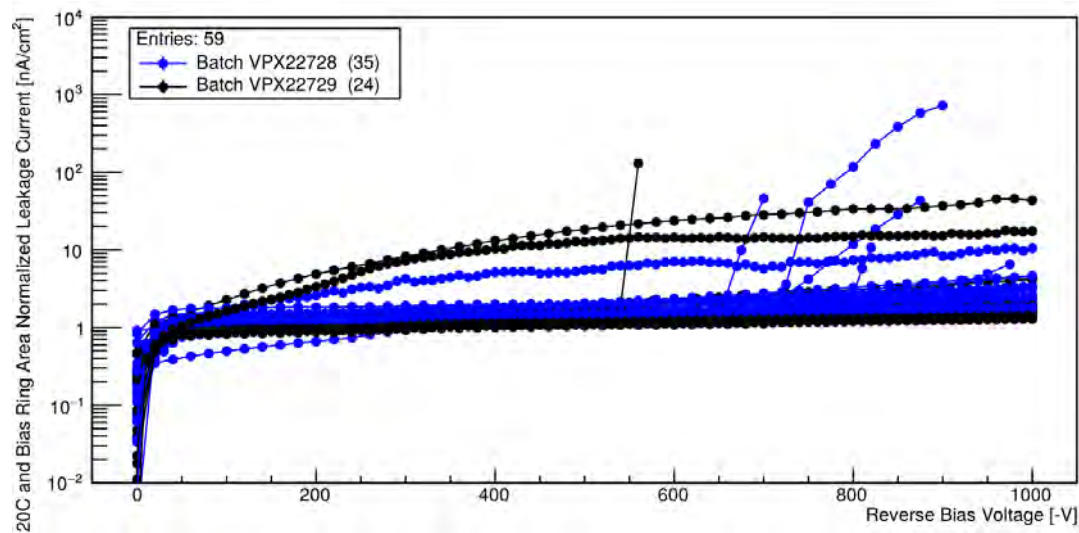
IV Curves (Over the Generations)



L.B.A. Hommels *et al.*, "Detailed Studies of Full-Size ATLAS12 Sensors". *Nucl. Instr. Meth. Phys. Res. A*, vol. 831, pp. 167–173, 2016.



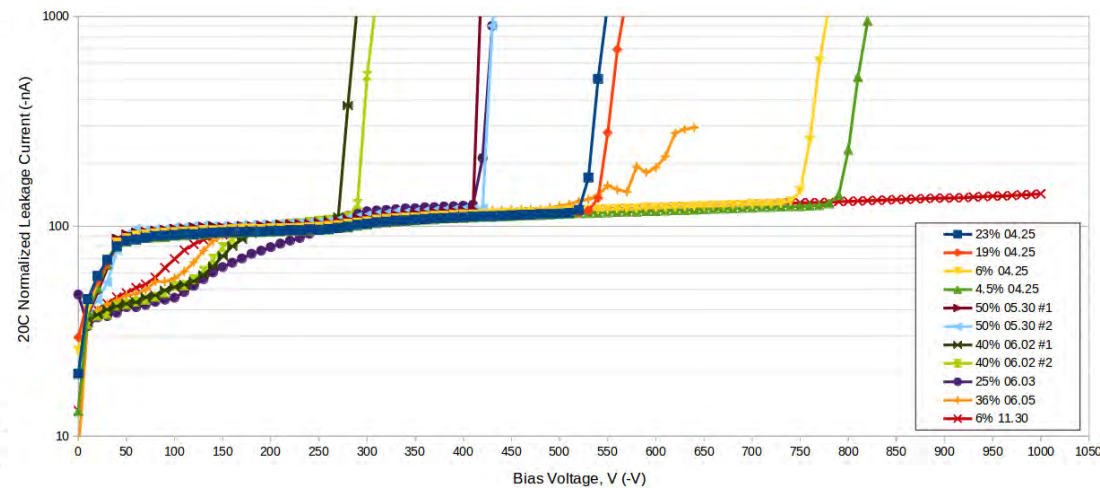
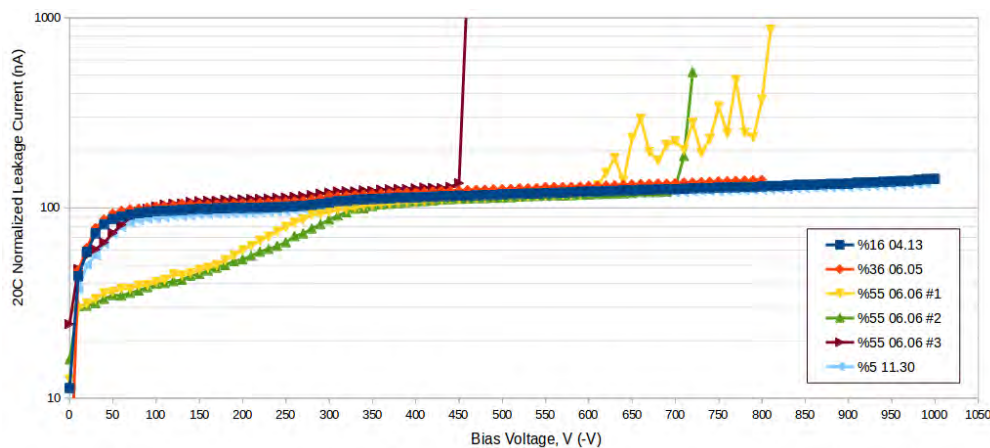
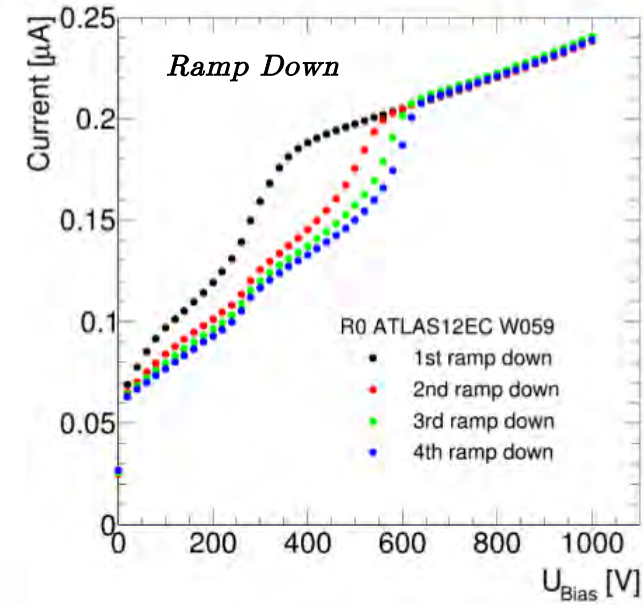
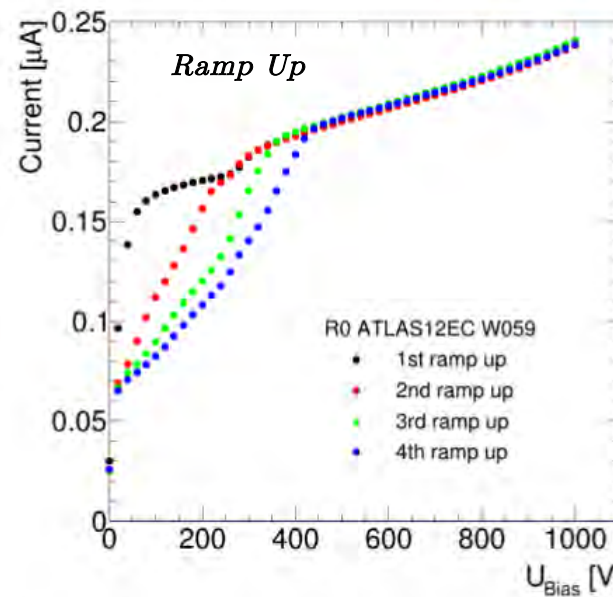
J. Bohm. *et al.*, "Evaluation of the bulk and strip characteristics of large area n-in-p silicon sensors intended for a very high radiation environment," *Nucl. Instr. Meth. Phys. Res. A*, vol. 636, pp. S104–S110, 2011.



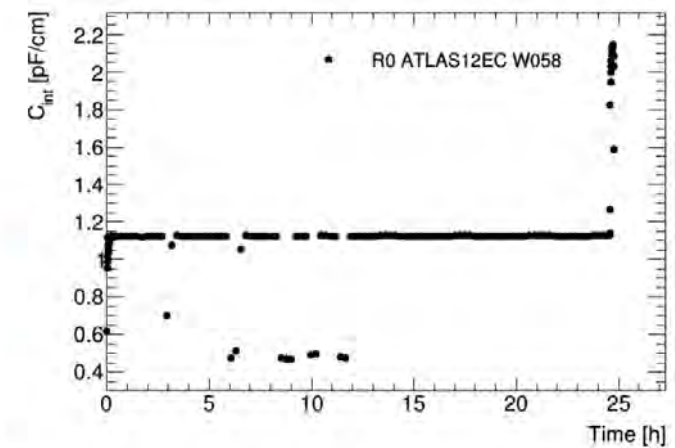
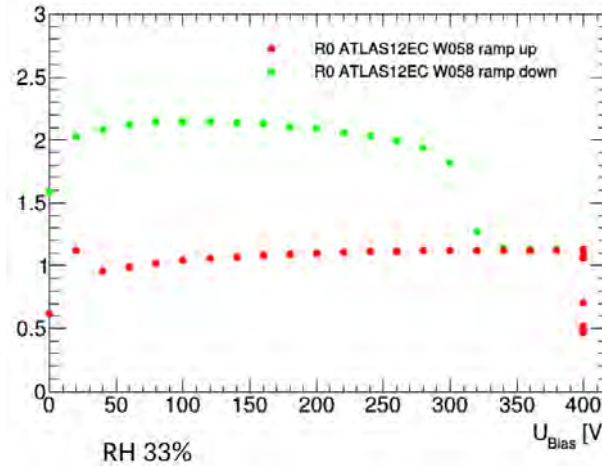
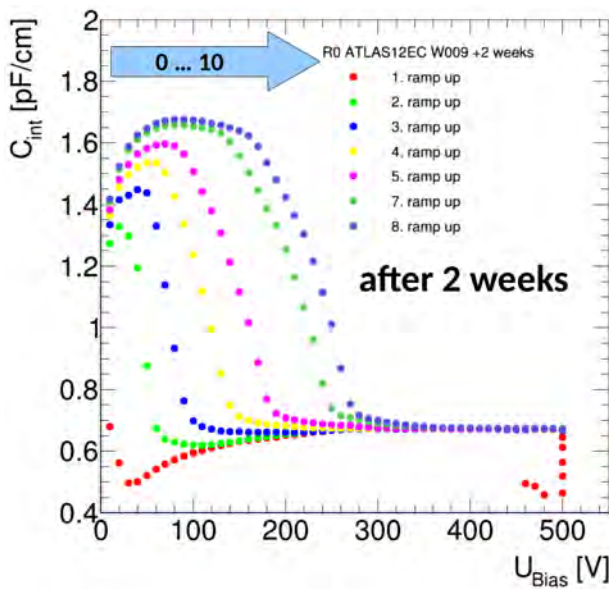
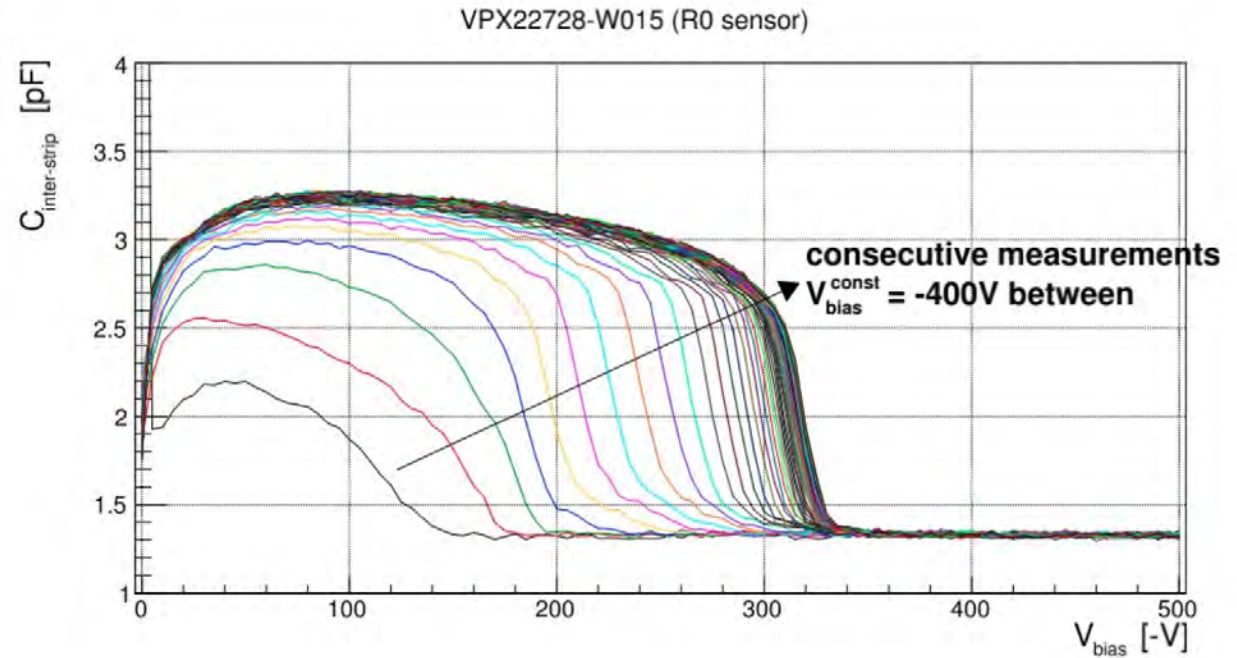
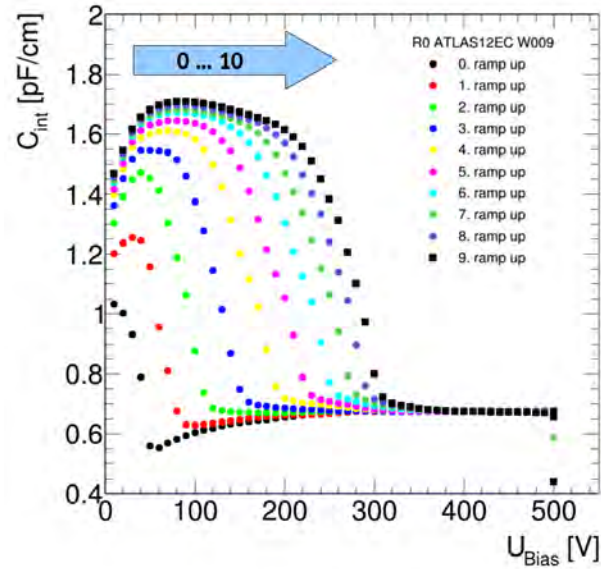
IV Hysteresis

- Observed in sensors with and without strenuous humidity history
 - Evidence for bias activated interface states

5-10min Unbiased between Ramps

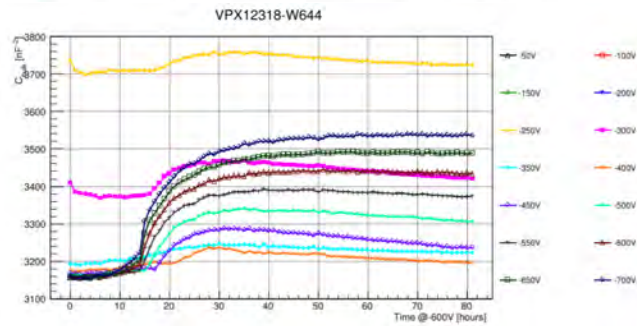
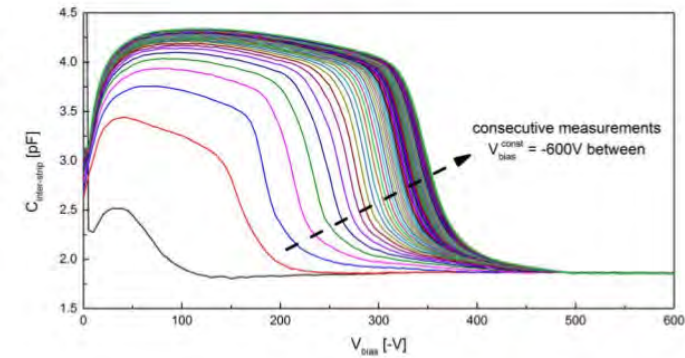
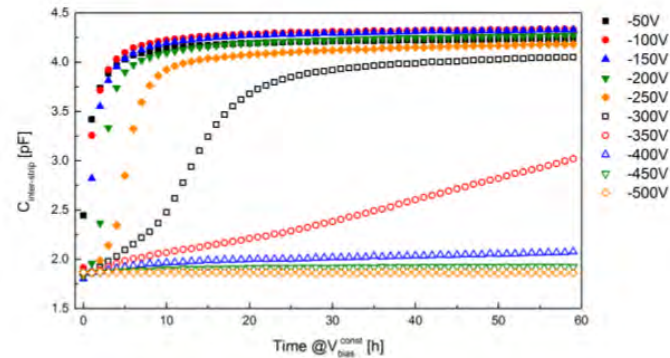
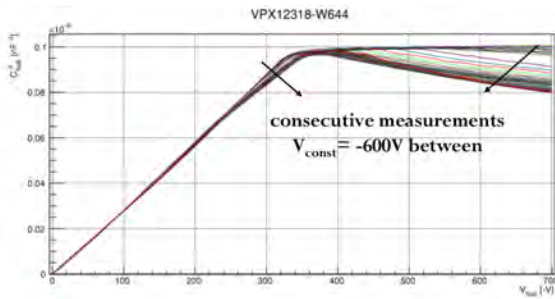


Hysteresis of Interstrip Capacitance

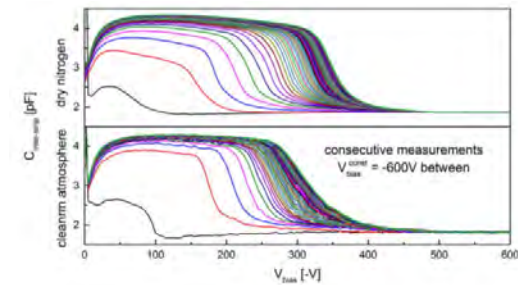


Hysteresis in ATLAS07 and ATLAS12

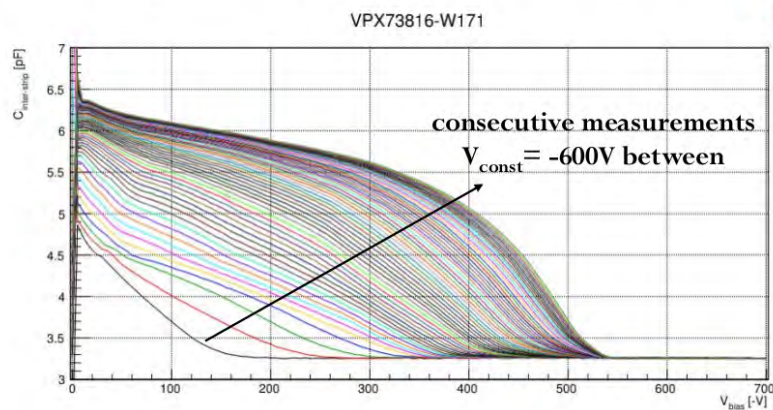
ATLAS12 Cbulk



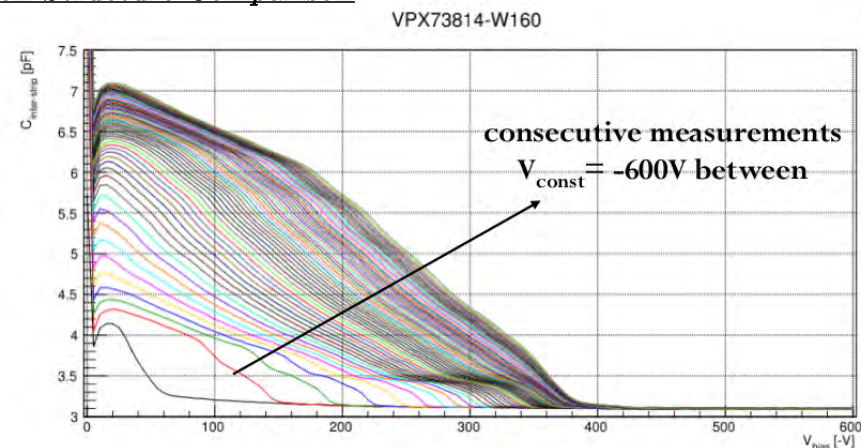
ATLAS12 Cis



ATLAS07 Cis Strip Isolation Structure Comparison



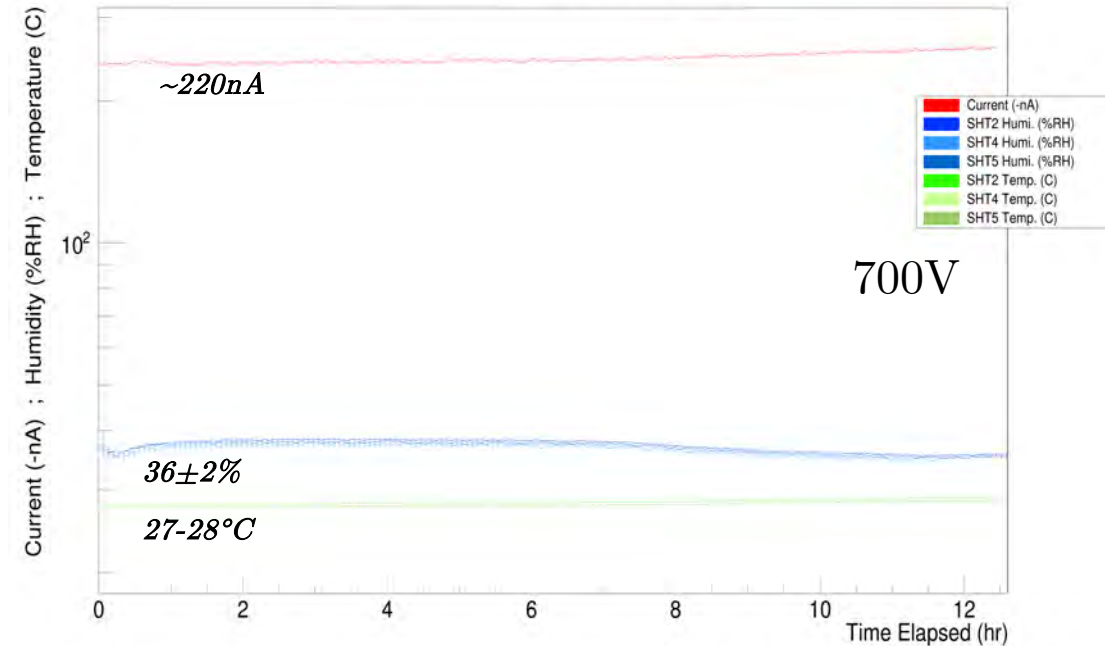
p-stop



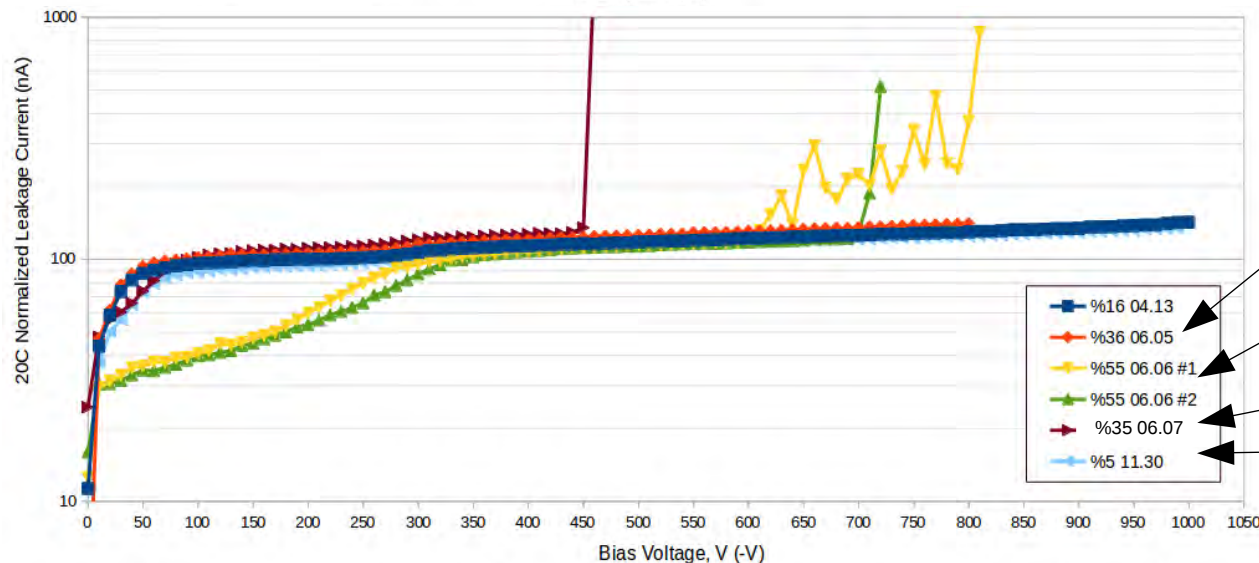
p-spray

Humidity Sensitivity – A Tale of Two Sensors

IVStab_CombData_W042_H36pm2



- W042 showed good IV character
- Both poor and well behaved sensors (in an IV curve respect) can show humidity sensitivity
- Recovery of sensors after long-term dry storage
 - Complete recovery of microdischarge onset
 - Some hysteresis remains (ion activated interface traps)



(Dry storage = 0.1%)

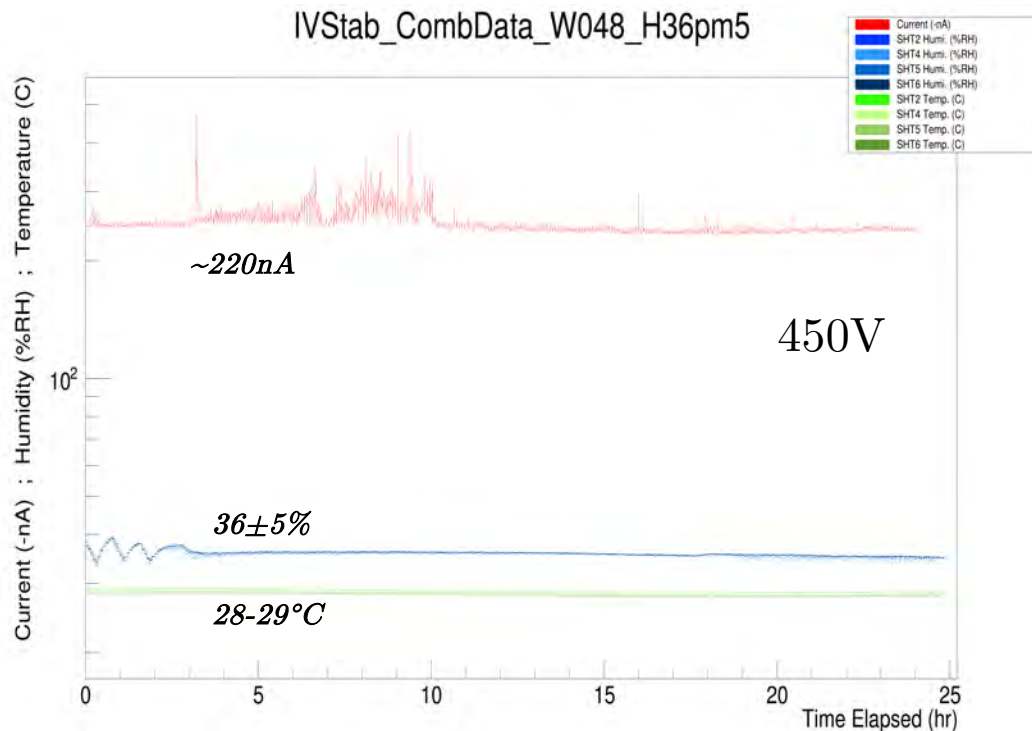
After weeks in dry storage

After 24hr at 700V, 36% and then 26hrs in dry storage.

After 3 hr at 55% and 13hr at 35%

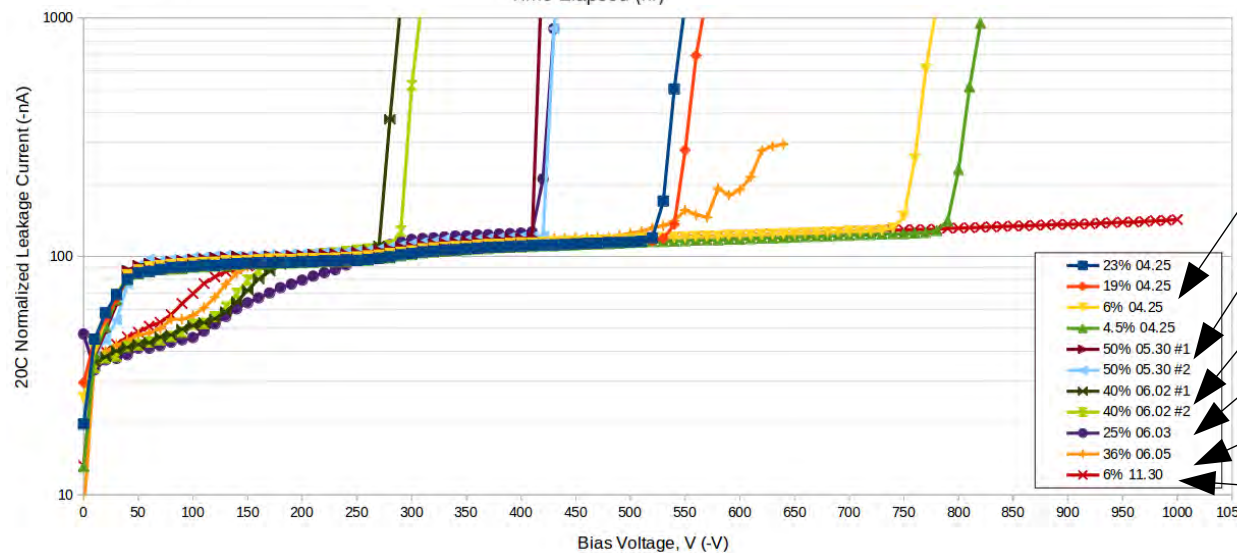
After nearly six months in dry storage

Humidity Sensitivity – A Tale of Two Sensors



- W048 showed early onset microdischarge and a humidity dependency therein
- Both poor and well behaved sensors (in an IV curve respect) can show humidity sensitivity
- Recovery of sensors after long-term dry storage
 - Complete recovery of microdischarge onset
 - Some hysteresis remains (ion activated interface traps)

(Dry storage = 0.1%)



Taken consecutively.

Consecutive after weeks in dry storage

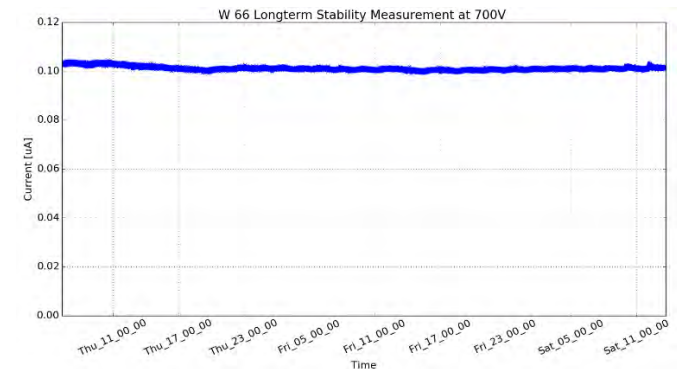
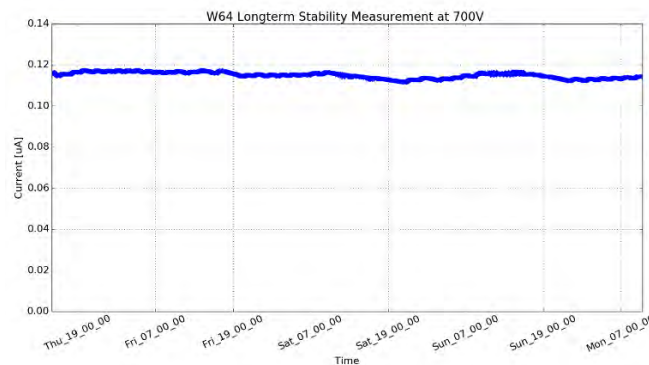
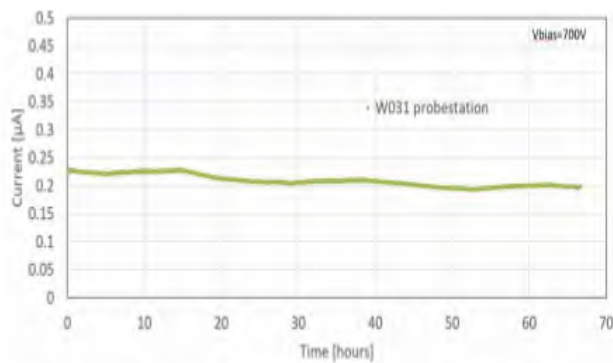
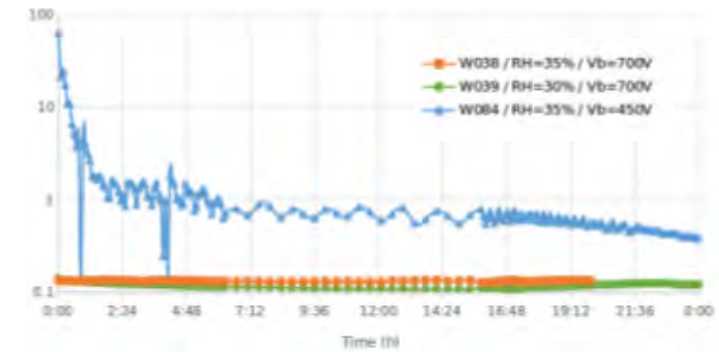
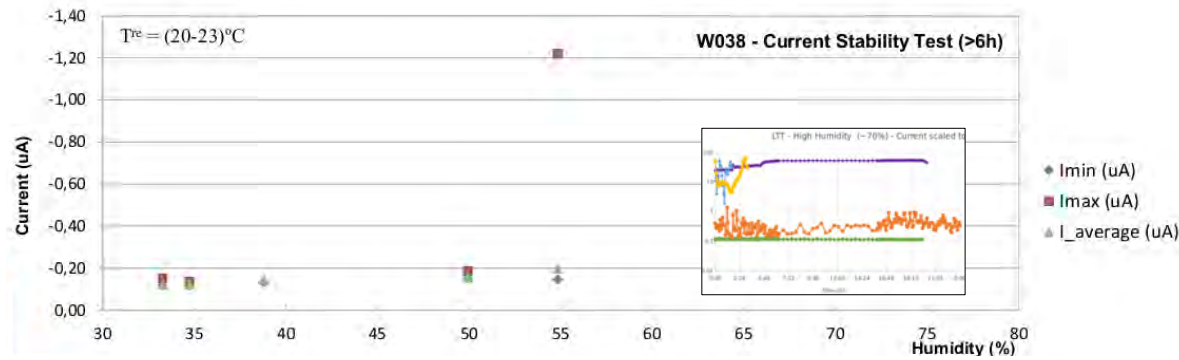
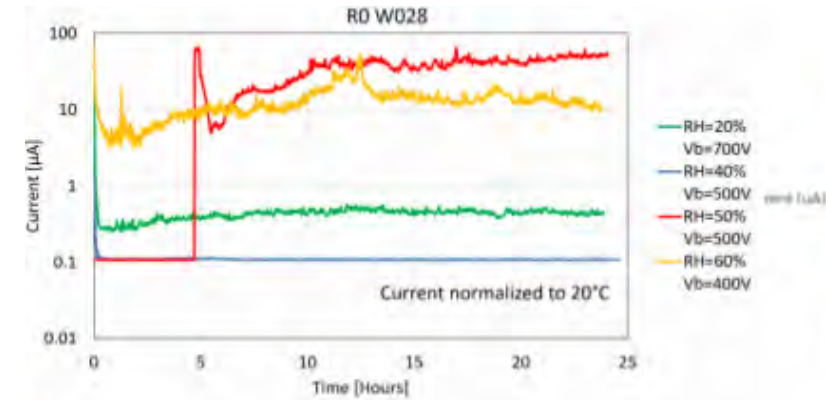
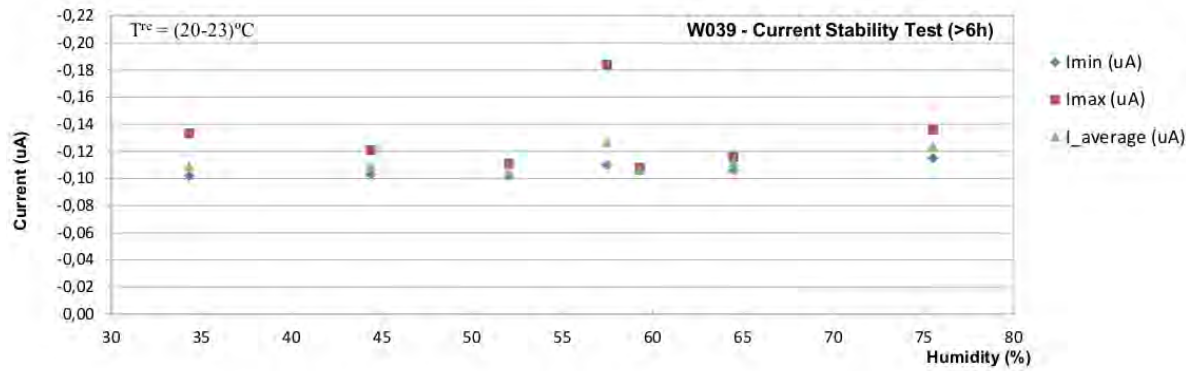
Consecutive after 24hr at 400V, 55% and then 48hr in dry storage

After 24hr at 280V, 40%

After 24hr at 280V, 25% and 15hr in dry storage

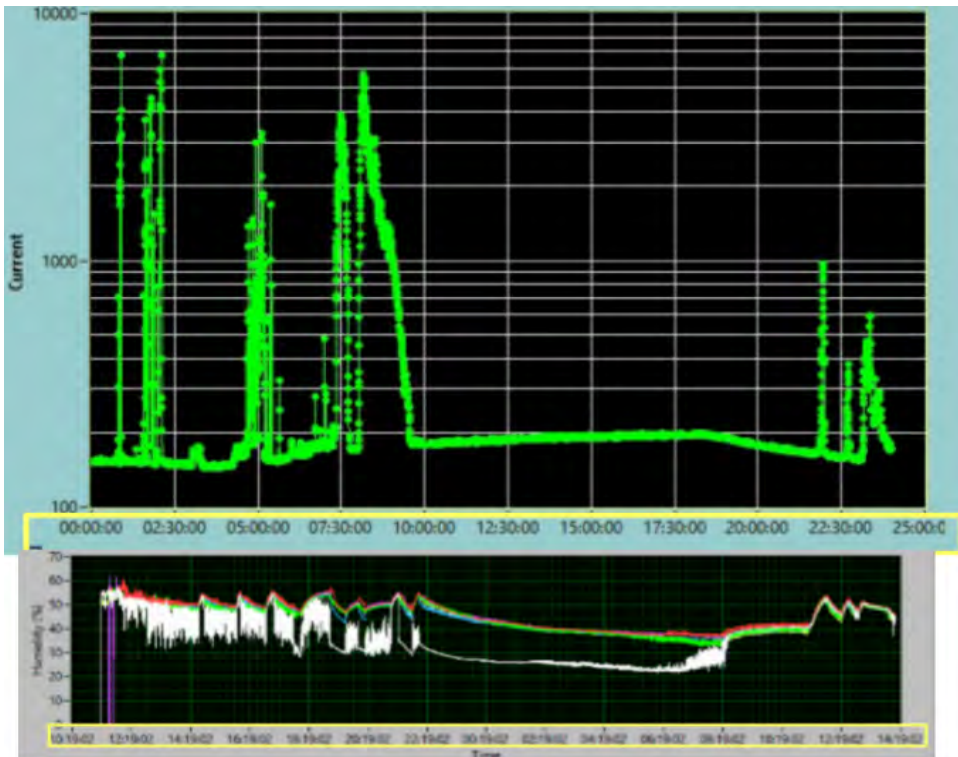
After nearly six months in dry storage

Long Term IV Stability and Humidity



More Evidence for Passivation Issues

- Immediate response to changes in humidity in long term tests



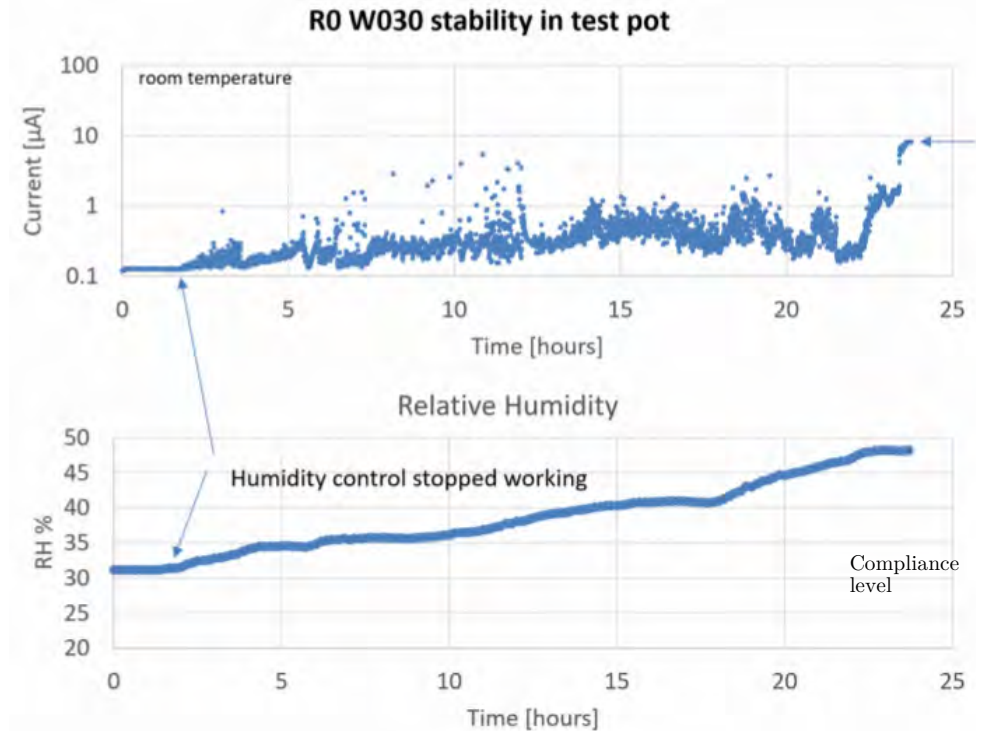
400V

Triple peak at end of run:

1st peak: ~51.5% up , quick I decrease

2nd peak: ~50.5% up , quick I decrease

3rd peak: ~49.75% up, leave fan slow to bring down H slow, instability lasts to lower H than with quick fall

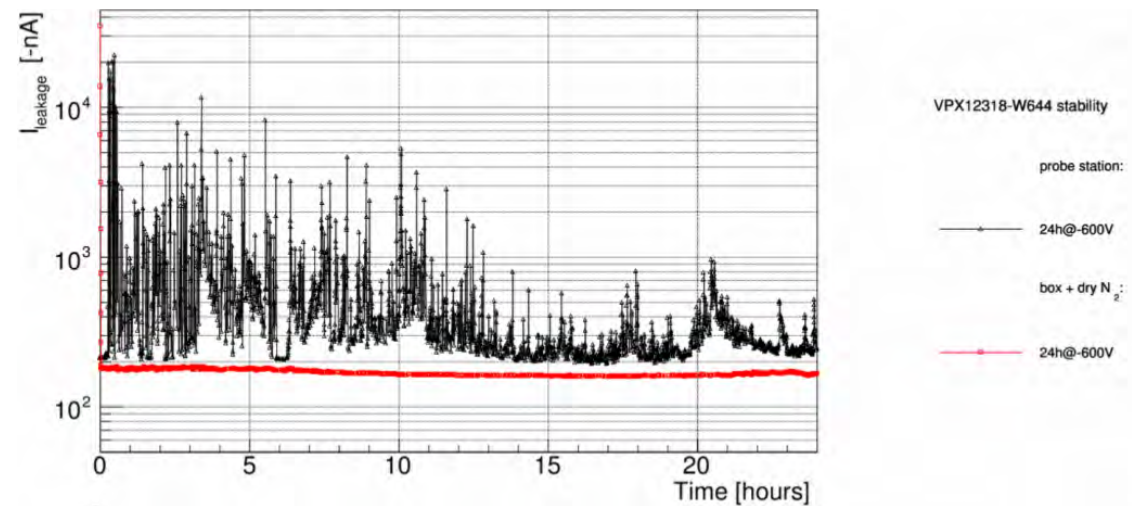
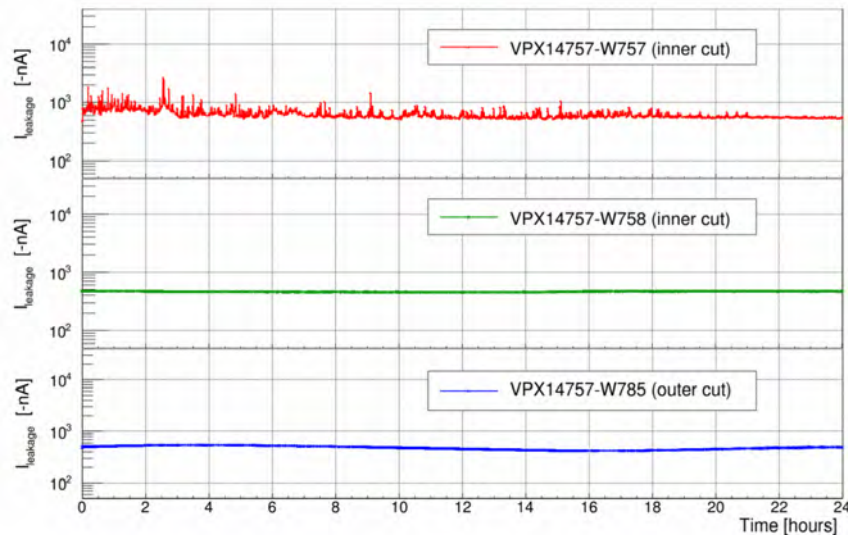
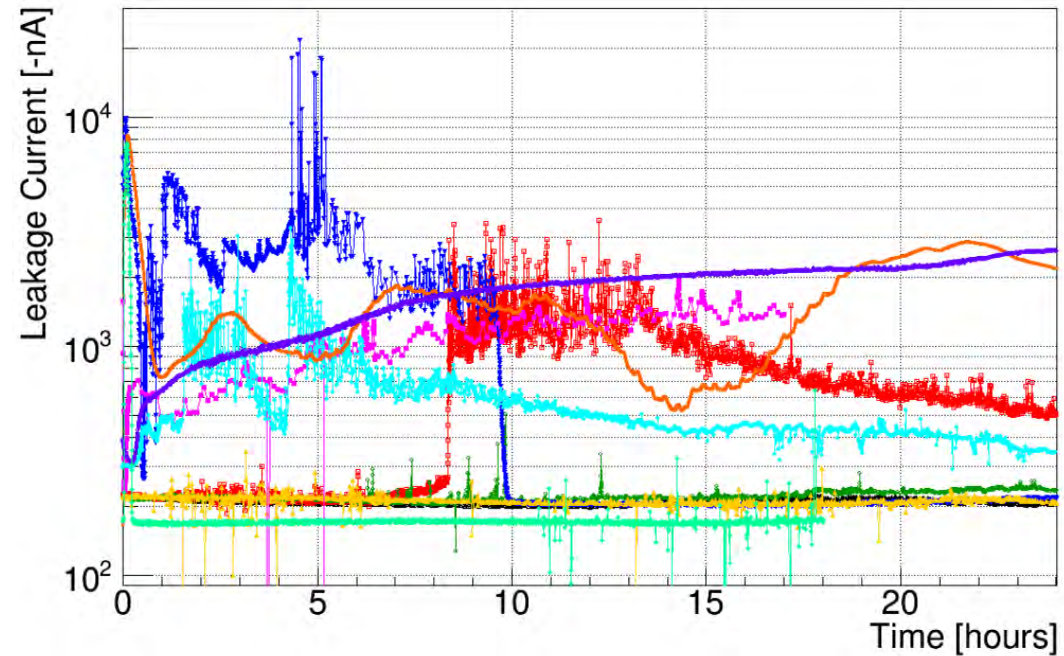
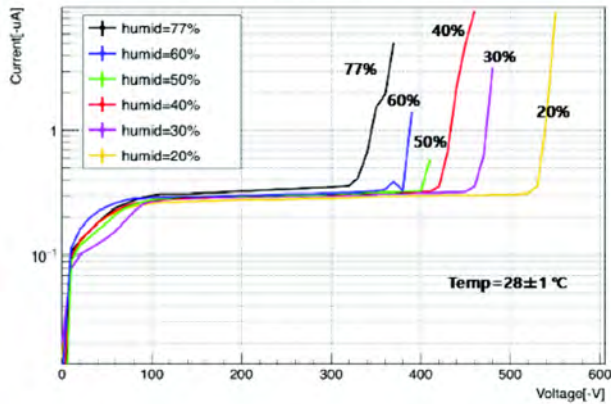


ATLAS12 Humidity Sensitivity

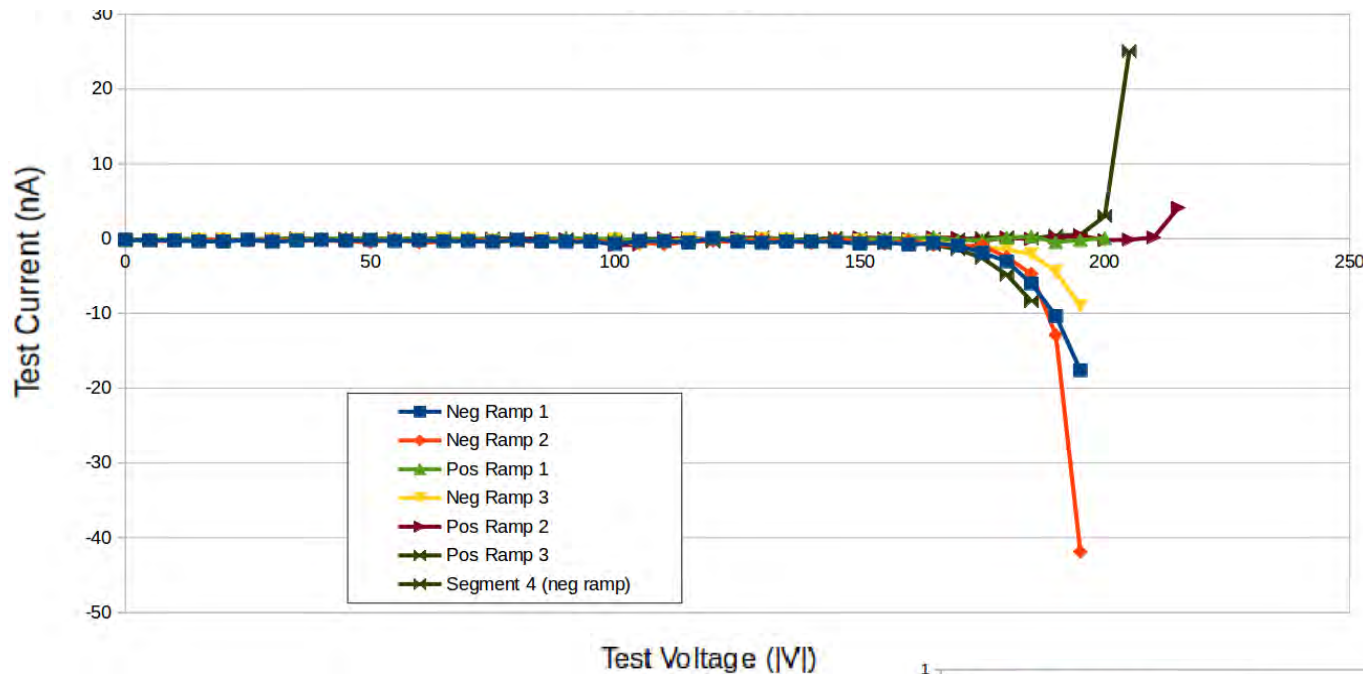
ATLAS12

- VPX12318-W602
- 65h@-600V
- VPX12318-W603
- 24h@-600V
- VPX12318-W606
- 24h@-600V
- VPX12318-W608
- 24h@-600V
- VPX12318-W612
- 24h@-600V
- VPX12518-W684
- 17h@-300V
- VPX12518-W697
- 24h@-600V
- VPX12519-W736
- 24h@-200V
- VPX12519-W746
- 24h@-600V
- VPX12519-W748
- 18h@-130V

W705 IV_scan @KEK



Dielectric Breakdown Voltage

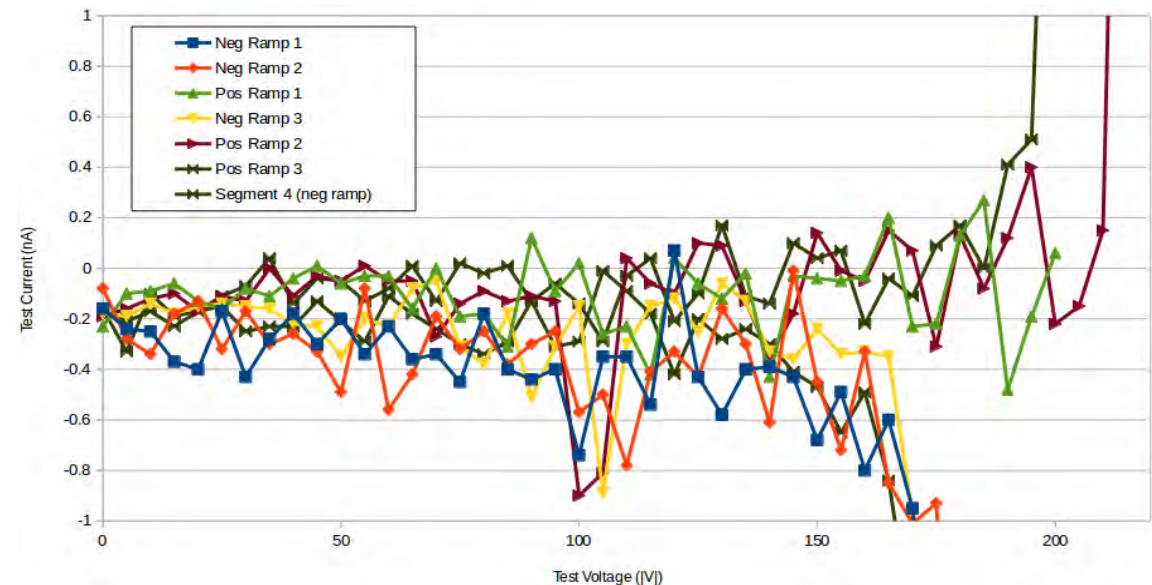


Positive Voltage on Strips:
~200V-210V

Negative Voltage on Strips:
~150V-170V

Specification: > 100V

- Understandable discrepancy between negative and positive voltage breakdowns
 - Sensor unbiased, inversion layer opposes the positive strip voltage, reinforces the negative



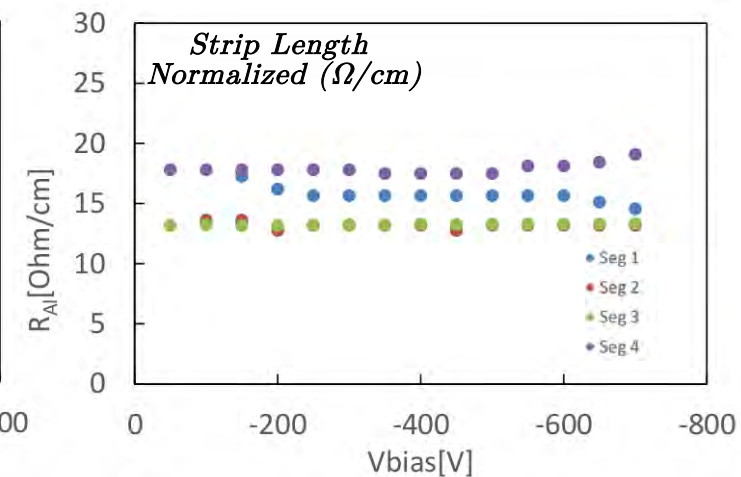
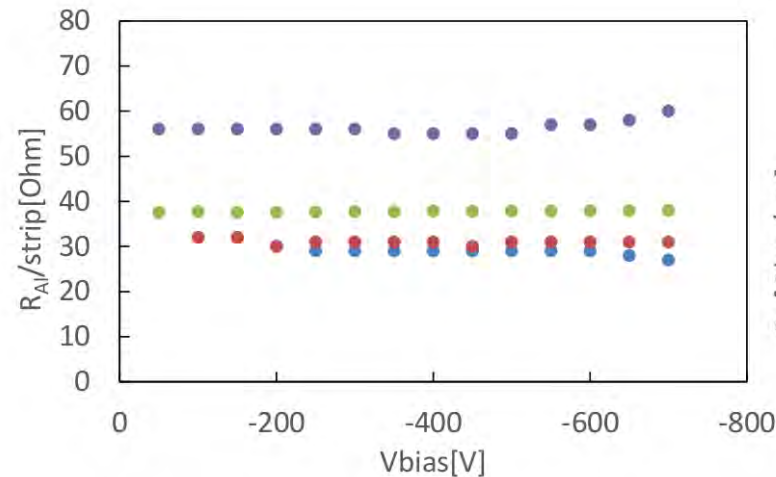
Strip and Implant Resistance

- Must be 'small' to maximize signal integrity and consistent for comparable channel response

Aluminum Strip Resistance

Range: **12.1 – 21.05 Ω/cm ***
 *No. of Strips Measured: 17

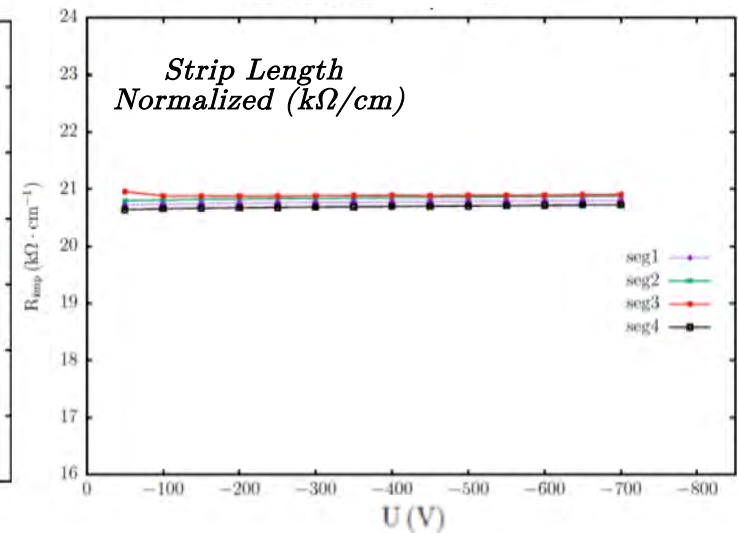
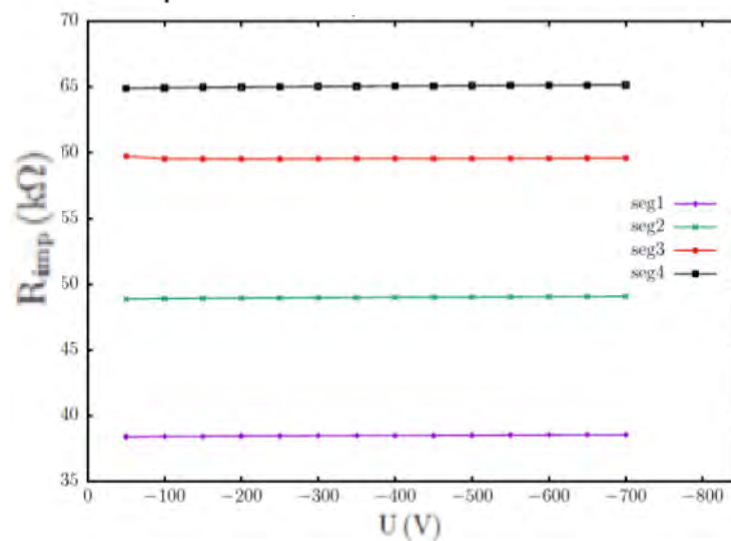
Specification: **< 30 Ω/cm**



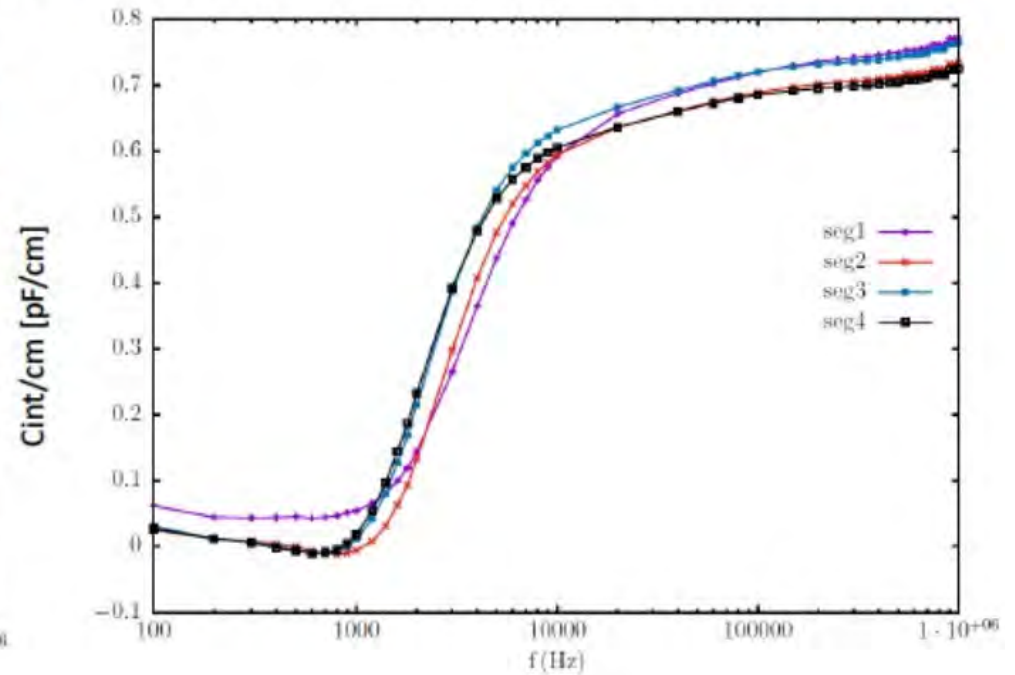
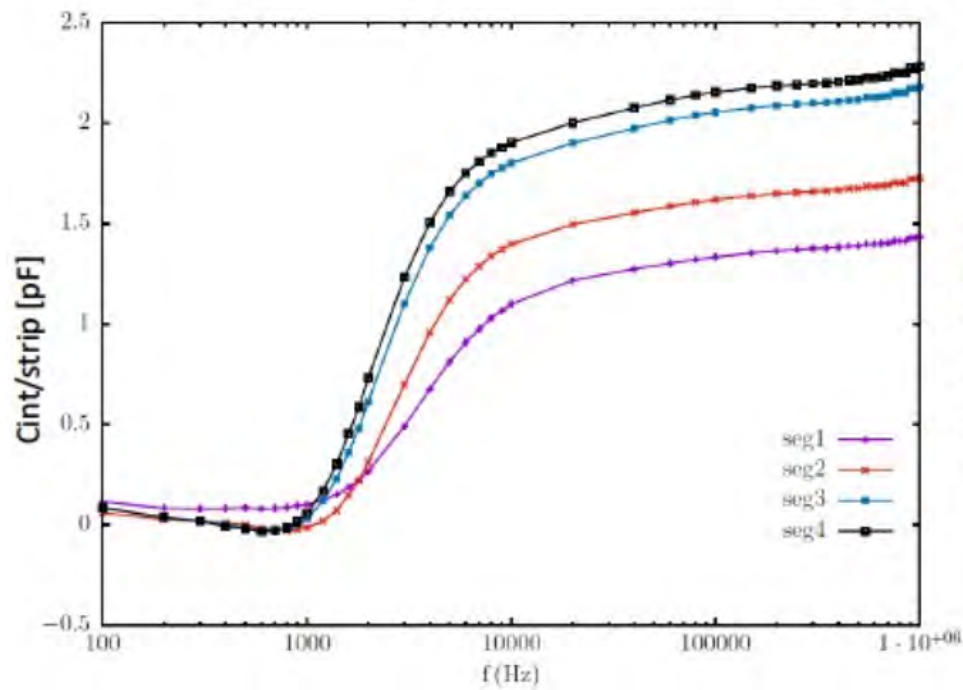
n^+ Implant Resistance

Average: **20.38 \pm 0.21 $k\Omega/cm$ ***
 *No. of Strips Measured: 7

Specification: **< 50 $k\Omega/cm$**



Frequency Dependence of Interstrip Capacitance



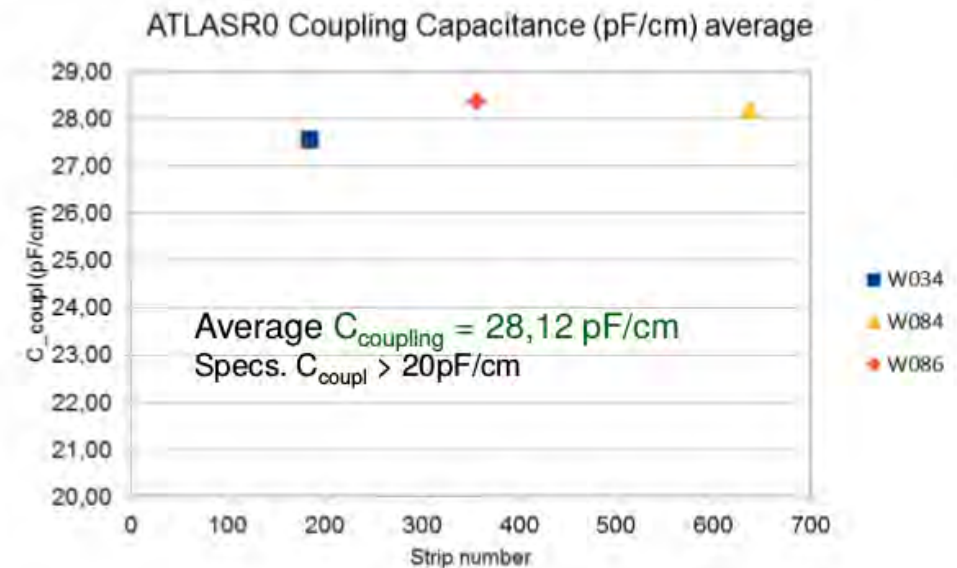
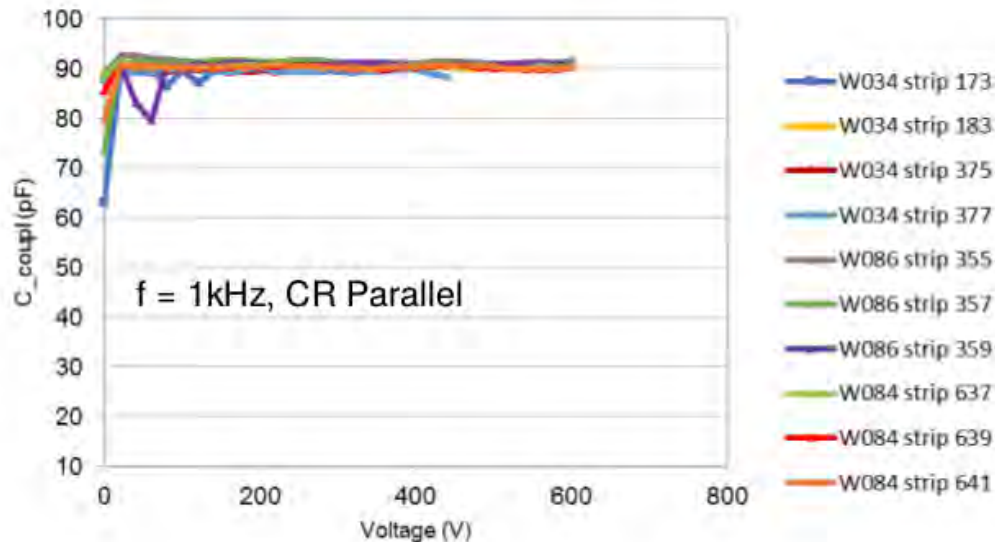
Unirradiated

100kHz is chosen as test frequency (sits well into the plateau region)

More Measurements of Coupling Capacitance

Segment	1	2	3	4
Number of Measurements	17	4	3	4
Range (pF)	46.42-46.95	58.21-59.02	69.75-72.28	76.24-77.42
Average (pF)	46.70	58.51	70.90	77.09
Average (pF/cm)	25.24	24.90	24.88	24.55

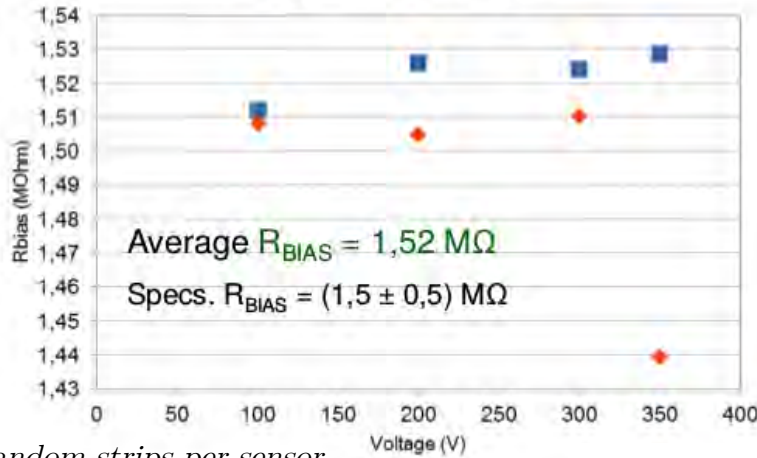
Sensor ID	C_{coup} [pF]
W031	24-25
W034	27.55
W084	28.19
W086	28.37



More Results for Bias and Interstrip Resistance

Polysilicon Bias Resistor (R_{BIAS})

Average R_{bias} vs Voltage

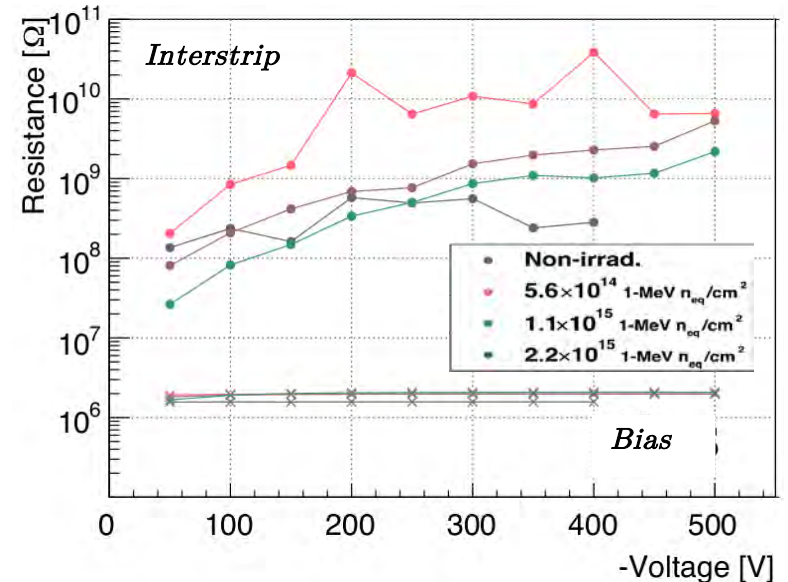
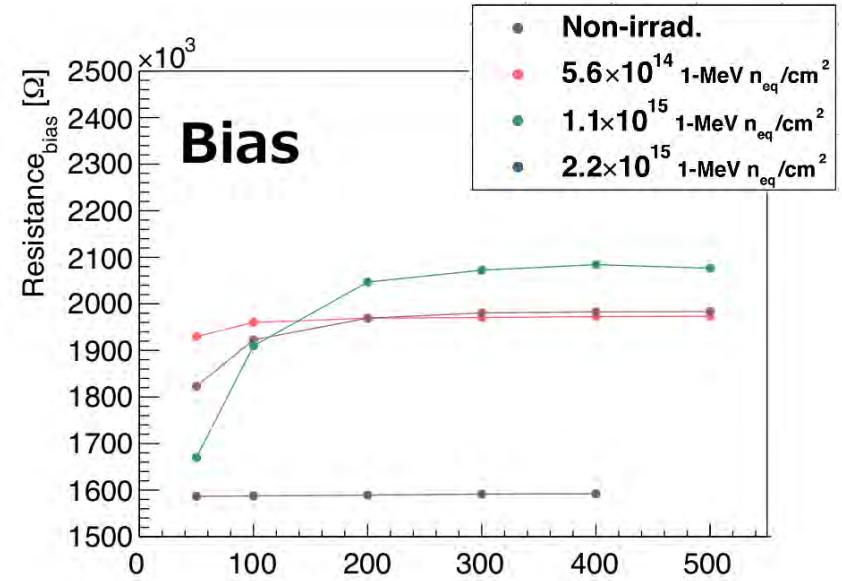
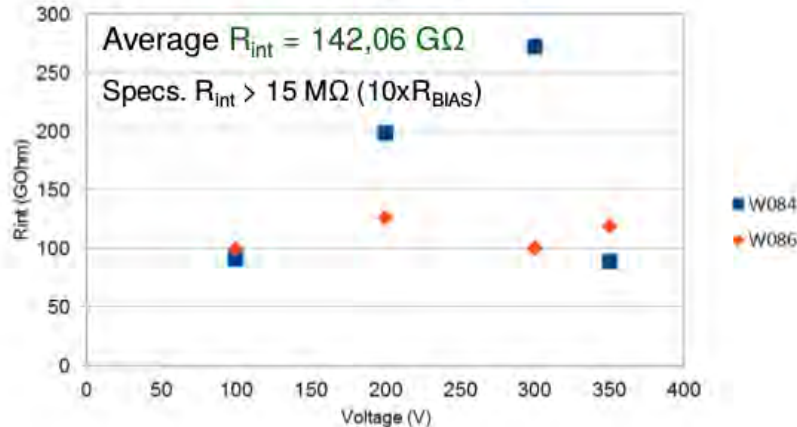


3 random strips per sensor

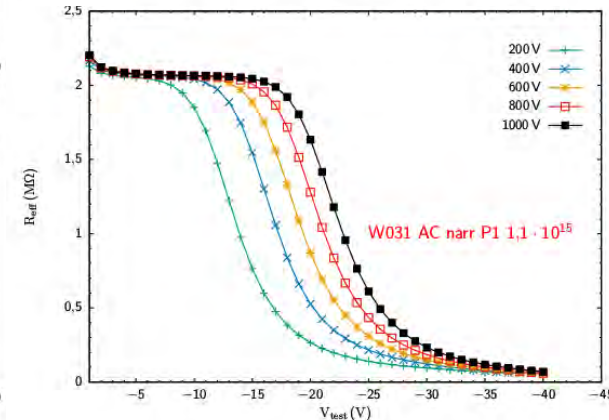
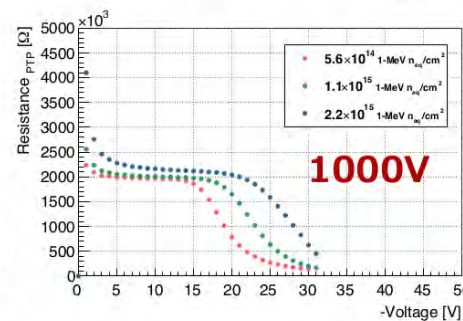
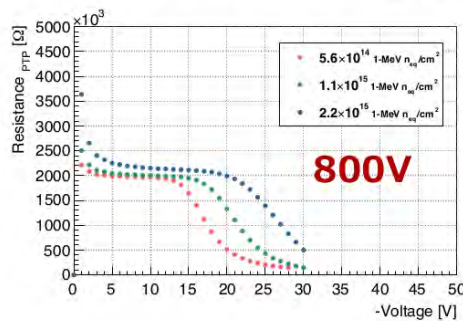
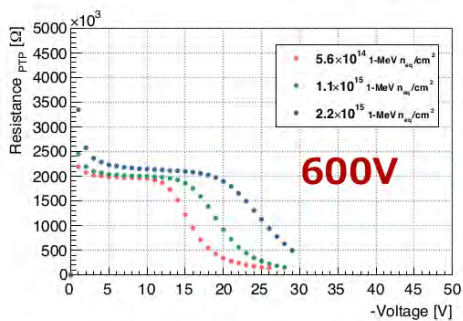
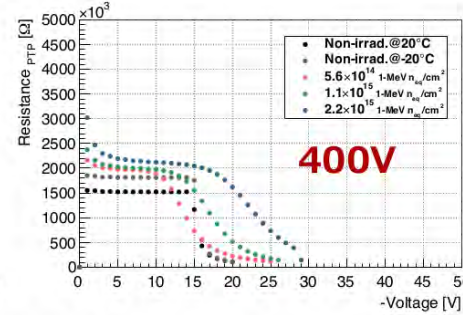
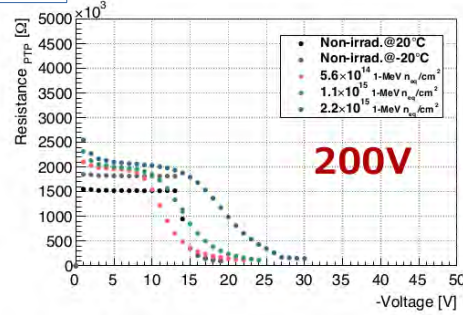
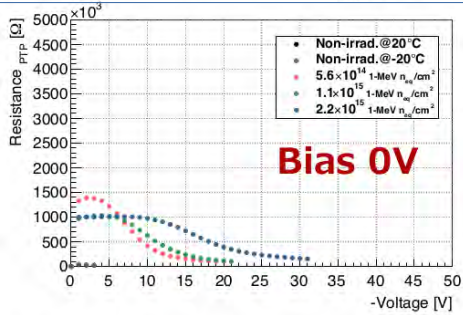
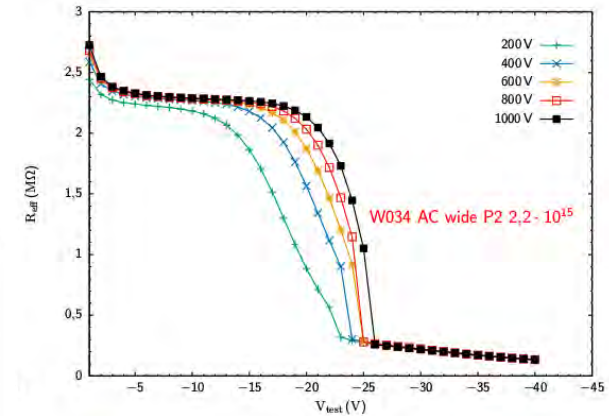
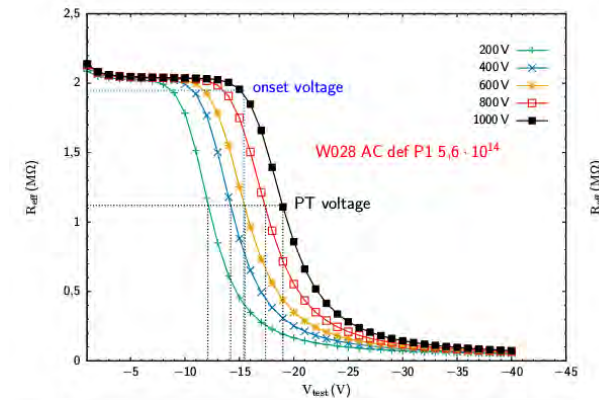
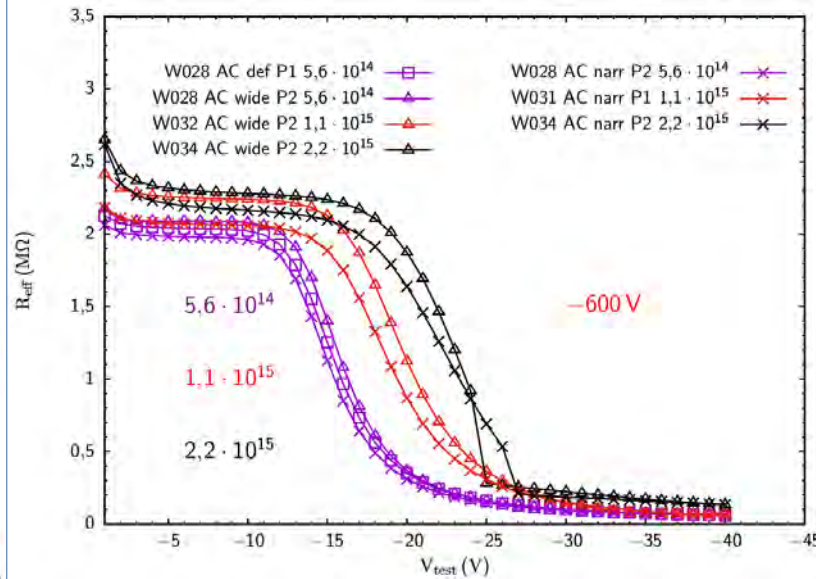
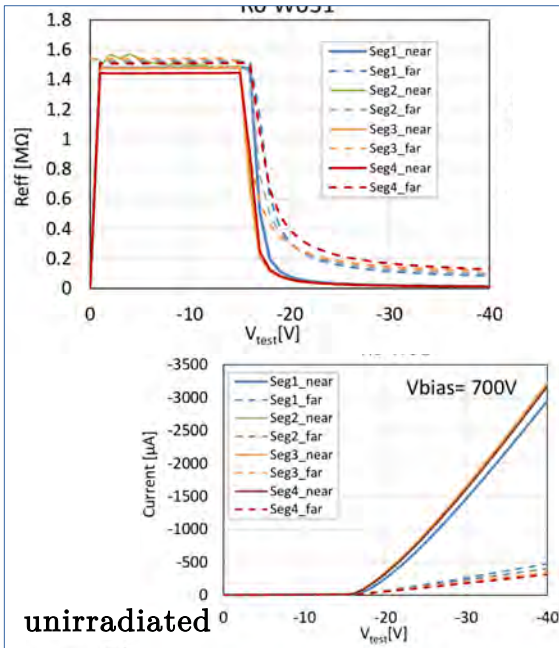
Sensor ID	R_b [MΩ]	R_{is} [GΩ]
W031	1.47	10-120
W084	1.52	271
W086	1.49	99.8

Interstrip Resistance (R_{int})

Average R_{int} vs Voltage



(Irradiated) Performance of the PTP



Irradiated Performance of the Interstrip Capacitance

